INVESTIGATING CORAL DISEASE SPREAD ACROSS THE HAWAIIAN ARCHIPELAGO

A DISSERTATION SUBMITTED TO THE GRADUATE DIVISION OF THE UNIVERSITY OF HAWAIʻI AT MĀNOA IN PARTIAL FULFILLMENT OF THE REQUIREMENTS FOR THE DEGREE OF

DOCTOR OF PHILOSOPHY

IN

ZOOLOGY (MARINE BIOLOGY)

MAY 2017

By

Jamie Sziklay

Dissertation Committee:

Megan Donahue, Chairperson
Greta Aeby
Ruth Gates
C. Drew Harvell
Margaret McManus

ACKNOWLEDGEMENTS

I am thankful for the incredible support of my committee and offer my heartfelt thanks to each of them. First and foremost, I would like to thank my advisor, Megan Donahue, for her years of unwavering dedication to making me a better scientist and communicator. She has been an amazing mentor and will continue to be a lifelong colleague. I would like to thank Ruth Gates for her infectious enthusiasm for science and her ability to simultaneously discuss fine scale details and big picture ideas, a unique quality which was incredibly helpful throughout my PhD. I am thankful to Greta Aeby for always encouraging me to get in the field, for valuable feedback on my scientific writing and for always challenging me to defend my hypotheses and results with ecological information. I am thankful to Margaret McManus for helping me understand how the physical environment can influence disease transmission and for being an outstanding role model for women in science. Finally, I would like to thank Drew Harvell for her help with my experimental design and for introducing me to the broad world of marine infectious disease ecology. I am incredibly grateful to have her as a role model and for her support in networking and communicating with scientists from across the country.

I am grateful for the many people who helped me conduct fieldwork and who shared their own field data for my analyses. Thank you to field assistants Debra Ford, Iain Caldwell, Christina Curto, Courtney Couch, Chelsie Counsell, Katie Lubarsky, Julie Zill, Nyssa Silbiger, Raphael Ritson-Williams, Sean Dimdoff, John Burns, Ingrid Knapp, Kiesha Bahr, Heather Ylitalo-Ward, Amanda Shore-Maggio, Laura Nunez-Pons, David Slater and Ariana Marie-Snow. This fieldwork could not have been conducted without

the University of Hawai‘i dive support of Jason Jones and Dave Pence, and from the crew of the NOAA R/V Hi‘ialakai and chief scientists Randall Kosaki and Scott Godwin. Thank you to Greta Aeby, John Burns, Courtney Couch, Jean Kenyon, Megan Ross, Christina Runyon, William Walsh, Maya Walton, Darla White and Gareth Williams for sharing your field data with me; without your shared knowledge I would not have been able to draw conclusions about broad scale, long term coral disease patterns in Hawai‘i.

I would especially like to give a heartfelt thanks to my family. Their unwavering support is the reason I have been able to reach many achievements in my life. To my parents, Carol and Barry, thank you for inspiring me to explore the world, to seek the best education possible and for supporting me no matter how far my endeavors took me away from home. To Jeremy and Mellissa, thank you for always reminding me there are more things to life besides science, and for consistently telling me to enjoy my time in Hawai‘i! To Dana and Drew, thank you for your love, support and wonderful memories. To Lynn, Claude, Treasa, Mike, Laura and Richard, thank you for treating me as part of the family long before it became official and always supporting my ambitions. Finally, I would like to thank my husband, Iain, for his friendship, support, guidance and help throughout this journey. You inspire me every day to be a better person.

This research was supported by grants from the National Aeronautics and Space Agency Earth and Space Science Fellowship, the PADI Foundation and the Hawai‘i Community Foundation.

ABSTRACT

Coral diseases negatively impact reef ecosystems and they are increasing worldwide; yet, we have a limited understanding of the factors that influence disease risk and transmission. My dissertation research investigated coral disease spread for several common coral diseases in the Hawaiian archipelago to understand how host-pathogen-environment interactions vary across different spatial scales and how we can use that information to improve management strategies. At broad spatial scales, I developed forecasting models to predict outbreak risk based on depth, coral density and temperature anomalies from remotely sensed data (chapter 1). In this chapter, I determined that host density, total coral density, depth and winter temperature variation were important predictors of disease prevalence for several coral diseases. Expanding on the predictive models, I also found that colony size, wave energy, water quality, fish abundance and nearby human population size altered disease risk (chapter 2). Most of the model variation occurred at the scale of sites and coastline, indicating that local coral composition and water quality were key determinants of disease risk. At the reef scale, I investigated factors that influence disease transmission among individuals using a tissue loss disease outbreak in Kāneʻohe Bay, Oʻahu, Hawaiʻi as a case study (chapter 3). I determined that host size, proximity to infected neighbors and numbers of infected neighbors were associated with disease risk. Disease transmission events were very localized (within 15 m) and rates changed dramatically over the course of the outbreak: the transmission rate initially increased quickly during the outbreak and then decreased steadily until the outbreak ended. At the colony scale, I investigated disease

progression between polyps within individual coral colonies using confocal microscopy (chapter 4). Here, I determined that fragmented florescent pigment distributions appeared adjacent to the disease front of infected coral and had fewer intact polyps than in healthy coral fragments. These results suggested that disease progression within colonies affected with chronic and acute *Montipora* white syndromes are highly localized rather than systemic and their bacterial pathogens directly attack the coral tissue rather than zooxanthellae. Overall, my dissertation research indicates that watershed condition and coral community configuration can facilitate and/or inhibit coral disease spread, and that disease transmission may be more spatially constrained than previously thought.

TABLE OF CONTENTS

LIST OF TABLES

LIST OF FIGURES

CHAPTER 1

INTRODUCTION

Although diseases are often viewed negatively, they are an integral component of normally functioning ecosystems, maintaining healthy populations and communities. For individual hosts within a population, diseases have deleterious effects. Infectious diseases cause acute and chronic illnesses in humans, plants, and wildlife, resulting in decreased immune function, reduced physical fitness and mortality. From the perspective of the host population, however, diseases can have positive effects, removing weaker individuals and leaving a stronger pool of individuals to survive and reproduce. Diseases influence population structure indirectly by affecting host development, physiology or behavior, which changes the way the host interacts with resources and other organisms (Hatcher, Dick, and Dunn 2006; Hatcher, Dick, and Dunn 2014), or directly through mortality or reduced fecundity (Anderson 1978; Scott and Dobson 1989). From an evolutionary standpoint, disease-induced mortality can regulate species diversity and genetic composition over relatively short timescales (decades or shorter) and buffer host populations against future epidemics (Altizer, Harvell, and Friedle 2003). Thus, diseases can act as keystone species, modifying community structure and competitive interactions to maintain ecosystem diversity and function (Chapin III et al. 1997; Lafferty et al. 2008; Preston et al. 2016).

Diseases become problematic for host populations and communities when there is a disruption in the host-pathogen balance, leading to large-scale epidemics, die-offs, and host extinctions. Some notable widespread disease outbreaks include Ebola (Kramer et al. 2016), sudden oak death (Rizzo and Garbelotto 2003), potato blight (Smart and Fry 2002), eelgrass wasting disease (Short, Muehlstein, and Porter 1987), canine distemper

virus in seals (Kennedy et al. 2000), chytridiomycosis in amphibians (Skerratt et al. 2007), white plague disease in corals (Miller et al. 2009) and seastar wasting disease (Eisenlord et al. 2016). In general, epidemics are projected to become more frequent and intense in the future due to ongoing climate change (Harvell et al. 2002). It is important to note, however, that projected range expansions for some well-studied diseases such as malaria have not materialized as expected with recent climate change (Lafferty 2009; Lafferty and Mordecai 2016).

For coral reefs, one of the most highly vulnerable ecosystems on Earth, disease outbreaks have contributed to significant declines in coral cover worldwide and outbreaks are predicted to increase in prevalence due to climate change (Harvell et al. 2002; Altizer et al. 2013; Burge et al. 2013). Coral bleaching and subsequent disease outbreaks have been a major driver of reef declines worldwide, first in the Caribbean, and more recently in the Pacific (Aronson and Precht 2001; Miller et al. 2009; Hobbs et al. 2015). Such declines have initiated cascading effects throughout the ecosystem (Hughes et al. 2007; Alvarez-Filip et al. 2009), in turn, affecting the important economic, ecological and cultural roles reefs play in society. Climate change is shifting environmental conditions in favor of disease persistence. Environmental stressors, such as high temperature and rainfall, make corals more susceptible to disease by reducing their immune capacity while simultaneously increasing the abundance and virulence of many pathogens (Ward, Kim, and Harvell 2007; Haapkyla et al. 2011; Burge et al. 2013; Burge et al. 2014). As environmental conditions known to influence disease prevalence

become more common, coral diseases are expected to increase in frequency and severity.

Coral diseases in the Indo-Pacific have recently been identified as one of the 15 most globally important environmental issues that require conservation attention (Sutherland et al. 2015). While coral disease outbreaks often affect relatively small geographic regions, they can cause disproportionately large amounts of damage to coral reefs. Diseases lead to reduced coral growth, fitness, fecundity and/or colony mortality (Sutherland, Porter, and Torres 2004). Both sub-lethal (e.g., reduced fecundity) and lethal effects of disease directly affect reef persistence by restricting gene flow. Under normal conditions, the majority of coral larvae are thought to remain within local populations with limited larval dispersal over moderate to long distances (Vollmer and Palumbi 2006; Combosch and Vollmer 2011). Disease outbreaks can further limit gene flow by initiating a negative feedback, where individuals are removed from a population through mortality (or reproduction is depressed), leaving fewer individuals to reproduce and source local populations, the effect of which is amplified through time. Therefore, one outbreak can affect the future trajectory of a single reef, or a system of interconnected reefs.

Although disease prevalence in Hawai‘i is relatively low compared to most of the Indo-Pacific, disease events have already increased in frequency and geographic extent over the past few decades. In 2003, an outbreak of *Acropora* white syndrome occurred at remote French Frigate Shoals in the Papahānaumokuākea Marine National Monument

(Aeby 2005), perhaps indicating a climate-associated, rather than direct, anthropogenic cause. Outbreaks have been more common in the Main Hawaiian Islands where corals face both global temperature stress and local stress from pollution, nutrient runoff, overfishing and sedimentation. Outbreaks of acute *Montipora* white syndrome were reported in Kāneʻohe Bay, Oʻahu in 2010 and 2012 (Aeby et al. 2016) and in Molokini, Maui in 2013 (Darla White, Maui Division of Aquatic Resources, personal communication). In 2013, Black Band Disease was also discovered for the first time in Hawaiʻi on the north shore of Kauaʻi (Aeby et al. 2015). These outbreaks all resulted in localized mass mortality of the host coral species. The increasing prevalence of coral disease and gradient of human pressure, water quality, habitats and temperature regimes in Hawaiʻi makes this region an ideal location to investigate coral disease transmission.

The disease triangle is one framework that helps us understand the dynamics of infectious diseases in general and can be used to investigate coral diseases in particular (Figure 1.1). George McNew introduced the disease triangle in the 1960s to help identify host-pathogen-environment interactions that result in disease epidemics (McNew 1960). This concept is still used to visualize and articulate disease processes, and examine methods to predict and limit or control future epidemics. Each component of the disease triangle (pathogen, host, environment) influences the behavior of a disease. The efficacy of a pathogen to cause disease depends on the pathogen's ability to invade, proliferate, persist, and disseminate in a host. The susceptibility of a host to infection varies with host traits such as age, sex, size and pre-exposure to infection.

Host-pathogen interactions are often mediated by anomalous environmental events such as high temperatures or rainfall, which can alter interactions in favor of the host or the pathogen (e.g., promoting pathogen growth while reducing host immune efficacy). Although not explicitly integrated into the disease triangle, evolution modifies host-pathogen interactions over time, changing suitable environmental conditions, improving pathogen invasion strategies and increasing host resistance. Importantly, these host-pathogen-environment interactions occur on a multitude of temporal and spatial scales.

At broad spatial scales, climate patterns can mediate coral host-pathogen interactions. For several coral diseases, disease prevalence significantly increases with region-wide warm temperature anomalies (Bruno et al. 2007; Selig, Casey, and Bruno 2010; Ruiz-Moreno et al. 2012), high rates of temperature change (Randall and van Woesik 2015) and extreme climatic events such as the El Niño Southern Oscillation (Selig, Casey, and Bruno 2010). The relationship between coral diseases and temperature anomalies is strongest on scales of approximately 50 km or less (Selig, Casey, and Bruno 2010), suggesting that widespread anomalous conditions may prime reef regions for disease events. However, within anomalously warm reef regions where disease development is favorable, local and micro-scale conditions likely determine which individuals become infected.

On a local scale (within/among reefs), host structure, habitat composition and the physical environment can affect disease transmission among individuals. Specific host traits associated with genetics and physiology can make certain individuals more

susceptible to disease than others. The variation in susceptibility can influence disease spread over small spatial scales. Habitat composition of non-host species (i.e., other coral species and benthic invertebrates, fish community) can also influence pathogen dispersal. Non-host species can both suppress disease transmission by acting as low competency/dead-end hosts or amplify disease transmission by serving as a source pool or reservoir for existing and new pathogens (Johnson and Thieltges 2010). A third constraint on disease transmission at the local scale is the physical environment, which can result in high local spatial variability in conditions such as diurnal warming, stratification and internal waves – all of which influence temperature variability. For example, seawater temperatures often increase in embayments, which can allow pathogens to remain viable throughout winter months (e.g., Vanoy et al. 1992). The interactions among host, pathogens and environment at the local scale can vary on daily to seasonal time scales and regulate the severity and duration of disease events.

For disease progression to occur within a coral host (microscale), pathogens must overcome physical barriers, chemical gradients, microbiota and the host immune system. As a first line of defense, the coral epidermis acts as a physical barrier to prevent pathogen entry (Mullen, Peters, and Harvell 2004; Reshef et al. 2006). A surface mucus layer covers the epidermis and consists of numerous microorganisms, many of which actively produce antibiotics (Shnit-Orland and Kushmaro 2009). Internally, cnidarians can elicit a suite of innate immune responses, which include pathogen recognition, signaling cascades, and effector responses (reviewed by Augustin & Bosch 2010; Dunn 2010; Palmer and Traylor-Knowles 2012). In all

organisms, including corals, pathogens have developed various strategies to evade a host immune response, from neutralizing mechanisms to inhibiting signaling pathways to disguising oneself as part of the host organism (Finlay and McFadden 2006), prompting an arms race between the host and pathogen. The strength and speed in which corals can elicit an immune response underpins their capacity to resist and recover from an infection.

The overarching objective of my dissertation research was to understand marine disease spread at multiple spatial scales using coral as a model system. Each chapter addresses one or more interrelationships in the disease triangle (Figure 1.1). In Chapter 2, I develop forecasting models of coral disease risk for three common coral diseases in Hawai‘i using conditions that can be measured remotely for the entire archipelago. In Chapter 3, I more broadly examine biotic and abiotic conditions associated with disease prevalence across Hawai‘i for four common coral diseases. In chapter 4, I investigate how disease risk varies by host traits, habitat and time in Kāne‘ohe Bay, O‘ahu using a tissue loss disease outbreak in *Montipora capitata* as a case study. In chapter 5, I explore intra-colony disease progression by quantifying changes in the natural fluorescence of *M. capitata* affected by chronic and acute tissue loss diseases. In chapter 6, I discuss the results of chapters 2-5 on our understanding of coral disease in Hawai‘i and how that information improves our overall understanding of marine disease transmission globally.

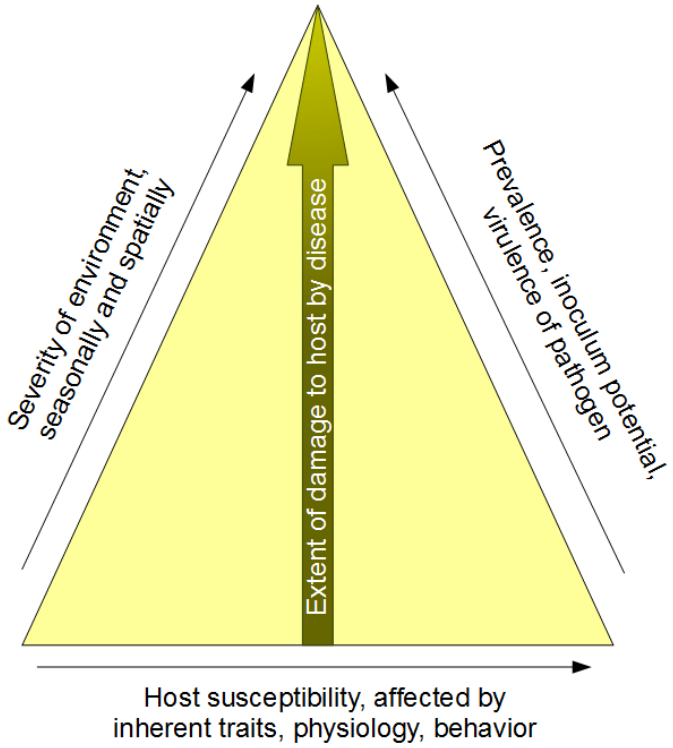

Figure 1.1 Modified disease triangle (adapted from Scholthof 2007). The extent of damage caused during an epidemic is influenced by complex interactions among the pathogen, host and environment.

CHAPTER 2

SATELLITE SST-BASED CORAL DISEASE OUTBREAK PREDICTIONS FOR THE HAWAIIAN ARCHIPELAGO

Published as:

Caldwell J, Eakin CM, Heron SF and Donahue M (2016). Satellite SST-Based Coral Disease Outbreak Predictions for the Hawaiian Archipelago. Remote Sensing 8 (2): 93.

Abstract

Predicting wildlife disease risk is essential for effective monitoring and management, especially for geographically expansive ecosystems such as coral reefs in the Hawaiian archipelago. Warming ocean temperature has increased coral disease outbreaks contributing to declines in coral cover worldwide. In this study we investigated seasonal effects of thermal stress on the prevalence of three widespread coral diseases in Hawai‘i: *Montipora* white syndrome, *Porites* growth anomalies and *Porites* tissue loss syndrome. To predict outbreak likelihood we compared disease prevalence from surveys conducted between 2004 and 2015 from 18 Hawaiian islands and atolls with biotic (e.g., coral density) and abiotic (satellite-derived sea surface temperature metrics) variables using boosted regression trees. To date, the only coral disease forecast models available were developed for *Acropora* white syndrome on the Great Barrier Reef (GBR). Given the complexities of disease etiology, differences in host distribution and environmental conditions across reef regions, it is important to refine and adapt such models for different diseases and geographic regions of interest. Similar to the *Acropora* white syndrome models, anomalously warm conditions were important for predicting *Montipora* white syndrome, possibly due to a relationship between thermal stress and a compromised host immune system. However, coral density and winter conditions were the most important predictors of all three coral diseases in this study, enabling development of a forecasting system that can predict regions of elevated disease risk up to six months before an expected outbreak. Our research indicates satellite-derived systems for forecasting disease outbreaks can be appropriately adapted from the GBR tools and applied for a variety of diseases in a new region.

These models can be used to enhance management capacity to prepare for and respond to emerging coral diseases throughout Hawai‘i and can be modified for other diseases and regions around the world.

Introduction

Climate change and associated ocean warming have been linked to increasing frequency and severity of infectious diseases in several economically and ecologically important marine organisms (Harvell et al. 2002; Burge et al. 2014). While diseases are an integral component of normally functioning ecosystems, outbreaks can alter population structure, lead to large-scale die-offs and even host extinctions (Vredenburg et al. 2010; Fisher et al. 2012). Host-pathogen interactions often shift in response to prolonged or severe environmental disturbance, such as high temperatures or rainfall, which alters interactions in favor of either the host or the pathogen (e.g., promoting pathogen growth while reducing host immune efficacy) (Altizer et al. 2006). Temperature changes alone can affect host and pathogen behavior, shift pathogen ranges and increase host susceptibility and pathogen virulence (Altizer et al. 2006; Burge et al. 2014). For example, a +1 °C increase in water temperature increases the abundance of pathogenic bacteria *Vibrio harveyi* in the water column and the susceptibility of its abalone host *Haliotis tuerculata* (Travers et al. 2009). As periods of anomalously high ocean temperatures occur more frequently, marine disease outbreaks are expected to become more common and more severe.

Links between warming ocean temperatures, increased temperature variability and coral disease outbreaks threaten coral reef ecosystems across the globe. With increasing disease outbreaks and coral bleaching, many corals worldwide are threatened by extinction (Carpenter et al. 2008), presenting concerns for food security, livelihoods and shoreline protection for coastal communities (Reytar, Spalding, and Perry 2011). Disease prevalence patterns vary across ocean basins and, for several diseases, are strongly correlated with regionally warm temperature anomalies (Ruiz-Moreno et al. 2012). Previous studies investigating temperature-disease relationships have found that increased ocean temperatures promote lesion and pathogen growth rates (Bruckner and Hill 2009; Miller and Richardson 2014), increase transmission and virulence of pathogens, and reduce coral resistance to pathogens for a variety of coral diseases such as Black Band Disease, Yellow Band Disease and White Plague (Harvell et al. 2002; Ward, Kim, and Harvell 2007; Sokolow 2009; Burge et al. 2014). While disease outbreaks have been most severe across the Caribbean, coral disease outbreaks have become increasingly common in the Indo-Pacific during the last decade (Aeby 2005; Williams et al. 2011; Hobbs et al. 2015). Mild winters and anomalously warm summers have coincided with many of these outbreak events (Carpenter et al. 2008; Eakin et al. 2010; Heron et al. 2010; Maynard et al. 2011) suggesting an association between broad scale oceanic temperature regimes and disease onset.

Four previous modeling efforts have advanced our ability to predict coral disease outbreaks using remotely sensed sea surface temperature (SST) anomalies. Bruno et al. (2007) used the weekly SST anomalies metric (WSSTA; the number of weeks in the

preceding year at or above +1 °C above the weekly mean), coral cover and long-term *Acropora* white syndrome observations to model outbreak events on the Great Barrier Reef (GBR). They found that sites with >50 % coral cover and more than five anomalously warm weeks were associated with higher disease abundance. Maynard et al. (2011) also assessed the relationship among white syndrome abundance, coral cover and warm-season high thermal stress using the Mean Positive Summer Anomaly (MPSA) metric in a regression model that predicted outbreak likelihood with >90 % accuracy on reefs with >26 % coral cover. This study revealed that as temperature stress increased, outbreaks could occur at lower threshold densities.

Heron et al. (2010) incorporated the magnitude (not just occurrence) of summer anomalies and also included anomalous winter temperature metrics (Winter Condition and Cold Snap) during the year prior to a disease event to predict an outbreak. Their study confirmed the importance of high coral cover (threshold >30 %) and anomalously warm summer temperatures for increased risk of *Acropora* white syndrome, but also demonstrated that mild winter temperatures may be equally as important factors in susceptibility to disease outbreaks. The National Oceanic and Atmospheric Administration (NOAA) now regularly produces a predictive tool for coral disease outbreak risk on the GBR based on these findings (coralreefwatch.noaa.gov/satellite/disease/dz_gbr.php).

Randall and van Woesik (2015) developed a model for white-band disease on *Acropora* in the Caribbean by comparing recent outbreaks with historical and contemporary SST

metrics. Their study revealed that the most useful predictors of white-band disease differed depending on the host species, where depth, 30-year rate of temperature change and minimum temperatures were most important for *Acropora palmata* while maximum, minimum and monthly rate of temperature change was most important for *Acropora cervicornis*. These four research efforts set the foundation to develop predictive models for different temperature-dependent coral diseases in other regions across the globe.

Scientists and managers currently use the Maynard et al. 2011 and Heron et al. 2010 *Acropora* white syndrome models to plan research and conservation efforts in Australia (Beeden et al. 2012). Remote sensing of environmental conditions associated with disease outbreaks is particularly useful for reef management agencies where time and financial resources are limited, allowing them to better monitor broad geographic regions with low background levels of disease and patchy distribution of outbreaks. Given the complexities of disease etiology, differences in host distribution and environmental conditions across reef regions, such models may need to be refined and adapted for different diseases and geographic regions.

Metrics from Heron et al. 2010 were adapted to produce a complementary, experimental predictive tool for the Hawaiian archipelago. The modifications included determining appropriate SST climatologies, adjusting metric thresholds to represent the new location, and refining the release schedule for seasonal risk outlooks and

assessments. However, these metrics and thresholds had, until now, never been quantitatively evaluated using disease observations.

Here, we evaluate the applicability of SST-based metrics describing anomalously warm and cold conditions for forecasting three common coral diseases in Hawai‘i: *Montipora* white syndrome, *Porites* growth anomalies and *Porites* tissue loss syndrome. These diseases have caused significant morbidity, reduced fecundity, and often colony mortality in the region's dominant reef-building corals. *Montipora* white syndrome and *Porites* tissue loss syndrome are characterized by gradual to rapid tissue mortality as the disease progresses across the colony, sometimes killing colonies in less than two weeks (Aeby et al. 2010; Aeby et al. 2011; Work et al. 2012); *Porites* growth anomalies are chronic, protuberant masses of the coral skeleton that do not cause rapid mortality, but do have a number of deleterious effects on coral including reduced growth, fecundity, fitness and overall survival (Stimson 2010).

Montipora (and *Acropora*) white syndrome, *Porites* tissue loss syndrome, and to a lesser extent, *Porites* growth anomalies, have been observed to be related to anomalous temperature (Williams et al. 2010; Aeby et al. 2011), which suggests that these three diseases are good candidates to test thermal stress metrics for forecasting future outbreaks. Pathogenic bacteria that can cause white syndromes in *Acropora* and *Montipora* (*Vibrio* spp.) have been observed to alter their disease presentation, decrease time until disease onset and/or shorten the incubation period in higher water temperatures (Kimes et al. 2012; Ushijima et al. 2014). The pathogens that cause

Porites growth anomalies and tissue loss syndrome are currently unknown, but previous studies have shown slight associations between sites with lower thermal stress and higher disease prevalence (Aeby et al. 2011). To determine outbreak risk in this study, we used boosted regression trees, an ensemble statistical modeling approach that allowed us to identify optimal predictors and their relative importance while minimizing predictive deviance.

Methods

Field Surveys of Coral Diseases

We used 789 coral health surveys from the Hawai'i Coral Disease database (HICORDIS; Caldwell et al. 2016) conducted in the Hawaiian archipelago between 2004 and 2015 to explore associations among SST, biotic factors and disease prevalence. Surveys were conducted by ten different research groups on 18 islands and atolls across the ~2400 km Hawaiian archipelago (Figure 2.1) representing large variations in coral community composition, densities and disease prevalence across nine degrees of latitude (Table 2.1).

Coral health observations were collected using one of three methods: belt transects, line-intercept and estimated prevalence, across a 1–24.5 m depth range. For the belt transect method, divers recorded health information on all coral colonies within a specified length and width (average length = 20 m, range = 8–50 m; average width = 1 m, range = 1–6 m). In the line-intercept method, divers recorded coral health information

for all colonies lying directly beneath 25 m of transect tape. In the estimated prevalence method, divers counted the number of colonies in a subset of a belt transect (average = 10 × 2 m^2, range = 10 × 2 m^2 to 10 × 6 m^2), and counted all diseased colonies within the larger belt transect area (average = 25 × 2 m^2, range = 25 × 2 m^2 to 25 × 6 m^2).

For each survey, we calculated disease prevalence as the number of infected colonies divided by the total number of host colonies (*i.e.*, *Montipora* or *Porites*) observed. For the estimated prevalence method, we extrapolated the total number of host colonies observed for the entire transect surveyed from the abundances counted in the subset region. We excluded surveys that had <20 total coral colony observations from the data because they disproportionately resulted in exceptionally high prevalence values. We calculated densities as the total number of colonies divided by the area surveyed.

Defining Disease Outbreaks

We calculated disease prevalence thresholds by statistically isolating outliers as outbreaks (i.e., above average levels of disease prevalence), according to the Heron et al. (2010) method. Briefly, for each disease, we first isolated the maximum disease prevalence value for each year from 2004 to 2015 and calculated the mean and standard deviation (SD) of the maximum prevalence across years. Any annual values that exceeded the mean plus one SD were replaced with the next highest value from that year and the mean and SD recalculated. This was iteratively repeated until no

values were above the threshold. Any values above the final threshold were considered outbreaks.

Sea Surface Temperature Based Metrics

To hindcast SST anomalies over the same time period as our disease observations and to develop a tool relevant for forecasting disease risk into the future, we concatenated three SST datasets. We used an updated release (v5.2) of the retrospective Pathfinder SST dataset (Casey et al. 2010) used in other studies (Heron et al. 2010) that spanned the period 1985–2012. Daily data were composited to weekly temporal resolution, maintaining the native 1/24° (~4 km) resolution and gap filled following Heron et al. (2010). The second dataset was the NOAA/NESDIS Blended 5 km (precisely 0.05°) dataset available in near real-time since March 2013 with daily temporal resolution (Liu et al. 2014). This was composited as a weekly average for consistency of temporal resolution with the 4 km dataset. As the 5 km dataset is produced in near real-time, it is the leading option on which to build any future forecasting of disease risk. To bridge the gap between these datasets and to facilitate the bias adjustment between them (ensuring consistency of the time series), the blended 11 km SST predecessor to the 5 km product was used. This product spanned the period February 2009–October 2013 and was also composited to weekly resolution. The three datasets were concatenated by linearly regressing paired weekly values in the temporal overlap and adjusting the relative bias of the 4 km and 11 km values to emulate the 5 km data. This resulted in an internally consistent SST time series at weekly resolution for each survey location and for

the period January 1985–June 2015. This covered the period of observations (2004–2015) and allowed development of long-term climatologies used in the calculation of SST metrics.

To examine heat stress preceding each disease survey, we used two SST metrics that have been successfully used to hind/forecast *Acropora* white syndrome on the Great Barrier Reef (Table 2.1). Mean Positive Summer Anomaly (MPSA) is the average of SST anomalies above the corresponding monthly mean climatology plus one standard deviation (SD), calculated across the three summer months and is expressed as °C (Maynard et al. 2011). Hot Snap (Heron et al. 2010) is another indicator of unusually warm conditions experienced primarily during the summer period accounting for both the magnitude and duration of heat stress. The Hot Snap metric uses a single summertime baseline to identify stressful temperature, one SD above the summer mean SST, and integrated the magnitude of temperature anomalies above this baseline through time (units of °C-weeks). Hot Snaps also include positive anomalies outside of the climatological warmest months to include warming prior/subsequent to the three-month summer season.

We also examined two winter metrics that were designed to determine if unusually cold or warm temperatures affect pathogen loading and/or host susceptibility, ultimately increasing risk of disease in the subsequent warmer months as thermal stress accumulates (Heron et al. 2010). Cold Snap (Heron et al. 2010) combines the magnitude and duration of wintertime cold stress by integrating temperatures that are

one SD below the mean winter SST (climatological mean across three coldest months of the year). The Cold Snap metric consists of only negative values and is calculated across the nine months preceding the summer. The Winter Condition (Heron et al. 2010) complements the Cold Snap metric to provide an overall measure of winter pre-conditioning throughout the year. The Winter Condition consists of positive and negative anomalies accumulated about the mean winter temperature through the defined three-month winter period and also incorporates additional non-winter cool periods when temperatures are below one winter SD above the winter mean.

While the temperature profile in the ocean varies with depth, temperature anomalies from the surface provide an effective estimate of anomalies to at least a few tens of meters as well as at the surface (Heron et al. 2010). As each of these metrics was derived using temperature anomalies, they are indicative of conditions experienced at the depth of corals. However, depth may contribute significant information to the models, so it is independently included as a model parameter and as an interactive term with other SST metrics. We calculated all SST-based metrics for each pixel containing a disease survey using the concatenated SST time series.

Determining Outbreak Risk

To assess the relationship among SST metrics, biotic factors (e.g., host density) and disease prevalence, we used boosted regression trees. Boosted regression trees (BRTs) fit response variables (i.e., disease prevalence) to their predictors through recursive binary splits in an additive fashion in which simple regression trees are combined using a boosting

algorithm (an algorithm to reduce deviance at each iteration) to improve predictive performance (Elith, Leathwick, and Hastie 2008). BRTs are models built in a stage-wise fashion using machine-learning techniques to minimize predictive error at each stage of model building and have superior predictive performance compared to other modeling techniques (Elith, Leathwick, and Hastie 2008; Cappelle et al. 2010; Franklin, Jokiel, and Donahue 2013).

Three parameters need to be defined to optimize model performance in BRTs: tree complexity, learning rate, and bag fraction. Tree complexity (*tc*) controls the number of nodes in a tree based on whether interactions are fitted. Learning rate (*lr*) reduces the contribution of each tree as it is added to the model. Together, tree complexity and learning rate determine the number of trees required for optimal predictive power. Number of trees (*nt*) is the number of consecutive trees used to build a BRT. The optimal *nt* indicates the point just before the model begins to overfit the data. Using an *nt* beyond the optimal *nt* may increase predictive deviance. Stochasticity adds accuracy and reduces over-fitting and is controlled in BRTs through a bag fraction, which uses a bootstrapped subset of data to fit each new tree. A bag fraction of 0.5 means that at each iteration, individual trees are fitted with 50% of the data that are drawn at random, without replacement, from the dataset.

To determine the optimal values of learning rate, tree complexity and bag fraction, we examined the cross-validation deviance over *lr* values of 0.01, 0.001, 0.005, tc values of 1–5 and bag fraction values of 0.1, 0.5, 0.75. Cross validation is a technique for

evaluating the model using withheld portions of the data and the cross-validation deviance measures how much the predicted values based on the non-withheld data differ from the observations from the withheld data (Elith, Leathwick, and Hastie 2008). We ran all possible combinations using *gbm.step* in the *gbm* package in R statistical program version 3.3.1 (R Core Team 2014) with 10-fold cross-validation in each model run and selected the three-parameter combination that produced the lowest cross-validation deviance to produce the optimal BRT. We further optimized the final BRT model by removing redundant, non-informative predictor variables selected through *gbm.simplify*, a method analogous to backwards selection in regression.

For each disease we developed hierarchical BRT models to account for zero-inflated data. The majority of surveys (50%–91% across the three diseases) had no diseased colonies (i.e., a prevalence of zero). We accounted for the zero-inflated data distribution using an approach similar to Cappelle et al. (2010), where we combined two BRT models: a presence-absence model assuming a Bernoulli response distribution and a prevalence-if-present model using a Gaussian response distribution on square-root transformed prevalence data. The final prevalence prediction was calculated as the probability of disease presence given by the presence-absence model (0 or 1) multiplied by the predicted prevalence given by the prevalence-if-present model.

To test predictive accuracy, we created all models using the parameters described above on a training dataset consisting of a randomly selected 75% subset of surveys and used the withheld 25% of surveys (test data) for independent validation of the

models. To evaluate the performance of each BRT individually, we calculated the cross-validation (CV) deviance and the standard error of CV deviance (SE). Here, we used CV deviance as a measure of each model's ability to explain the withheld data in the training dataset.

To determine model performance of the hierarchical BRTs, we calculated the area under the receiver operating characteristic curve (AUC) and model deviance for each hierarchical model. To quantitatively measure goodness-of-fit, we used AUC values, which provide a metric for how well the model distinguishes presences and absences by comparing rates of true positives and false positives. A model that is unable to assign presences more often than random is indicated by an AUC value of 0.5 whereas a model that always assigns presences with a higher probability than absences (perfect fit) is indicated by an AUC value of 1.0. The percentage of test data explained by the model is called deviance (D). We calculated D as the average difference between true observations of disease prevalence in the test dataset and predicted estimates of disease prevalence made by the model.

Results and Discussion

Defining Disease Outbreaks

Using the method described in Heron et al. (2010), we defined the occurrence of a disease outbreak for *Montipora* white syndrome, *Porites* growth anomalies and *Porites* tissue loss syndrome in Hawai'i as any survey where prevalence values exceeded 8.5%, 45.5% and 16.2% respectively. According to these thresholds, outbreaks

(surveys with statistically high disease prevalence) of *Montipora* white syndrome were recorded in 10 surveys (1.3%), outbreaks of *Porites* growth anomalies were recorded in 26 surveys (3.3%) and outbreaks of *Porites* tissue loss syndrome were recorded in 43 surveys (5.4%); there were 789 surveys in total for each disease. Mean prevalence values previously reported for *Montipora* white syndrome and *Porites* tissue loss syndrome in Hawai‘i ranged from 0%–1% and increased several-fold during outbreak events, previously reported as high as 35.95% and 29.17% respectively (Aeby 2009; Aeby et al. 2011). In contrast, mean prevalence values previously reported for *Porites* growth anomalies across the Indo-Pacific (including Hawai‘i) ranged from 0%–13.7% illustrating relatively high endemic levels of disease prevalence (Aeby 2009; Aeby et al. 2011; Couch et al. 2014). The large size of this dataset allowed us to define regionally specific outbreak thresholds for the first time. As with all studies in wildlife disease ecology, these thresholds should neither be considered an exact or fixed threshold. However, they provided a meaningful metric to distinguish locations with average versus above average disease prevalence.

Many coral disease outbreaks between 2004 and 2015 occurred clustered in space and time (Figures 2.1 and 2.2). The most severe outbreaks for all three diseases occurred in the Main Hawaiian Islands. *Montipora* white syndrome outbreaks primarily occurred during the winter of 2010 and 2012 on O‘ahu and in 2014 on Maui. Given the importance of host density for *Montipora* white syndrome transmission (Aeby et al. 2010), the high number of susceptible hosts at these specific locations may partially explain this spatial pattern. The majority of outbreaks for *Porites* growth anomalies and

tissue loss syndrome also occurred between 2010 and 2015, with the most severe events in 2010 and 2011. Thirteen *Porites* growth anomalies outbreaks (48%) were recorded around the island of O‘ahu with six outbreaks (22%) recorded around Hawai‘i Island. The spatial clustering of *Porites* growth anomalies around Hawai‘i may be partially explained by the correlation between disease prevalence and high host densities whereas the spatial clusters of outbreaks on O‘ahu may be explained by the correlation between disease prevalence and large human populations sizes (Aeby et al. 2011). Ten *Porites* tissue loss syndrome outbreaks (29%) also occurred on O‘ahu. Prior studies have shown a positive correlation between *Porites* tissue loss syndrome and coral cover/host density (Williams et al. 2010; Aeby et al. 2011). *Porites* is the dominant coral genus on all of the Main Hawaiian Islands, including O‘ahu (Franklin, Jokiel, and Donahue 2013), which suggests there are additional factors driving tissue loss syndrome prevalence that are currently unknown.

Determining Outbreak Risk

We used hierarchical BRT models to retrospectively predict coral disease prevalence. Optimal parameters for these models ranged from 750–3500 trees, tree complexities of 3–5, learning rates of 0.001 or 0.005 and a bag fraction of 0.75 (Table 2.2). Model cross-validation deviances for the training data ranged from 0.048–1.213 (Table 2.2). Cross-validation deviances closer to zero indicate greater predictive accuracy. AUC values ranged from 0.67–0.85. Large AUC values indicate higher performance models. All models predicted disease prevalence better than random (i.e., AUC > 0.5) but the model for *Porites* growth anomalies performed best in the independent validation tests

using the test dataset with an AUC value of 0.85 (Table 2.2). Coral distribution (i.e., *Montipora* density, *Porites* density and/or colony density) and Winter Condition were important for all models; however, relative contributions differed among models (Figure 2.3). For example, the relative influence of Winter Condition in the *Montipora* white syndrome model was 54.1% compared to only 14.5% in the *Porites* growth anomalies model suggesting that Winter Condition plays a much more important role in disease dynamics of *Montipora* white syndrome (Figure 2.3). We show the relative influence of each predictor variable and the relationship between the fitted model functions and predictor variables in Figure 2.3.

Montipora White Syndrome

Winter Condition, Cold Snap, Hot Snap and host density were the most informative predictors of *Montipora* white syndrome prevalence (Figure 2.3); all other predictor variables were determined non-informative. The mean predictive accuracy for *Montipora* white syndrome (AUC) was 0.70 and explained 30% of the deviance using the test data (Table 2.2). The Winter Condition metric had the highest relative influence in the model, highlighting a relationship between mild Winter Conditions (>0.85 °C-weeks) and higher disease prevalence. This relationship is similar to the relationship between winter temperatures and *Acropora* white syndromes on the Great Barrier Reef where Winter Conditions of 2.5–6.5 °C-weeks were associated with higher disease abundance (Heron et al., 2010). Also consistent with *Acropora* white syndrome on the GBR (Heron et al. 2010), few or no Cold Snaps were associated with high disease prevalence, possibly

suggesting the pathogenic bacteria that cause *Montipora* white syndrome may have a lower likelihood of survival during very cold winters.

The model results indicated unexpected relationships between disease prevalence and Hot Snaps and host (*i.e.*, *Montipora*) density. The Hot Snap metric had a non-linear relationship with disease prevalence. Similar to *Acropora* white syndrome, there was an association between Hot Snaps above 2 °C-weeks and higher disease prevalence. In contrast to *Acropora* white syndrome however, high disease prevalence was also associated with Hot Snaps less than 1.3 °C-weeks. This relationship may help explain why several *Montipora* white syndrome outbreaks have occurred during winter months in Hawai‘i (Figure 2.2). However additional factors not included in the study may be needed to better understand the seasonality of *Montipora* white syndrome such as increased rainfall and associated runoff. Surprisingly, disease prevalence increased as host density decreased with the highest disease prevalence at sites with <2.7 colonies m^{-2}. More studies are needed to further examine this relationship, however, this result may reflect host densities in locations with high disease prevalence events such as Kāne‘ohe Bay, O‘ahu, rather than real threshold host densities needed for disease establishment.

Porites Growth Anomalies

The model developed for *Porites* growth anomalies prevalence had the highest predictive performance where depth and colony density were the strongest drivers of

disease prevalence (Figure 2.3). The AUC value for the hierarchical *Porites* growth anomalies model was 0.85 and explained 41% of the deviance using the test data (Table 2.2). Given the high relative influence of site level characteristics in predicting disease prevalence, thermal stress is a relatively weak driver of disease and most likely to increase disease prevalence at sites in specific depth and host density ranges. Spatially explicit maps of such site level characteristics can be developed (and subsequently updated) to complement thermal risk assessments. There were negative relationships between both depth and colony density and disease prevalence, where shallower coral communities (<12.7 m) and lower colony densities were associated with higher disease prevalence. Although the relationship between shallower depths and *Porites* growth anomalies prevalence is currently unclear, one previous study determined that UV radiation does not explain this relationship (Stimson 2010). Within Kāneʻohe Bay, Oʻahu, Williams et al. (2010) found a negative relationship between coral cover and *Porites* growth anomalies prevalence; our study includes the Williams et al. dataset and suggests a similar relationship may exist across the entire archipelago. One possible explanation for the negative relationship between colony density and disease is that higher colony density often reflects a community of very small colonies, and *Porites* growth anomalies appear to be more common on larger corals (Couch et al. 2014).

Associations between *Porites* growth anomalies, Winter Condition, MPSA and Hot Snap (Figure 2.3) slightly improved predictive accuracy of the model. A bi-modal relationship exists between Winter Condition and disease prevalence where cold (<−5 °C-weeks) and warm (>8.8 °C-weeks) conditions were associated with higher disease prevalence.

There was a negative relationship between disease prevalence and both Mean Positive Summer Anomaly (MPSA) and Hot Snap, indicating high thermal stress is associated with lower disease prevalence. This combination of colder winters and mild summers compliments a prior study that found a negative association between *Porites* growth anomalies and average occurrence of anomalously warm temperature (WSSTA) over the four years prior to a survey (Aeby et al. 2011). This combination may also help explain the shorter-term seasonality associated with increased growth anomaly density and subsequent growth in the fall (Stimson 2010).

Porites Tissue Loss Syndrome

Host and coral density, depth, Winter Condition, MPSA and Hot Snap were important for predicting *Porites* tissue loss syndrome prevalence and this model explained the most deviance (Figure 2.3). The mean predictive accuracy for *Porites* tissue loss syndrome (AUC) was 0.67 and explained 44% of the deviance using the test data (Table 2.2). There was an interaction between host density, coral density and disease prevalence, in which sites with high coral density but lower host density were associated with the highest disease prevalence values. Disease prevalence was also highest in shallower water (<7 m). The Winter Condition metric shows a negative association between disease prevalence and cold temperature (<0.3 °C-weeks) and a positive relationship between disease prevalence and warm temperature (>4.4 °C-weeks). The Hot Snap metric above 2 °C-weeks supports a positive relationship between thermal stress and disease prevalence, also shown in the MPSA, however, the Hot Snap metric

<1.6 °C-weeks contradicts this pattern. Our conclusion is that our data are likely missing an important predictor variable for explaining tissue loss prevalence such as additional metrics of coral distribution, water quality, or subsurface temperature fluctuations.

Very little is currently known about the disease etiology of *Porites* tissue loss syndrome and the role of thermal conditions in influencing disease dynamics. The results here suggest extreme thermal conditions in the winter may contribute to coral susceptibility to disease, but more information is needed to build a robust predictive model. The bimodal relationship between thermal stress and disease could support one or two complimentary hypotheses about winter pre-conditioning and disease prevalence: (1) during anomalously warm winters pathogens do not undergo winter mortalities leading to higher densities of pathogenic organisms in the water column; and (2) thermal stress prior to the summer contributes to compromised host immune systems. Both hypotheses require further exploration.

Forecasting Disease Risk

To accurately predict coral disease risk in Hawai‘i, information on both coral distribution and thermal stress is needed. For all three diseases modeled in this study, thermal stress was only important for predicting disease risk in communities within a specific range of colony densities.

A fundamental principle of epidemiological theory is that there is a minimum population threshold for pathogen invasion and a critical community size required for disease persistence for diseases with density dependent transmission (Kermack and McKendrick 1927). While exact thresholds in wildlife populations are difficult to determine, identifying host distribution ranges around these thresholds, as we did here, can improve our understanding of disease dynamics (Lloyd-Smith et al. 2005) and therefore ability to forecast future outbreak events. For non-infectious diseases, where pathogens are endemic in the population and infection results from an imbalance in the host–pathogen relationship, variables besides host density may be important determinants of disease prevalence (Hawley and Altizer 2011). For example, in this study we found that depth was an important determinant of disease prevalence for *Porites* growth anomalies and tissue loss syndrome. Depth may be an important predictor of coral disease in Hawai‘i because shallower sites are often exposed to greater environmental stress such as nutrient runoff, pollution, salinity changes, increased UV radiation and destructive human activities (e.g., spearfishing). Incorporating size-frequency distributions into future models may also improve predictive accuracy as disease susceptibility often varies with size and/or age structure, such as in the relationship between the fungal pathogen *Aspergillus sydowii* and its sea fan coral host *Gorgonia ventalina* (Dube et al. 2002).

Winter Conditions were strong predictors of all three coral diseases, highlighting the importance of winter pre-conditioning of hosts and pathogens for disease onset and making it possible to evaluate disease risk several months before an expected

outbreak. Warm winter temperature was an indicator of increased disease risk for all three diseases, whereas cold winter temperatures appeared to lower the risk for *Montipora* white syndrome, but not for *Porites* growth anomalies or tissue loss syndrome. High thermal stress in the summer indicated an increased likelihood of *Montipora* white syndrome and *Porites* tissue loss syndrome; however, more information is needed to better understand these relationships at lower levels of thermal stress (i.e., Hot Snaps <2 °C-weeks) given the nonlinear relationships displayed in partial dependence plots (Figure 2.3).

Uncertainties, Errors and Accuracies

Modeling host–pathogen–environment relationships has led to interesting insights into the relationships between coral disease, host distributions, and thermal stress; however, many aspects of how environmental stressors drive coral diseases still remain uncertain. For all three diseases modeled here, the presence-absence models had lower predictive accuracy than the prevalence-if-present models (indicated by the several-fold higher cross-validation deviances). The lower predictive accuracy of the presence-absence models suggests more information is needed to differentiate sites with and without disease. Given that low background levels of disease are natural in all populations, environmental conditions may not differ between places with no visible disease and those with very low levels of disease prevalence. While our results suggest these models can provide an early and good first approximation of expected levels of

disease prevalence prior to a disease event, additional environmental information could improve model accuracy.

Several studies have shown relationships between water quality (e.g., turbidity, chlorophyll *a* concentration, sedimentation, nutrient pollution) and disease prevalence (Williams et al. 2010; Haapkyla et al. 2011; Vega Thurber et al. 2013; Ban, Graham, and Connolly 2014) and incorporating such predictor variables could improve disease predictions. Remotely sensed ocean color metrics may provide a useful tool to account for broad scale variation in water quality. However, ocean color metrics require further development and validation for shallow, coastal habitats and would need surface-measured data to validate and/or complement such a study. The relationships with temperature identified here for three diseases can provide the basis for the development and delivery of monitoring tools that can help managers now and can subsequently guide further evaluation of temperature-disease relationships along with those of other environmental parameters.

Conclusions

Coral diseases arise from dynamic interactions between host, pathogens and their environment. Climate change is altering these interactions and thus increasing the magnitude and severity of outbreaks worldwide. Modeling efforts such as the one described here help elucidate environmental drivers of disease and may provide risk assessments for future disease outbreaks months before an expected event. Using a

combination of methods used for forecasting *Acropora* white syndrome outbreaks on the Great Barrier Reef and white-band disease on *Acropora* in the Caribbean (Heron et al. 2010; Randall and van Woesik 2015), we were able to develop separate predictive models for *Montipora* white syndrome, *Porites* growth anomalies, and *Porites* tissue loss syndrome in Hawai‘i using boosted regression trees. Our research highlights the need for disease- and regionally-specific models given the differences among the models for each host–pathogen relationship and between models developed for Hawai‘i and Australia. One reason seasonal thermal stress may be less influential for coral diseases in Hawai‘i compared to the Great Barrier Reef is that SST stress is ameliorated through flushing of near shore waters with deep oceanic water found close to shore and through high wave energy found at many locations in Hawai‘i (Gove et al. 2013).

As the frequency of extreme temperature events continues to increase in Hawai‘i, forecasting models of temperature-driven diseases will become increasingly useful to resource managers and scientists alike. Before 2014, the Main Hawaiian Islands had only experienced one severe thermal stress event that resulted in mass coral bleaching (Jokiel and Brown 2004). Now mass bleaching events have occurred in two consecutive years as a result of thermal stress (NOAA Coral Reef Watch Report 2014a; Department of Land and Natural Resources 2015). This study has confirmed that Coral Reef Watch’s Experimental Coral Disease Outbreak Risk product for the Hawaiian archipelago (http://coralreefwatch.noaa.gov/satellite/disease_haw/dz_hawaii.php) provides valuable insights that can be used by local managers, but the addition of other

biotic and abiotic factors could increase predictive accuracy of the forecasts, which currently still produce some false positives and negatives. In addition to the SST metrics and biotic factors used in these models, other biotic and abiotic factors such chlorophyll-*a* concentration should be assessed to better understand coral susceptibility to disease and increase model predictive capabilities. The models we developed for *Montipora* white syndrome, *Porites* growth anomalies and *Porites* tissue loss syndrome can improve the capacity of local managers to prepare for and respond to disease outbreaks in Hawai‘i several months before an expected outbreak event. This may be especially useful for monitoring remote locations such as coral reefs in the Papahānaumokuākea Marine National Monument.

Table 2.1 Host distribution and environmental predictor variables used in boosted regression trees.

Variable	Type	Description and Unit	Min	Max
Total coral abundance	Biotic	Number of colonies/survey	20	2633
Total coral density	Biotic	Number of colonies/m^2	0.15	52.4
Porites density	Biotic	Number of colonies/m^2	0.02	9.49
Montipora density	Biotic	Number of colonies/m^2	0.02	8.4
Depth	Abiotic	Meters below sea surface	<1	24.5
Winter Condition	Abiotic	Accumulation of positive and negative thermal anomalies; °C-weeks	−10.162	21.465
Cold Snap	Abiotic	Magnitude and duration of cold stress; °C-weeks	−5.0255	0
MPSA	Abiotic	Mean number of degree heating days in summer; °C	0	0.78077
Hot Snap	Abiotic	Magnitude and duration of heat stress; °C-weeks	0	11.02

Table 2.2 Optimal setting and predictive performance of boosted regression tree analyses for three coral diseases. Models: PA: Presence-Absence; PIP: Prevalence-If-Present; *nt*: number of trees; *tc*: tree complexity; *lr*: learning rate; bf: bag fraction; cv dev: cross-validation deviance; SE: standard error; AUC: area under the operating curve; D: predictive deviance of the final BRT model. Large AUC values indicate higher performance models.

Coral Disease	Model	*nt*	*tc*	*lr*	bf	cv dev	se	AUC	D
Montipora white syndrome	PA	3500	5	0.001	0.75	0.262	0.036	0.70	0.30
	PIP	1400	4	0.001	0.75	0.113	0.086		
Porites growth anomalies	PA	1350	4	0.005	0.75	1.061	0.031	0.85	0.41
	PIP	1900	5	0.005	0.75	0.048	0.005		
Porites tissue loss	PA	750	3	0.005	0.75	1.213	0.027	0.67	0.44
	PIP	2700	4	0.005	0.75	0.33	0.004		

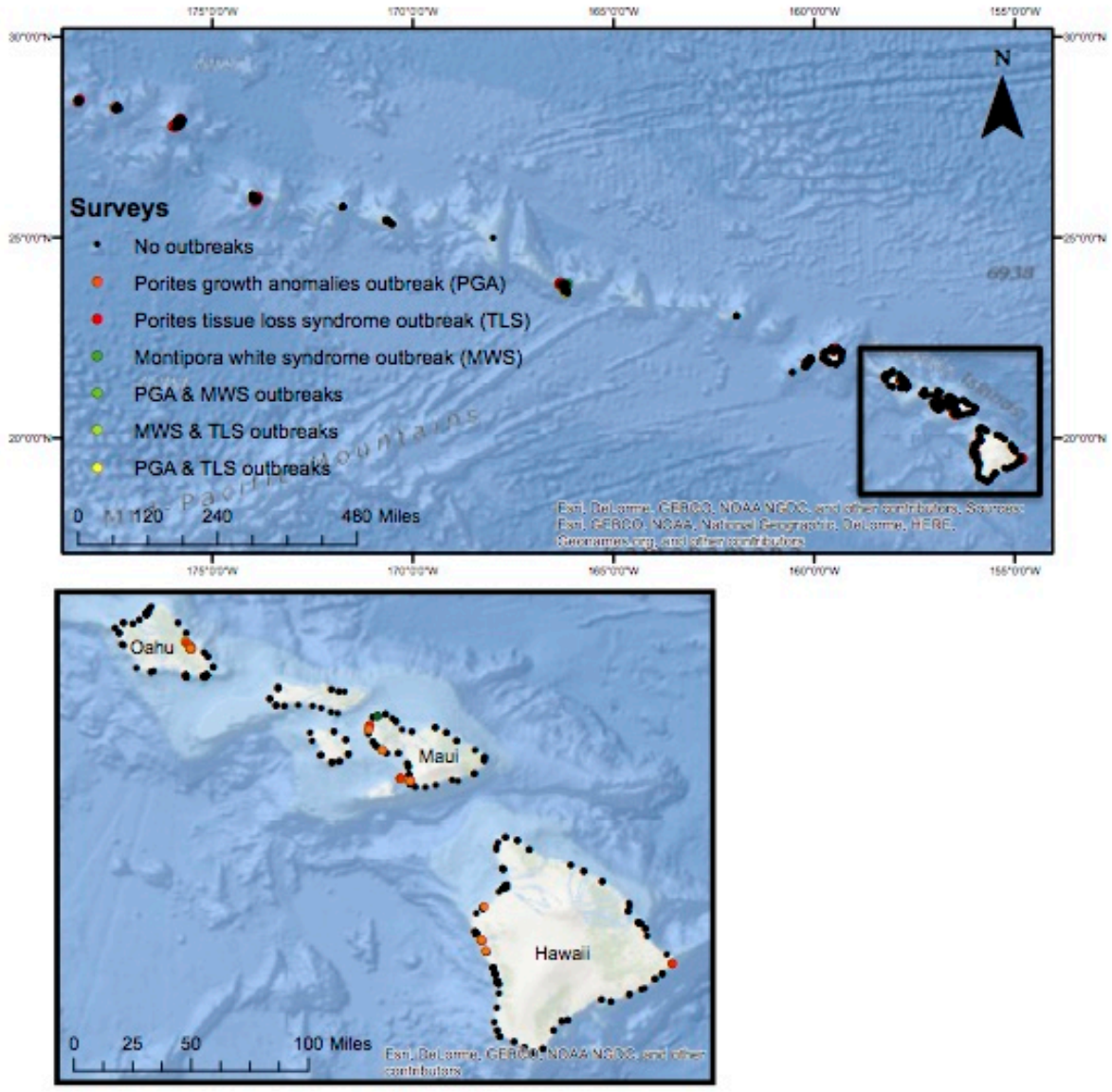

Figure 2.1 Map of disease surveys in the Hawaiian archipelago. Survey locations (dots) between 2004 and 2015 were along the extent of the archipelago. Colored dots indicate locations where an outbreak occurred.

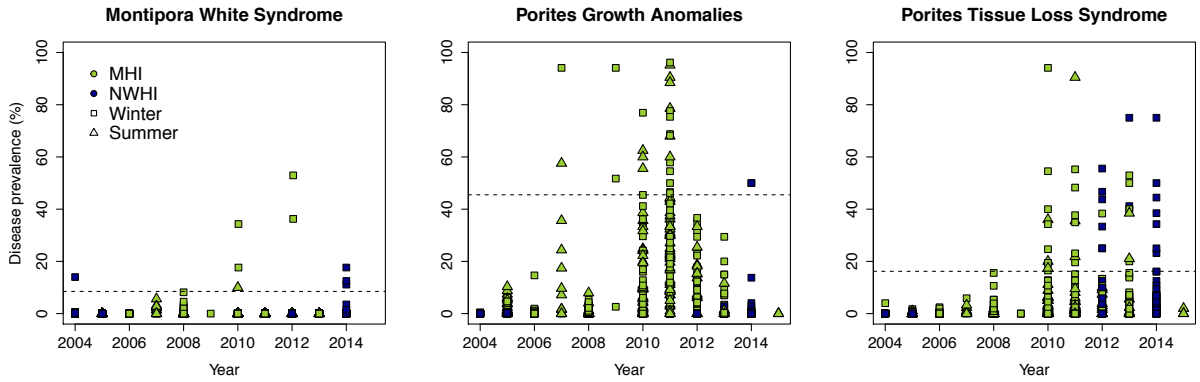

Figure 2.2 Disease prevalence by disease, year, season and region. Scatterplots of *Montipora* white syndrome, *Porites* growth anomalies and *Porites* tissue loss syndrome prevalence through time. Dashed horizontal lines represent outbreak thresholds determined by the iterative analysis described in the methods. MHI: Main Hawaiian Islands; NWHI: Northwestern Hawaiian Islands. Winter includes surveys conducted in November–April; summer includes surveys conducted in May–October.

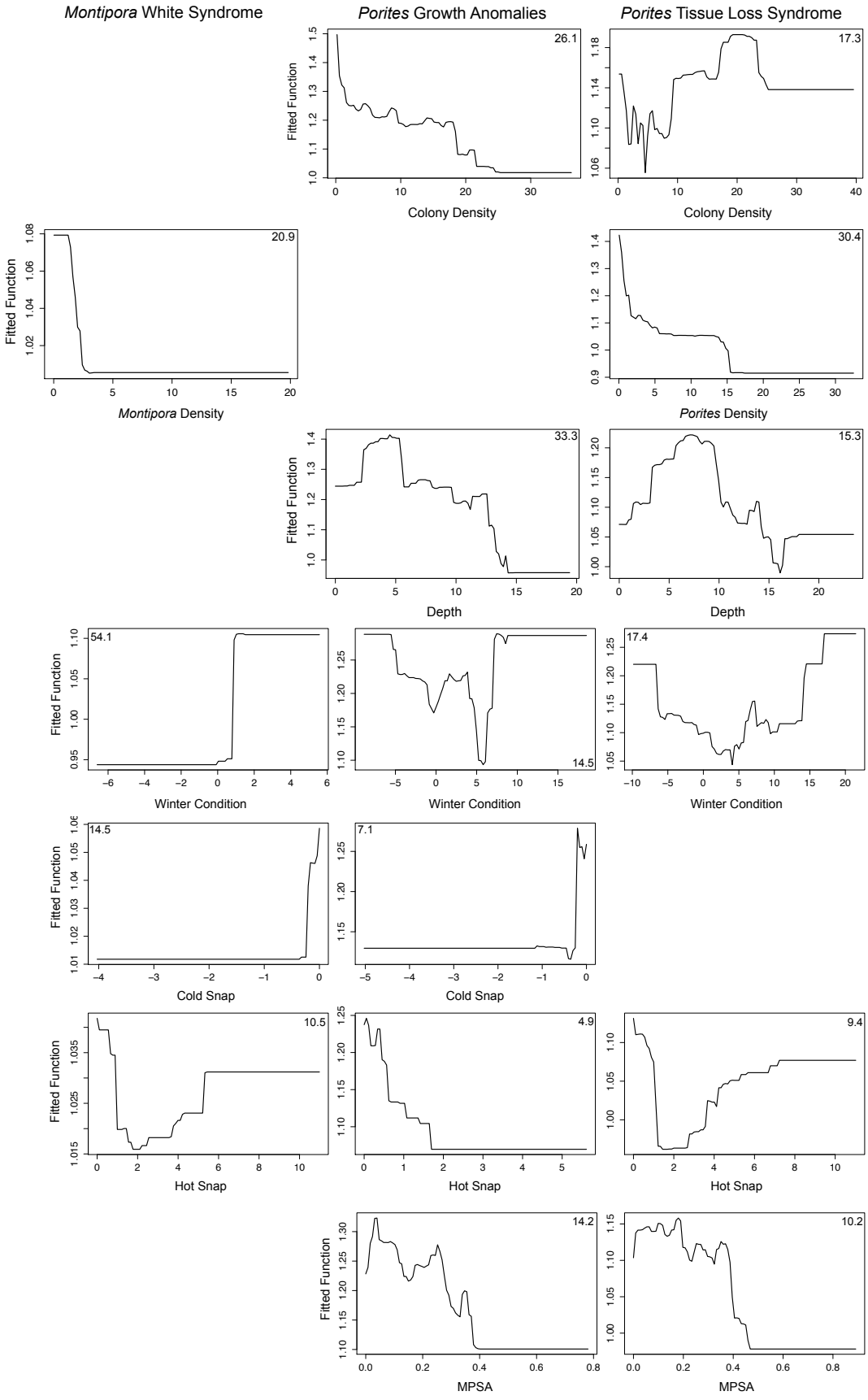
Montipora White Syndrome
Porites Growth Anomalies
Porites Tissue Loss Syndrome
Fitted Function
Colony Density
Montipora Density
Porites Density
Depth
Winter Condition
Cold Snap
Hot Snap
MPSA
26.1
17.3
20.9
30.4
33.3
15.3
54.1
14.5
17.4
14.5
7.1
10.5
4.9
9.4
14.2
10.2

Figure 2.3 Partial dependence plots relating coral disease prevalence to demographic and thermal predictor variables for prevalence-if-present models. Plots show the probability of disease prevalence across a range of values for the predictor variable, while accounting for the average effects of all other variables in the model. Models were developed with a randomly chosen 75% of the dataset and were tested using the 25% withheld. Relative influence of each predictor variable is shown as a percentage in a corner of each graph. We did not incorporate non-informative predictors, which were determined using the R function gmb.simplify, and therefore we do not show partial dependence plots for those variables (blank spaces). Host density is specified by genus (i.e., *Montipora* or *Porites* density). MPSA is Mean Positive Summer Anomaly.

CHAPTER 3

HABITAT COMPOSITION AND ENVIRONMENTAL CONDITIONS DRIVE VARIATION IN CORAL DISEASE PREVALENCE IN HAWAIʻI

To be submitted as:

Caldwell J, Aeby G and Donahue M. 2017. Habitat composition and environmental conditions drive variation in coral disease prevalence in Hawaiʻi for submission to Diseases of Aquatic Organisms.

Abstract

Coral diseases are a major conservation threat, yet we have a limited understanding of natural and human-influenced variation in disease risk. In this study, we demonstrate that interacting biotic and environmental conditions affect coral disease risk and these relationships vary by disease type. We investigated disease risk for tissue loss diseases and growth anomalies in *Montipora* and *Porites* in the Hawaiian archipelago, where there is a natural gradient of habitats and human influence. Using a hierarchical modeling approach, we found that the majority of variation could be explained at local scales (survey site and sector of coastline). All disease types were associated with host density, indicating the importance of relatively static conditions associated with disease risk. Habitat composition was more closely associated with disease risk for growth anomalies compared to tissue loss diseases for both genera, likely because growth anomalies are chronic diseases. All four diseases were associated with different water quality metrics (e.g., chlorophyll-*a*, terrestrial runoff), highlighting the importance of watershed health on disease risk. Interestingly, the effect of rainfall anomalies on *Montipora* tissue loss disease risk varied across islands, potentially indicating the importance of stream channelization for this disease. We also found a positive association between *Porites* tissue loss disease risk and fish abundance suggesting fish are potential disease vectors of this disease. For *Porites* growth anomalies, we found that the effect of human population on disease risk varied across islands, likely indicating that human behavior, rather than density alone, affects disease risk.

Introduction

Coral diseases in the Indo-Pacific are considered one of the biggest global conservation issues (Sutherland et al. 2015). Coral disease outbreaks have been a major contributor to reef declines worldwide, first in the Caribbean and more recently in the Indo-Pacific (e.g., Aronson and Precht 2001; Miller et al. 2009; Williams et al. 2011; Hobbs et al. 2015), often resulting in loss of functional and structural integrity of coral reefs (Hughes et al. 2007; Alvarez-Filip et al. 2009). Coral diseases have been recorded in remote and protected areas (e.g., Aeby et al. 2003; Hobbs et al. 2015), suggesting that disease may arise in certain types of physical environments, such as semi-enclosed bays, and/or from global anthropogenic stress. However, diseases are more common in populated regions, suggesting that human activities increase disease risk above some natural threshold. Both natural gradients in environmental conditions and variation in human-induced stressors contribute to differences in disease prevalence across local (e.g., survey site, section of coastline) and regional (e.g., island, archipelago) spatial scales.

Diseases can shift between endemic and outbreak states, often in response to both natural and human-induced environmental variability. Previous studies have demonstrated links among increased disease prevalence, progression, and severity, anomalously warm ocean temperatures and poor water quality for a variety of coral diseases (Sutherland, Porter, and Torres 2004; Vega Thurber et al. 2013; Haapkylä et al. 2007; Ban, Graham, and Connolly 2014; Sheridan et al. 2014). Increased seawater temperature can increase pathogen growth rates and reduce coral resistance to disease (Ben-Haim and Rosenberg 2002; Cervino et al. 2004; Ward, Kim, and Harvell 2007;

Frydenborg et al. 2013), while terrestrial runoff and sediments associated with poor water quality can serve as pathogen reservoirs (Sheridan et al. 2014). While exposure to stressful conditions can increase disease risk, reducing stress exposure can decrease disease risk. For example, experimental evidence indicates that improving water quality, even after long periods of chronic exposure, can reduce disease prevalence (Vega Thurber et al. 2013).

Coral diseases vary in their mortality rates, endemic disease prevalence levels, and tendency to cause outbreak events. There are three major types of coral diseases in the Indo-Pacific that are categorized based on their disease lesion appearance: diseases that cause 1) tissue loss, 2) discoloration, and 3) growth anomalies. Tissue loss diseases of unknown etiologies (white syndromes) usually have very low endemic prevalence levels but they are often associated with rapid outbreak events resulting in localized mass mortality (George Roff et al. 2011; Aeby et al. 2010; Hobbs et al. 2015; Chapter 4). Tissue loss diseases with known etiologies that can be diagnosed in the field (e.g., Black Band Disease, Brown Band Disease, Skeletal Eroding Band) are common in many parts of the Indo-Pacific and they are associated with outbreak events that usually cause partial colony mortality (Sutherland, Porter, and Torres 2004). Discoloration refers to a broad range of coral diseases that vary in prevalence across regions and rarely cause outbreak events; little is known about their etiology and host effects. Growth anomalies are common, long-lasting diseases (Sutherland, Porter, and Torres 2004; Aeby et al. 2011) that can cause reduced growth and fecundity (Sutherland, Porter, and Torres 2004; Stimson 2010; Burns et al. 2011). In this study,

we investigated drivers of tissue loss diseases and growth anomalies in two dominant reef-building genera in the Hawaiian archipelago, *Montipora* and *Porites,* because they are widespread and represent acute and chronic diseases that have high and low mortality rates respectively.

Tissue loss diseases, or white syndromes, are among the most widespread and destructive types of coral disease. Tissue loss diseases have been recorded in several species of coral in the family Acroporidae and Poritidae across the Indo-Pacific (George Roff et al. 2011; Aeby et al. 2010), and, in some cases, have significantly reduced coral cover and community composition (e.g., Hobbs et al. 2015). This suite of diseases is characterized by gradual to rapid tissue mortality as the disease front progresses across the colony, often killing colonies in a few weeks. Multiple studies have linked tissue loss diseases to a variety of bacterial pathogens (Cervino et al. 2004; Cohen et al. 2012; Ushijima et al. 2014). Several studies have also demonstrated that increased tissue loss disease prevalence is strongly correlated with high coral cover and increased ocean temperatures (Bruno et al. 2007; Heron et al. 2010; Maynard et al. 2011).

Growth anomalies are another widespread disease affecting at least 16 different coral species across the Indo-Pacific (Sutherland, Porter, and Torres 2004). Growth anomalies are chronic, protuberant masses of coral skeleton (i.e., tumors) that do not cause rapid mortality, but do have a number of deleterious effects including reduced growth, fecundity, and overall survival (Sutherland, Porter, and Torres 2004; Stimson 2010; Ruiz-Moreno et al. 2012). In Hawai‘i, growth anomalies typically appear during

the summer with subsequent growth in the fall (Stimson 2010). This disease can be more common on larger colonies than smaller colonies (Couch et al. 2014), potentially indicating a relationship between growth anomaly formation and age or chronic stress. Growth anomalies can be found in shallow water (<3 m) (Stimson 2010), in association with sewage outfall (Kaczmarsky 2006), and are strongly correlated with human population size (Aeby et al. 2011).

In this study, we expand upon several coral disease studies that have been conducted in the Hawaiian Islands (Williams et al. 2010; Couch et al. 2014; Aeby et al. 2010; Aeby et al. 2011; Aeby et al. 2016) by using a more spatially and temporally comprehensive dataset to assess correlative relationships between disease risk and hypothesized disease drivers that have not been previously tested in Hawaii or elsewhere.

Hypotheses

For each of the four diseases we examined in this study (*Montipora* tissue loss disease, *Porites* tissue loss disease, *Montipora* growth anomalies, *Porites* growth anomalies), we tested specific hypotheses regarding biotic and environmental drivers of disease based on known relationships from the literature. However, we included host size and density in all models because these metrics are commonly associated with disease risk across a variety of disease types and taxa (e.g., Groner et al. 2014; Eisenlord et al. 2016; Aeby et al. 2011). Host size may indicate exposure time to chronic stress or age, while host density is an important factor for density-dependent disease transmission (McCallum et al. 2001). In this study, we refer to host density as congeneric density because we pooled observations to the genus level.

Tissue loss diseases in Montipora

Outbreaks of tissue loss diseases in *Montipora* often appear in the winter months (i.e., the rainy season) in semi-enclosed reef systems (Aeby et al. 2016; Ross et al. 2012) and have been linked to temperature-dependent bacterial pathogens (Ushijima et al. 2012; Ushijima et al. 2014; Ushijima et al. 2016). Based on these known relationships, we hypothesized that coral disease risk is associated with seasonal temperature and rainfall variation, stream exposure, chlorophyll-*a*, embayments and wave energy (Table 3.2). Since the amount of rainfall that reaches any given coral reef is dependent upon the topography, watershed area, and soil permeability, we hypothesized that the effect of rainfall on disease risk could vary by island. We opted to model this relationship exclusively for the main Hawaiian Islands because *Montipora* tissue loss diseases are primarily found in the main Hawaiian islands and rainfall dynamics differ dramatically between the main Hawaiian Islands (high islands) and the low lying northwestern Hawaiian islands, which are primarily atolls and have no streams.

Tissue loss diseases in Porites

Despite the wide distribution of *Porites* tissue loss disease throughout the Hawaiian archipelago (Aeby et al. 2011), little is known about its pathogenesis; therefore, we made hypotheses about disease risk based on the behavior of tissue loss diseases in other coral species (such as *Montipora spp.*) and personal observations. Similar to *Montipora* tissue loss diseases, we hypothesized that *Porites* tissue loss diseases were associated with temperature variation, water quality, water motion and embayment. In

addition, we hypothesized that *Porites* tissue loss disease is related to depth and herbivorous fish abundance. Depth indirectly relates to sunlight exposure, which under optimal conditions is vital for coral's intracellular algae to photosynthesize (reviewed in Roth 2014). Sunlight exposure can also be harmful in cases of excessive sunlight or under exposure (reviewed in Roth 2014). Herbivorous fish abundance could be positively or negatively correlated with disease risk based on direct or indirect relationships. For instance, herbivorous fish consume algae on coral, which could directly control bacterial populations on the algae itself, or indirectly control macroalgae overgrowth (Hughes et al. 2007) relieving mechanical stress on coral. At the same time, fish may be vectors of pathogenic organisms, excreting them directly on coral surface tissue. Another alternatively hypothesis is that sites with specific fish community compositions also have higher or lower disease risk due to some latent variable, indicating an indirect relationship between fish abundance and disease risk even if there is no causal relationship.

Growth anomalies in Montipora and Porites

Growth anomalies are chronic diseases that can be associated with host density and human population sizes. We were interested in further investigating how community composition and human populations influence disease risk. Thus, in addition to host density and human population within 20 km of the coastline, we hypothesized that growth anomalies were related to wave energy, total colony density, and land-based sources of pollution. Wave energy can indirectly relate to coral species composition (Franklin, Jokiel, and Donahue 2013). We analyzed three measures of land-based

sources of pollution: agriculture and golf runoff, new coastal development and urban runoff. We used the same hypotheses for growth anomalies in *Porites* and *Montipora* because 1) the disease lesions are similar, and 2) *Porites* growth anomalies are well studied (Aeby 2009; Aeby et al. 2011; Williams et al. 2010; Stimson 2010; Couch et al. 2014), while little is known about *Montipora* growth anomalies.

Methods

Data sources

We compared coral health observations from belt transect surveys (average survey area = 10 m^2) in the Hawai‘i Coral Disease Database (HICORDIS; Caldwell et al. 2016; Figure 3.1) with predictor variables capturing potential biotic and abiotic coral disease drivers. For each survey, all coral species and diseases were recorded; however, not all coral species were present at all sites. Therefore, there were different numbers of observations and surveys for each host genus. There were 169,020 *Porites* colonies and 83,561 *Montipora* colonies observed from 1,058 surveys at 16 Hawaiian islands and atolls collected between 2004 and 2015 (Table 3.1). Predictor variables included biotic variables (e.g., colony size, host density) and abiotic variables (e.g., depth, stream exposure) (Table 3.2).

In order to assess disease variation associated with biotic and abiotic variables across varying spatial scales, we included predictor variables at the colony, survey and sector scales. At the colony scale, the only predictor was colony size, which was measured as the longest horizontal diameter of a colony (Table 3.2). If colony size was categorized

into a size class, we used the average colony size within that size class (e.g., for a size class of 0-5 cm we used a colony size of 2.5 cm). Only 37% of surveys in the HICORDIS database included colony size. At the survey scale, we used survey depth, congeneric and total colony density, chlorophyll-*a* anomalies, wave energy, temperature anomalies, land-based sources of pollution, rainfall anomalies, stream exposure, human population density and embayment as predictor variables (Table 3.2). At the sector scale, which refers to the section of coastline where the survey was conducted (Figure 3.1), we used fish abundance as a predictor variable. Fish abundance data was collected by the National Oceanic and Atmospheric Administration Coral Reef Ecosystem Program (NOAA CREP) and calculated as pooled estimates of herbivorous fish abundance per sector for all sectors within the Hawaiian archipelago between 2010-2012 (1-6 sectors/island; Heenan et al. 2014; Table 3.2).

Predictor variables at the survey scale were compiled from the HICORDIS database, NOAA, and the University of Hawai‘i. We calculated depth, total colony density and congeneric density from the HICORDIS database. Total colony density was calculated as the number of colonies divided by the survey area. Similarly, congeneric density was calculated as the number of colonies of a given genus divided by survey area. As a measure of water quality, we used maximum anomaly values of chlorophyll-*a* for each survey, which were calculated using a 30 m boundary around each island following the procedure used by Gove et al. (2013). We used long-term (2003-2013) maximum monthly mean values of chlorophyll-*a* from NASA MODIS satellite imagery with eight-day temporal and 4 km spatial resolution. To assess water motion at each survey

location, we used the maximum monthly mean of wave energy flux (kW m^{-3}; Gove et al. 2013) provided by NOAA CREP. We used three temperature anomaly metrics provided by NOAA Coral Reef Watch based on remotely sensed sea surface temperature data at ~4 km weekly resolution: Hot Snap, Cold Snap and Winter Condition. All three metrics measure the magnitude and duration of thermal stress. Hot Snap and Cold Snap metrics measure positive and negative conditions based on the three climatological warmest and coldest months, respectively, while Winter Condition measures positive and negative temperature stress over the winter months (Heron et al. 2011; Caldwell et al. 2016). To examine the role of human activities associated with disease risk, we used land-based sources of pollution data from the University of Hawai‘i (Lecky 2016). Agriculture and golf runoff was used as a proxy for pesticide and fertilizer discharge. New development was used as a proxy for new coastal construction, and urban runoff was used as a proxy for trash, household chemicals and oils produced per watershed. We used rainfall anomaly data from the Rainfall Atlas of Hawai‘i (Frazier et al. 2016), which was interpolated from rain gauge data, expert knowledge, radar observations, meteorological model simulations and vegetation data. Anomalies were calculated as the rainfall variation in any given month and year from the 1978-2007 mean (Frazier et al. 2016). We extracted rainfall anomaly values for the month prior to each survey at the nearest coastal location in ArcGIS. We calculated stream exposure (inverse polar distance between stream mouth and survey site) and inside/outside of embayment for each survey point in ArcGIS using watershed, stream, and coastline shapefiles from the State of Hawai‘i Office of Planning. Human population density within 20 km of coastline from each survey site was provided by NOAA CREP based on 2010 US Census Data.

Statistical analysis

To investigate the effect of different stressors on coral disease risk, we analyzed our dataset using a hierarchical modeling framework. The data are naturally hierarchical, with individual colony nested within survey, surveys within sectors, and sectors within island, with predictor variables (Table 3.2) included at the colony, survey, and sector levels. Year was included as an orthogonal (non-nested) random effect. We analyzed each disease individually, restricting the data to surveys where *Montipora* or *Porites* was present and using only predictor variables hypothesized to affect disease risk for each disease.

For each disease, we modeled the probability of any given coral colony exhibiting disease signs using a multilevel logistic regression. Resolving the response variable at the colony scale allows the model to incorporate predictors at the colony scale (here, colony size), and accounts for the variation in observation effort among surveys that arise from different survey methodologies as well as the local density of congeneric colonies. In the equation below, y_i is the health state of the ith colony observation, which equals 0 if the colony is healthy and 1 otherwise. The inverse logit function is used to scale the probability of disease based on a set of predictor variables between 0 and 1. $\beta_{0.survey}$, $\beta_{0.sector}$ and $\beta_{0.island}$ are intercepts that vary by number of surveys, k, number of sectors, l, and number of islands, m, respectively. β, δ and λ are coefficients for predictor variable(s) at the colony (β), survey (δ), and sector (λ) scales. β corresponds to the coefficient for colony size, which is then multiplied by each observation of colony size, x_i. δ is the vector of coefficients at the survey scale multiplied by matrix H_k of

survey-scale predictors (e.g., coral density, depth, temperature anomalies; see Table 3.2). λ is the vector of coefficients at the sector scale multiplied by z_l observations of sector level predictors (fish abundance). α_{year} is the random intercept included for year, and σ^2_{year}, σ^2_{survey}, σ^2_{sector} and σ^2_{island} are the variances associated with the random intercepts at each scale.

$$\text{Prob}(y_i = 1) = logit^{-1}(\beta^{0.survey}_{k[i]} + \beta x_i + \alpha^{year}_{j[i]}) \qquad \text{Equation 3.1a}$$

$$\alpha_{year[j]} \sim N(0, \sigma^2_{year}) \qquad \text{Equation 3.1b}$$

$$\beta_{0.\text{survey}[k]} \sim \text{N}(\beta_{0.\text{sector}[k]} + \delta H_k, \sigma^2_{survey}) \qquad \text{Equation 3.1c}$$

$$\beta_{0.\text{sector}[l]} \sim \text{N}(\beta_{0.\text{island}[l]} + \lambda z_l, \sigma^2_{sector}) \qquad \text{Equation 3.1d}$$

$$\beta_{0.\text{island}[m]} \sim \text{N}(0, \sigma^2_{island}) \qquad \text{Equation 3.1e}$$

We created models for each disease iteratively, removing hierarchies and predictor variables that explained little variation in the dataset. We used AIC values to compare model fit (Table 3.3). We conducted all analyses in R statistical software using the lme4 package.

Results

Montipora tissue loss diseases

Montipora tissue loss diseases were positively associated with chlorophyll-*a*, stream exposure and the interaction between stream exposure and rainfall anomalies, and negatively associated with congeneric density and winter temperature variation (Figure 3.2A). Factors at the site scale explained 50.1 % of model variance. The effect of rainfall

on disease risk varied by island and the effect differed with stream exposure (Figure 3.4). Increasing chlorophyll-*a* by 1 mg m^{-3} corresponded to a 1 % increase in disease risk. Increasing the distance between a survey location and stream mouth by 1 % increased disease risk by 3.1 %. Increasing *Montipora* density by 1 colony m^{-2} corresponded to a 1.3 % decrease in disease risk. Increasing winter condition by 1 °C-wks corresponded with a 0.5 % decrease in disease risk. On Maui, Kaua‘i and Lānai there was a negative influence of rainfall on disease prevalence, in contrast to positive relationships for all other islands.

Porites tissue loss diseases

Porites tissue loss diseases were positively associated with herbivorous fish abundance, and chlorophyll-*a* and negatively associated with congeneric density, wave energy and depth (Figure 3.2B). There was no relationship between disease risk and host size, and, islands explained a negligible amount of model variance. A 1 % increase in fish abundance corresponded to a 1 % increase in disease risk. Increasing *Porites* density by 1 colony m^{-2} corresponded to a 1.7 % decrease in disease risk. A site with 1 % higher mean wave energy had a 1 % lower disease risk. An increase in chlorophyll-*a* and depth had negligible effects disease risk.

Montipora growth anomalies

Montipora growth anomalies were positively associated with host size, congeneric density and agriculture and golf runoff and negatively associated with total colony density (Figure 3.2B). Factors at the survey and sector scale explained the majority of

model variance. An 18 cm colony had a 1.8 % higher disease risk compared to a 17 cm colony. Increasing host density by 1 colony m^{-2} corresponded to a 6.6 % increase in disease risk whereas increasing total colony density by the same amount corresponded to a 18.4 % decrease in disease risk. Increasing agriculture and golf runoff in the watershed closest to the survey by 1 % corresponded to a 39.8 % increase in disease risk.

Porites growth anomalies

Porites growth anomalies were positively associated with depth, human population and congeneric density and negatively associated with total colony density (Figure 3.2D). There was no association between disease risk and host size. A 1 m increase in depth decreased disease risk by 3.1 %. Increasing the human population by 904 people per 20 km coastline (1 % increase) increased disease risk by 3.7 % Decreasing total colony density by 1 colony m^{-2} increased disease risk by 10.6 % while increasing *Porites* density by the same amount increased disease risk by 7.2 %. The effect of humans on coral disease risk differed by island: on Hawai‘i island, a 1 % increase in human population had a 21 % increase in disease risk, while on Ni‘ihau the same increase in human population decreased disease risk by 2 %.

Discussion

Relationships among disease risk, host size and congeneric density differed across disease types, likely reflecting differences in disease etiologies. Surprisingly, we only found a correlation between disease risk and host size for *Montipora* growth anomalies.

This result was unexpected, especially for *Porites* growth anomalies, where a previous study found that higher disease prevalence was associated with shallow sites with above average mean colony size (Couch et al. 2014). Our study suggests the relationship found in Couch et al. (2014) may be specific to the study location (West Hawai‘i) rather than a direct relationship between host size and disease risk reflective of each disease’s etiology. The relationship between congeneric density and disease risk differed between tissue loss diseases and growth anomalies, but were consistent with previous findings (Aeby et al. 2011; Caldwell et al. 2016). This difference may reflect mechanistic differences in disease transmission between potentially non-infectious growth anomalies and infectious tissue loss diseases.

Montipora tissue loss disease risk was associated with temperature variation and water quality. We found that disease risk was related to mild to warm winter temperatures and rainfall, which likely reflects the increase in tissue loss diseases in winter months (Aeby et al. 2016). Rainfall and associated runoff variables (indicators of water quality) were also strongly related to disease prevalence. Chlorophyll-*a,* stream exposure and an interaction between stream exposure and rainfall anomalies were all positively associated with this disease (Figure 3.4). This result could suggest that terrestrial runoff and sediments from rainfall are potential pathogen reservoirs (Sheridan et al. 2014; Pollock et al. 2014) and/or could increase host susceptibility. Therefore, terrestrial runoff and sediments should be considered in future studies. The differential effect of rainfall across islands warrants further investigation as well. Our results show that increased rainfall anomalies were associated with lower disease risk on Maui compared to other

islands. This result may arise because of Maui's geography, aquifer or coastal development/channelization practices or from coastal-trapped plumes (Storlazzi et al. 2006). Alternatively, but not mutually exclusive, coral or fish community composition at survey sites in Maui may be less sensitive to anomalous rainfall.

Porites tissue loss diseases were associated with wave energy, depth, herbivorous fish abundance and chlorophyll-*a*. Locations with higher wave energy had lower disease prevalence, which could reflect several mechanisms for reducing disease risk, including: flushing of particulates, pollutants, and/or pathogens in the water column and fast removal of sediment from corals (reducing the need for coral to expend energy removing sediment themselves). These mechanisms could allow for differences in disease prevalence across sites with similar exposure to nutrient runoff. Interestingly, there was a positive relationship between fish abundance and disease risk. This positive relationship could mean that fish are a potential disease vector, a hypothesis that could be tested in future studies. Alternatively, sites that attract high abundances of herbivorous fish could also be favorable for pathogen persistence and/or increase coral susceptibility to disease. Finally, higher disease risk was associated with lower summer time heat stress. This relationship could arise because cooler conditions are stressful to the coral itself or because cooler temperatures are better for pathogen survival. Differential disease responses between *Montipora* and *Porites* may arise because of physiological differences in the two host genera. For example, *Porites* is a slow growing, stress tolerant species with a greater ability to withstand harsh environments compared to corals with more weedy and competitive life-history strategies (e.g., *Montipora*)

(Darling et al. 2012). Regardless of the underlying mechanism, heat stress can be a useful indicator for predicting tissue loss disease risk.

For both *Montipora* and *Porites*, disease risk for growth anomalies was associated with community composition. There were positive associations between disease risk and congeneric density suggesting that disease is more common in sites with higher host densities. We also found negative associations between disease risk and total colony density, which could suggest a relationship between greater species diversity and lower disease risk, but more studies are needed to test this hypothesis directly. This type of relationship could support the disease dilution hypothesis, where increased diversity dilutes disease transmission by increasing the number of dead-end hosts within an ecosystem (Johnson and Thieltges 2010). Alternatively, increased colony density could indicate a greater distance between congeneric colonies for the vector/virus/parasite to cross for successful transmission.

We found different relationships between growth anomalies disease risk for *Montipora* and *Porites* and human populations. Interestingly, *Montipora* growth anomalies were associated with agriculture and golf runoff, which is a proxy for nutrients from fertilizers, pesticides and herbicides. Such toxins have been shown to increase rate of disease, deformities, and tumors in several fish species (reviewed in Islam and Tanaka 2004) and cause mortality in harbor porpoises (Kennedy et al. 1999) and may similarly increase coral susceptibility to disease, lending support for management actions that reduce fertilizer and pesticide use in coastal areas. For *Porites* growth anomalies

however, none of the land-based sources of pollution metrics could explain the relationship between human population density and disease risk. We did find the effect of human population on disease risk varied across islands for *Porites* growth anomalies. This response potentially demonstrates that it is not just the presence of humans that affects coral health, but perhaps, the behavior of humans. Alternatively, this result could indicate that differences in coral community composition across islands respond differently to human populations. The differences we found between drivers of growth anomalies in *Montipora* and *Porites* suggest that while the lesion appearances in both diseases are similar, disease etiologies may be drastically different.

Our study demonstrates that disease risk for four different coral diseases are associated with interacting biotic and environmental conditions, which must be considered when developing management programs to support long-term coral reef health. For all the diseases we investigated, habitat composition (e.g., host size, density) was an important driver of disease prevalence. Habitat composition was more important for growth anomalies than the tissue loss diseases, likely because these two diseases have very different types of pathogenesis. Growth anomalies tend to be chronic diseases that last for years while tissue loss diseases can move quickly and outbreaks are likely triggered by anomalous environmental conditions. Finally, for all disease types, the majority of variation was associated with factors at the survey and sector scales, suggesting drivers of disease risk are localized within a watershed. Understanding specific disease drivers for each disease type at the appropriate scale is vital for developing effective monitoring and managing strategies for coral reef conservation.

Table 3.1 Coral disease observation data.

Data description	*Porites*	*Montipora*
Number of surveys	809	716
Number of surveys where growth anomalies was observed	380	90
Number of surveys where tissue loss was observed	370	78
Number of colonies observed	169,020	83,561
Number of colonies exhibiting growth anomalies	8,374	227
Number of colonies exhibiting tissue loss	1,726	370

Table 3.2 Predictor variable data. Summary data for colony, survey, and sector level predictor variables. Anomaly data are based on long-term site-specific climatological means.

Predictor variable	Description	Minimum value	Maximum value	Source
Colony size	Maximum diameter (cm)	<1	450	HICORDIS
Depth	Distance below sea surface (m)	0.6 m	26 m	HICORDIS
Porites density	Number of colonies per m^2	0.02	9.49	HICORDIS
Montipora density	Number of colonies per m^2	0.02	8.4	HICORDIS
Coral density	Number of colonies per m^2	0.15	52.4	HICORDIS
Survey year	Year of survey	2004	2015	HICORDIS
Chlorophyll *a*	Max anomaly (mg m^{-3})	0.0004	0.357	NASA MODIS
Chlorophyll *a*	Max monthly mean (mg m^{-3})	0.056	0.409	NASA MODIS
Wave energy	Max anomaly (kW m^{-1})	0.003	285.7	NOAA
Wave energy	Max monthly mean (kW m^{-1})	0.002	103.5	NOAA
Hot snaps	Magnitude and duration of heat stress (°C-wks)	0	11.02	NOAA
Cold snaps	Magnitude and duration of cold stress (°C-wks)	-5.03	0	NOAA
Winter condition	Accumulation of positive and negative thermal anomalies (°C-wks)	-10.2	20.5	NOAA
New development	Coastal building	0	0.42	University of Hawai‘i
Agricultural golf runoff	Nutrient and chemical discharge from agricultural land and golf courses	0	0.53	University of Hawai‘i
Urban runoff	Trash, chemicals and oil discharge	0	0.73	University of Hawai‘i
Rainfall	Monthly rainfall anomaly	0.04	4.35	Rainfall atlas
Distance to stream	Planar distance between survey site and stream mouth	0.0008	∞	Hawaii.gov
Human population density	Number of people living within 20km of coastline	0	605,764	US Census/ NOAA
Embayment	Semi-enclosed habitat	0	1	Hawaii.gov
Herbivore fish abundance	Estimate of herbivorous fish within a specified sector	0.05 gm^{-2}	0.42 gm^{-2}	NOAA

Table 3.3 Top two models for tissue loss diseases and growth anomalies in *Montipora and Porites.*

Montipora tissue loss disease							
Host density	Cold Snaps	Winter Condition	Rainfall anomaly	Chlorophyll-a anomaly	Stream distance	Stream x rainfall	AIC
-0.02	0.01	-0.01	Varied by island	0.008	0.03	0.02	-1332.6
0.03	-	-0.004	Varied by island	0.007	0.03	0.02	-1330.6
Porites tissue loss disease							
Host density	Depth	Wave energy	Fish abundance	Chlorophyll-*a* anomaly	Hot Snaps	-	AIC
-0.02	-0.001	-0.01	0.01	0.003	-0.03	-	-1678.5
-0.02	-0.001	-0.01	0.01	0.003	-	-	-1677.5
***Montipora* growth anomalies**							
Coral size	Host density	Colony density	Agriculture & golf runoff	-	-	-	AIC
0.18	0.18	-1.44	-0.44	-	-	-	1924.8
0.18	0.67	-1.84	3.98	-	-	-	1924
***Porites* growth anomalies**							
Depth	Colony density	Host density	Urban runoff	Population	-	-	AIC
-0.02	-0.09	0.04	-0.17	Varied by island	-	-	-424.25
-0.02	-0.09	-0.02	-	Varied by island	-	-	-422.71

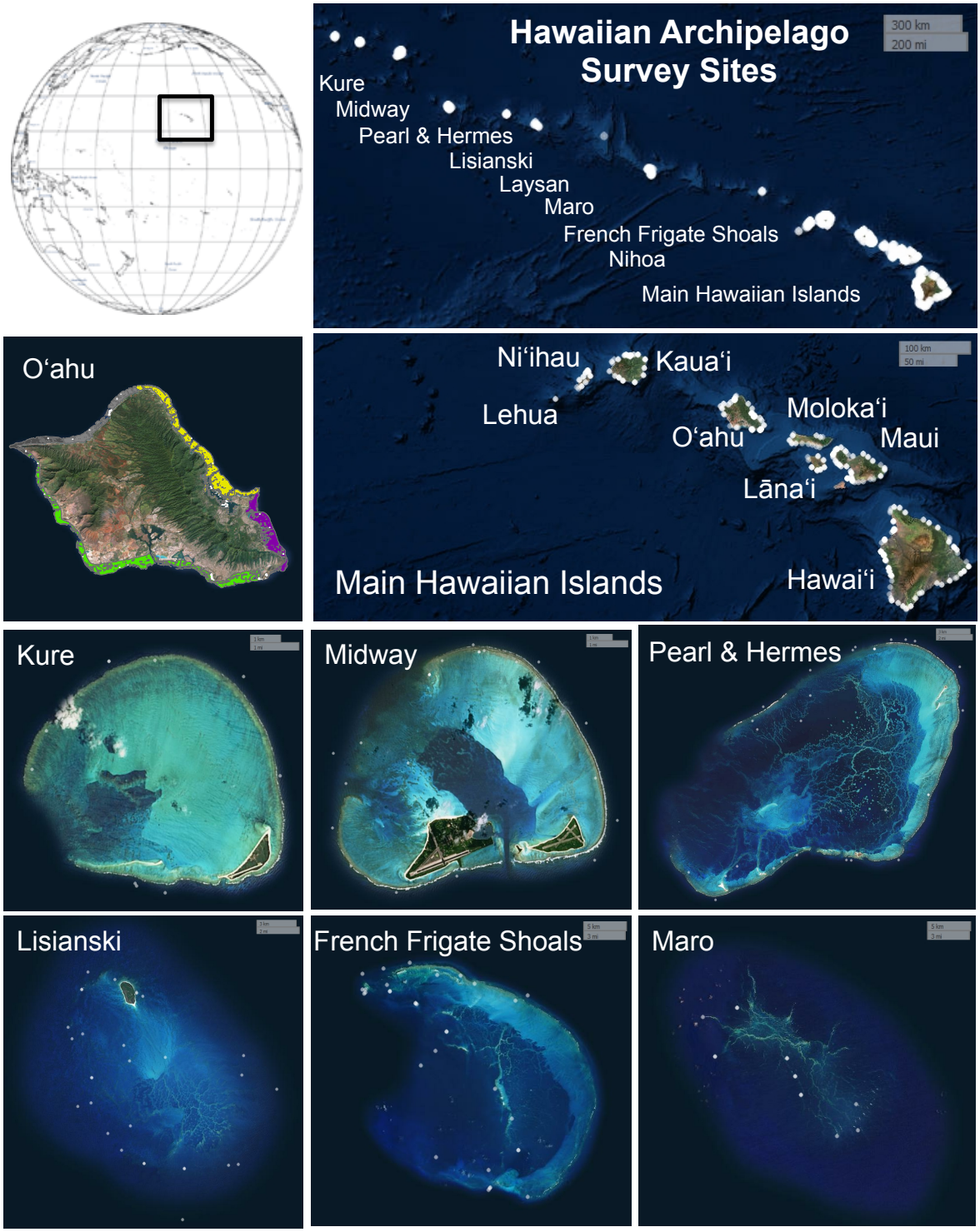

Figure 3.1 Map of survey locations. White dots indicate survey sites. Sites are nested within sectors (e.g., colored sections in O‘ahu subset) and sectors are nested within islands.

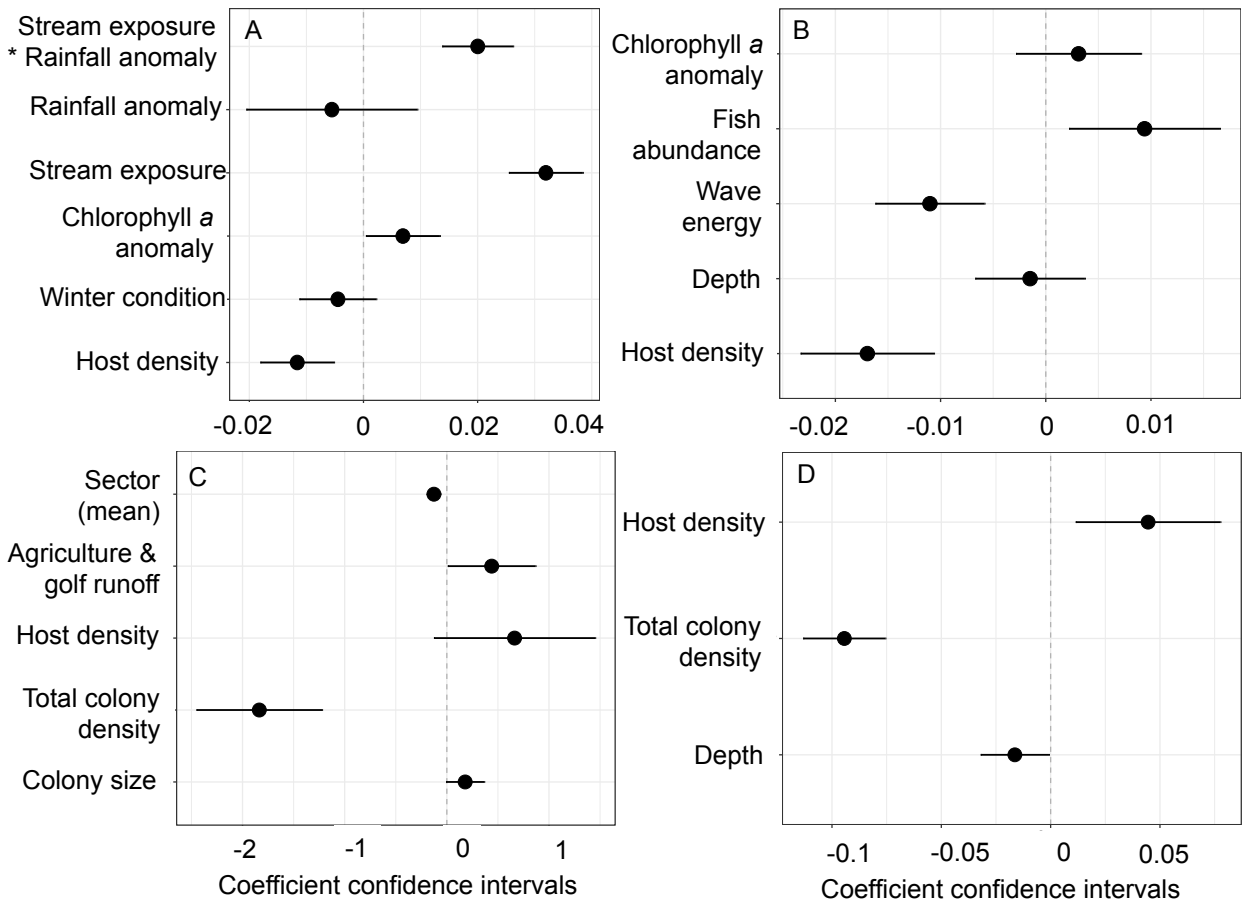

Figure 3.2 Coefficient plots for coral disease models. A) *Montipora* tissue loss disease, B) *Porites* tissue loss disease, C) *Montipora* growth anomalies and D) *Porites* growth anomalies.

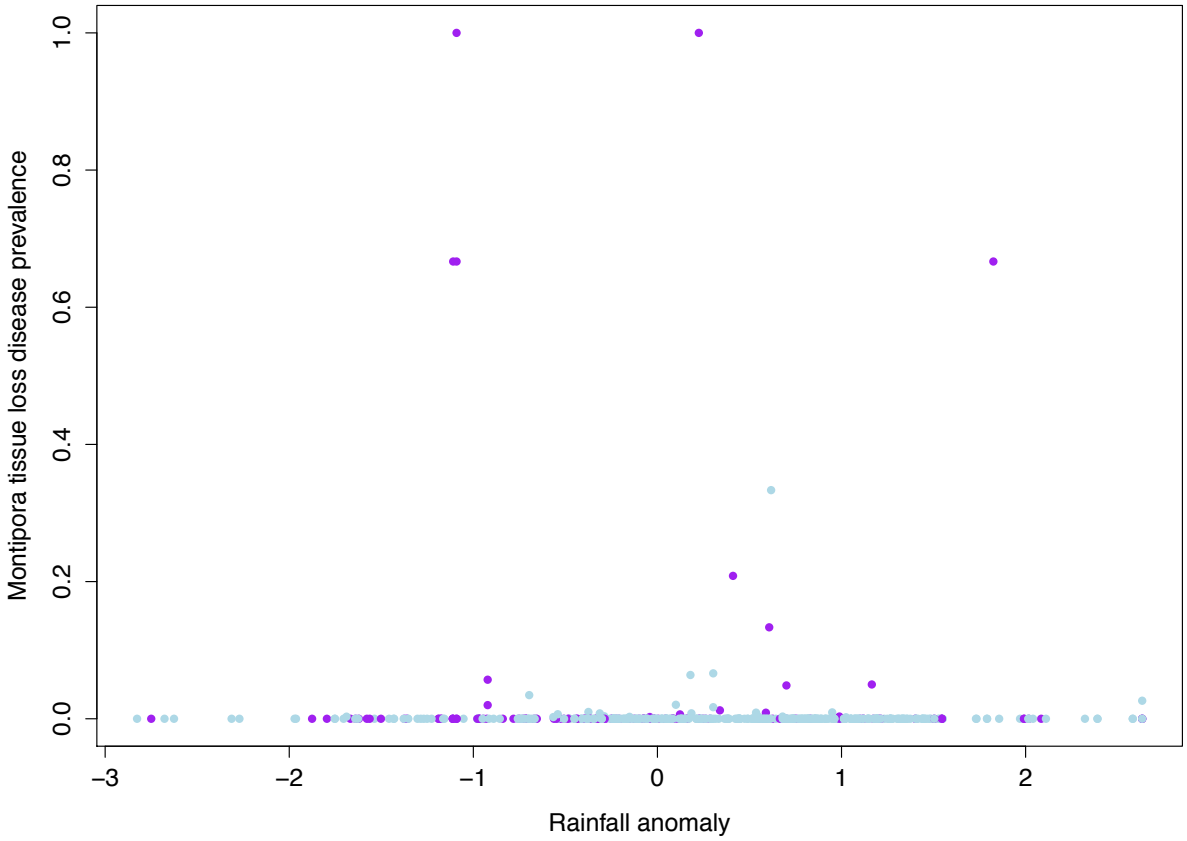

Figure 3.3 Scatterplot of disease risk, rainfall anomaly and stream exposure. Blue dots indicate sites with low stream exposure (i.e., far from stream mouth) and purple dots indicate sites with high stream exposure (i.e., close to stream mouth).

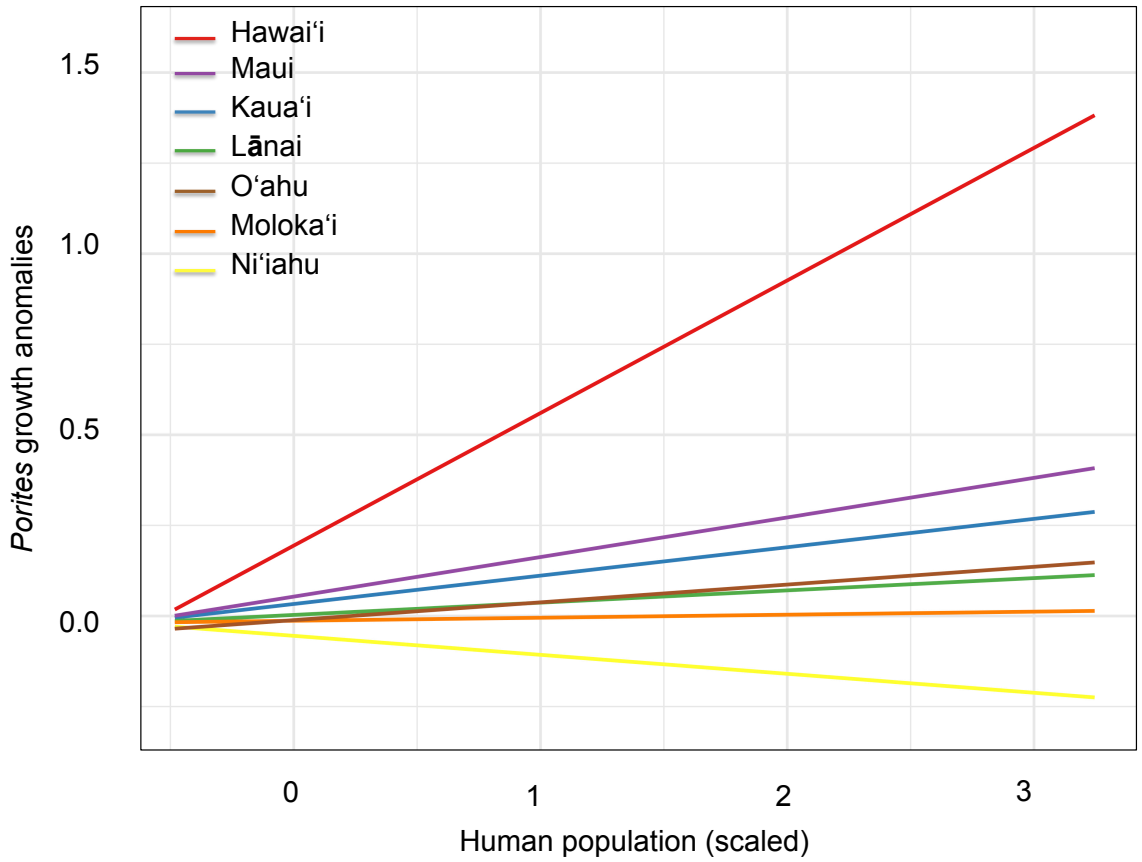

Figure 3.4 Effect of population size on *Porites* growth anomalies prevalence by island. Hawai‘i Island is indicated by the red line, Maui is indicated by the purple line, Kaua‘i is indicated by the blue line, Lānai is indicated by the green line, O‘ahu is indicated by the brown line Moloka‘i is indicated by the orange line, and Ni‘iahu is indicated by the yellow line.

CHAPTER 4

HOST TRAITS AND SEASCAPE ECOLOGY DRIVE THE SPREAD OF A MARINE DISEASE OUTBREAK

To be submitted as:

Caldwell J and Donahue M. 2017. Host traits and seascape ecology drive the spread of a marine disease outbreak to the journal Proceedings of the Royal Society B.

Abstract

We demonstrate that host and landscape heterogeneity drive the direction, duration and intensity of a marine disease outbreak. Understanding how disease risk varies over time and across heterogeneous landscapes is critical for managing disease outbreaks, but this information is rarely known for wildlife diseases. Here, we investigated how host and seascape heterogeneity influence disease risk and quantified key epidemiological parameters through time using a naturally occurring coral disease outbreak as a case study. We collected longitudinal health data for 200 coral colonies during the outbreak and found that disease risk increased with host size, severity of infected neighbors and number of infected neighbors. Disease risk increased by 2 % with every 10 cm increase in host size. Healthy colonies with high neighborhood severity (nearest three infected colonies had >75 % affected tissue) were 1.6 times more likely develop disease signs compared to colonies with moderate neighborhood severity (nearest three infected colonies had 25-75 % affected tissue). Disease transmission was highest within 15 m and this localized transmission may have contributed to the outbreak crashing as the local pool of susceptible individuals was depleted. We show that the per capita infection rate and the average number of secondary infections per individual varied through time (force of infection range: 0.007-0.02 newly infected corals per day; effective reproductive ratio range: 0.16-1.22) and peaked between days 6 and 11 of the study period. Our results provide estimates for rarely quantified time-varying epidemiological parameters for wildlife diseases. Furthermore, these outcomes indicate that marine disease transmission may be more spatially and temporally restricted than previously thought.

Introduction

Many aspects of terrestrial epidemiology do not apply to the ocean; therefore it is unclear whether the extent and rates of disease transmission in marine populations should be similar to their terrestrial counterparts. There are a few parallel modes of disease transmission in terrestrial and marine ecosystems such as pathogen dispersal via wind and ocean currents. At the same time, there are numerous transmission characteristics that differ between marine and terrestrial habitats. In the ocean for example, contact rates may be dependent on the movement of pathogens between hosts rather than rates of host-to-host contact (McCallum, Barlow, and Hone 2001). Theoretically, the openness and connectivity within marine populations may facilitate disease spread, while limited adult dispersal (long-distance dispersal typically occurs in planktonic larvae) may buffer marine populations from wide-scale disease spread (McCallum et al. 2004). Heterogeneity in host traits and habitat also affect the extent and rates of disease transmission, however, few studies have addressed how variation in body plans, life history traits, and landscape structure influence disease spread in the ocean. Coral reefs are an ideal marine ecosystem to test hypotheses about rates of disease transmission and factors that affect disease risk because coral colonies exist in discrete reef patches with variation in seascape configuration, composition and habitat quality.

For marine organisms, heterogeneity in host susceptibility to disease is influenced by traits such as genetics, immune capacity, and morphology. Some individuals are genetically predisposed to be more or less susceptible to disease, and this genetic

diversity has been shown to influence disease spread and severity in a variety of marine organisms from sea lions (Acevedo-Whitehouse et al. 2003) to brown algae (Gachon et al. 2009). Immune capacity also influences disease risk and can vary seasonally, with nutritional status, and during periods of reproduction and environmental stress (reviewed in Ellis et al. 2011). Morphology also affects disease risk. For example, host size has been associated with disease risk for sea fan aspergillosis (Bruno et al. 2011) and seastar wasting disease (Eisenlord et al. 2016). Functionally, the morphology of sessile and clonal marine invertebrates such as corals, sponges and bryozoans relates to high host genetic homogeneity which can enable build up of virulent pathogens and limited ability to ward off infectious agents relative to more mobile hosts (McCallum et al. 2004). Host heterogeneity may lead variation in disease spread over physical space resulting in patterns that reflect mechanistic processes underlying disease transmission.

Habitat configuration and composition also influence the spread and persistence of disease by increasing geographic connectivity or creating physical barriers preventing pathogen and/or host movement. On land for example, rivers and streams can act as semipermeable barriers to the movement of mammals affected by rabies (Smith et al. 2002) while serving as corridors for the spread of waterborne pathogens such as cholera and the Port Orford cedar tree pathogen, *Phytophthora lateralis* (Bertuzzo et al. 2010; Kauffman and Jules 2006). It is plausible therefore, that mosaic seascape habitats such as coral reefs, seagrass meadows and oyster reefs similarly affect disease spread in the ocean. A few studies have found relationships between coral reef configuration and clustering of diseased colonies, supporting different hypotheses about

modes of transmission specific to each coral disease (Jolles et al. 2002; Zvuloni et al. 2009; Lentz, Blackburn, and Curtis 2011; Zvuloni et al. 2015). In addition to habitat configuration, habitat composition can also influence disease risk as alternative hosts can act as pathogen reservoirs (sources) or sinks. However, the effect of alternative hosts is strongly dependent on the ability of a pathogen to multiply and transmit in both focal and non-focal hosts (Keesing, Holt, and Ostfeld 2006). Understanding the scale and affects of seascape heterogeneity on disease risk can be particularly valuable for diseases of management concern, where habitat manipulation can be incorporated into management programs.

The force of infection (FOI), or per-capita rate at which susceptible individuals acquire an infection, is a key parameter for quantifying how quickly and extensively a disease can spread through a population. FOI is used to estimate disease burden, effectiveness of intervention strategies, and related epidemiology parameters such as the basic reproductive ratio, R_0 (Hens et al. 2010). For example, French et al. (2013) compared FOI estimates to quantify the impact of national schistosomiasis control programs in several countries in sub-Saharan Africa. While previous approaches used models (e.g., the catalytic model; Muench 1934) to calculate time invariant values for FOI, recent studies have demonstrated that FOI can drastically change through time and can vary with host and pathogen heterogeneity based on longitudinal data sets (Howard and Donnelly 2000; Reiner et al. 2014).

In this study, we investigated how host and seascape heterogeneity influence marine disease risk and transmission rates through time using a naturally occurring coral disease outbreak as a case study. In winter 2015 a coral disease outbreak with an unknown origin occurred in central Kāneʻohe Bay, Oʻahu, Hawaiʻi (Figure 4.1). Histological investigation revealed microscopic lesions with dissociation of gastrodermal cells and mucus hypertrophy, leading to visual tissue loss exposing in-tact white skeleton (Work 2015). Even though this disease was newly described and the causative agent was unknown, we proceeded with an investigation assuming the disease was infectious based on initial epidemiology patterns. The tissue loss disease exclusively affected *Montipora capitata,* a dominant Hawaiian reef-building coral species (Concepcion, Baums, and Toonen 2014). *Montipora capitata* has two distinct morphologies: plating and branching; and exhibits coloration along a spectrum of red to orange. There have been two previous tissue loss disease outbreaks affecting *M. capitata* in Kāneʻohe Bay (Aeby et al. 2016), however there is no apparent link between the outbreak described in this study and previous outbreak events.

Methods

Field surveys

We identified 200 visually healthy branching *Montipora capitata* coral colonies of similar morphology and monitored their health state over the course of a tissue loss disease outbreak (Work 2015). The 200 focal colonies were distributed among three patch reefs directly adjacent to the epicenter of the outbreak, located in central Kāneʻohe Bay, Oʻahu, Hawaiʻi (Figure 4.1). There were no differences in disease risk among reefs, so

we pooled colonies from all reefs for our analysis. The outbreak was first discovered on February 3, 2015. We identified focal colonies and collected initial seascape measurements between February 5 and 7, 2015. We recorded health state of each focal coral colony daily for three weeks (February 8 - March 2, 2015) with follow up surveys once a week for two weeks (March 3 - March 16, 2015). We categorized coral health state as healthy (no actively affected tissue), severity 1 (≤25 % tissue actively affected), severity 2 (between 25 % and 75 % tissue actively affected), severity 3 (≥75 % tissue actively affected) or removed (no remaining actively infected tissue). No colonies experienced re-infection during the course of the study.

To investigate the role of host and seascape heterogeneity in disease susceptibility, we measured a range of host traits and seascape characteristics listed in Table 4.1. For host heterogeneity, we measured the size of each focal colony (longest horizontal axis), percent of surface tissue covered in sediment (visual estimate), water depth (m), and position of colony on the reef (reef flat, reef crest, reef slope). To understand how seascape heterogeneity influenced disease risk, we measured composition and configuration of fine scale reef habitat surrounding each focal colony. We surveyed the benthos surrounding each colony using 2 m x 1 m belt transacts measuring the percent cover of coral (*Porites compressa, Pocillopora damicornis, Leptastrea purpurea, Pavona varians, Montipora patula, Fungia scutaria, Cyphasrea ocellina, Palythoa spp.*), algae (filamentous and macro), sponge, sand and rock. To assess relative disease pressure surrounding each focal colony (i.e., relative amount of potential infectious particles in the water column), we measured distance to and size and severity of the

three nearest infected neighboring colonies. Based on those measurements, we calculated three metrics of disease pressure: 1) average neighborhood severity (where low = 12.5 % of colony visually affected; moderate = 50 % of colony visually affected; high = 90 % of colony visually affected); 2) average area of actively affected tissue (colony severity multiplied by colony diameter); and 3) average actively affected tissue scaled by an exponentially decreasing distance function (area of infection/distance^2). We measured and calculated disease pressure around each focal colony at the beginning (four days prior to the monitoring period) and end (1-3 days after the monitoring period) of the outbreak.

Associating host and seascape heterogeneity with disease risk

To assess variation in disease risk as a function of host and seascape heterogeneity, we used a spatio-temporal point process regression model (Höhle 2009). The regression model characterized the instantaneous rate of infection for each individual (*i*) at a series of time points (*t*) by incorporating a baseline hazard, log-linear covariate predictor variables (Table 4.1) and an additive-multiplicative model component that incorporated a distance-based measure of the number of infected individuals in the population at each time point (Equation 1a-c). The instantaneous rate of infection (Equation 1a) of each susceptible host, *i*, at time *t*, modeled as a Cox proportional hazards baseline, $\lambda_0(t)$, multiplied by covariates $v_i(t)$ and added to time-varying force of infection, $f(d_{ij})$. The covariates (Equation 1b) were host size, depth, reef position, sediment cover, coral cover, and the three disease pressure metrics. The force of infection (Equation 1c), $f(d_{ij})$, represents the force of infection of individual *i* based on

each diseased individual in the population within distance d_{ij} through a distance kernel, where B_m is a non-negative distance function. In our model, B_m is the Euclidean distance between two coral colonies. We conducted this analysis using twinSIR in the surveillance package in R statistical software v3.3.1.

$\lambda_i(t)=\lambda_0(t)v_i(t) + \sum_{j \in I(t)} f\left(d_{ij}\right)$ Equation 1a

$v_i(t) = \exp(z_i(t)^T \beta)$ Equation 1b

$f(u) = \sum_{m=1}^{M} B_m(u) \geq 0$ Equation 1c

Calculating FOI and R_{eff}

We calculated the mean and standard error of the mean of force of infection (FOI) at each time point *t* from individual FOI trajectories, which were calculated in the point process regression model.

The effective reproductive ratio, R_{eff}, is the average number of secondary infections in a population made up of susceptible and non-susceptible hosts. R_{eff} is calculated as the transmissibility (probability of contact between a susceptible and infected individual and the probability of infection given contact) divided by the duration an individual remains infectious. To calculate R_{eff}, we multiplied the FOI by the number of diseased individuals at each time step and divided that value by the recovery rate (analogous to the infectious period). We calculated recovery rate as the average duration an individual remained infected.

Results

Field surveys

During the five-week study period, 106 of the 200 (53 %) coral colonies that we monitored developed signs of disease. Of the diseased colonies, 83 individuals showed disease signs on ≤25 % of their surface tissue (severity 1), 22 individuals showed signs of diseases affecting between 25 % and 75 % of their surface tissue (severity 2) and 1 individual showed disease signs affecting more than 75 % of its surface tissue (severity 3) (Figure 4.1). Over 70 % of colonies showed signs of disease within the first two weeks of the study period. The peak of the outbreak within the study sites occurred on day 11 with a total of 65 colonies (32.5 %) exhibiting disease signs by that day (Figure 4.2).

Associating host and seascape heterogeneity with disease risk

Of the four host characteristics that we measured, disease risk only varied with host size. Host size ranged from 12-135 cm maximum diameter (Table 4.1, Figure 4.3A-C). Disease risk increased by 2 % with every 10 cm increase in host diameter (Table 4.3). Disease risk did not vary with sediment cover, position on reef (flat, crest and slope) or depth. Sediment covering the coral surface, including re-suspended sediment and fish excrement, which are potential disease vectors (Haapkylä et al. 2013), ranged from 0-33 % (Figure 4.3D-F). Depth, which can indicate solar radiation (both necessary for coral's symbiotic photosynthetic algae to translocate energy and harmful to coral in excessive sunlight conditions), ranged from 0.5-7 meters (Table 4.1, Figure 4.3G-I).

Disease risk increased with one measure of seascape heterogeneity: initial neighborhood disease severity. Disease risk did not vary significantly with host cover or coral cover, which were measured within 2 m^2 of each focal colony. Host cover, measured as the percent of *M. capitata* within 2m^2 of a focal colony, ranged from 4-67 % (Table 4.1, Figure 4.4A). Habitat composition measured by benthic cover, the percent of host and potential alternative host species within 2 m^2 of a focal colony (i.e., all coral species, algae and sponges), ranged from 11-100 % (Table 4.1, Figure 4.4B). Of the disease pressure metrics measured at the beginning (four days prior to the monitoring period) and after (1-3 days after the monitoring period) the outbreak, we found that disease risk was positively related to initial neighborhood severity. Neighborhood severity increased over the course of the outbreak from an initial neighborhood severity that ranged from low to high to a final neighborhood severity that ranged from moderate to high (Table 4.1, Figure 4.4C-D). Colonies with moderate severity neighbors were 1.13 times more likely to develop disease signs compared to colonies with low initial severity neighbors (Table 4.2). Colonies with high severity neighbors were 1.6 times more likely to develop disease signs compared to colonies with moderate severity neighbors (Table 4.2). Other disease pressure metrics included in the analysis such as the area of infected tissue of nearest neighbors or the area of infected tissue scaled by distance to neighbors (Table 4.1) did not perform as well as neighborhood severity.

Disease risk was also positively associated with the number of diseased individuals within a 15 m radius. The number of diseased individuals in our sample population and their distances to susceptible focal colonies continuously changed over the course of

the outbreak (Figure 4.2). Testing the relationship between number of individual colonies within 0 to 50 m while holding host size and initial neighborhood severity constant, the best-fit model included the number of infected neighbors within 15 m of the focal host colony and was slightly better than the model within 10 m (Table 4.3).

Calculating FOI, Recovery Rate and R_{eff}

Force of Infection (FOI) and the effective reproductive ratio changed through time, while recovery rate remained constant. Force of infection (i.e., the per capita rate at which healthy individuals become infected) ranged from 0.007 to 0.02 newly infected corals per day over the course of the outbreak with mean 0.015 (Figure 4.5). Mean recovery rate (or infectious period) was 7.15 days (SEM ±1.3 days) and was independent of all predictor variables that we measured in this study. The effective reproductive ratio (R_{eff}) is a metric that describes the average number of secondary infections in a population of susceptible and non-susceptible hosts; when R_{eff} is greater than 1, an outbreak can occur. For this tissue loss disease outbreak, R_{eff} ranged from 0.16 to 1.22 with a mean of 0.71 (Figure 4.6). R_{eff} exceeded 1 between days 6 and 11 of the study period.

Discussion

The disease outbreak described in this study affected over half the sample population, but 99% of infected coral colonies survived. This is in direct contrast to the high levels of disease-induced *M. capitata* colony mortality (~60 %) that occurred on patch reefs adjacent to our study sites prior to and during the study period (personal observation). The low mortality rate at our study sites may indicate that coral resistance was higher at

our sites compared to adjacent reefs, potentially because of spatial differences in environmental stress. Of the recovered colonies in our study, most experienced <25 % partial mortality. Like plants, partial mortality is a survival mechanism for coral, ensuring population persistence. As large colonies undergo partial mortality, the rest of the colony can facilitate survival (rather than putting energy into wound repair and recolonization) following mortality events (Lasker and Coffroth 1999). However, while colonies are recovering from partial mortality they are more vulnerable to predation, environmental stress and opportunistic pathogens (Guzner et al. 2010) and may have reduced growth rates and reproductive output for several years (Lirman 2000) hampering reef recovery. Our study took place over the course of five weeks; therefore, such long-term reef-wide effects are yet to be determined. In addition, the patch reefs in this study experienced moderate coral bleaching in 2014, which would make it difficult to tease apart the effects of bleaching from disease on survival and recruitment.

Similar to diseases in many other taxa, disease risk increased with host body size. Body size has been identified as a driver of disease risk for a variety of marine organisms (Dube et al. 2002; Groner et al. 2014; Eisenlord et al. 2016). There are two main arguments that could explain the positive relationship between host size and disease risk: 1) large adults have more surface area exposed to pathogenic organisms/particles relative to small colonies, and 2) large colonies tend to be older than small colonies (but see Hughes & Jackson 1980). While the association between age and disease resistance has not been tested for scleractinian corals, there is evidence that disease resistance decreases with increasing age for sea fan corals (Dube et al. 2002). A

related hypothesis is that older colonies have been exposed to stressful conditions for longer periods of time. If the surface area hypothesis were true, we would expect to see lesions on different areas of the colony, at a rate proportional to surface area; instead, lesions always began in the interior basal portion of the colony and moved upward. Several coral colonies split in half revealing further evidence of this distinctive pattern. Thus, this pattern does not support the surface area hypothesis. However, it is still unclear if the age/exposure hypothesis is true as there are other possible hypotheses that could also lead to the emergence of this lesion pattern, for example, local hydrodynamics restricts water flow at the base of the colony which could increase the likelihood of disease lesions in this region of the colony.

In addition to host size, local neighborhood composition played a significant role in disease risk: risk of infection increased with the density and severity of diseased neighbors. Healthy colonies were more likely to contract the disease if they were located near neighbors with moderate to severely diseased colonies at the beginning of the study (initial neighborhood severity). Interestingly, neighborhood severity was higher at the end of the outbreak relative to the beginning, potentially suggesting a saturation point for infectious particles in the water column or a change in virulence over time. We accounted for the changing number and distribution of infected neighbors during the study and found that number of infected neighbors within a 15 m radius increased transmission risk. The relationship among disease risk and seascape conditions (initial neighborhood severity and number of diseased colonies within 15 meters at any given

time) provides support for the hypothesis that this emerging tissue loss disease has density-dependent disease transmission that peaks within 15 m.

Surprisingly, for most of the study period, disease transmission rates were lower than the threshold for an outbreak to occur, and lower than known transmission rates for other coral diseases. The average R_{eff} in this study was 0.71, which is lower than 1, the expected R_{eff} needed for an outbreak to occur and lower than the R_0 (average number of secondary infections in a fully susceptible population) found for white plague and black band disease in the Red Sea (R_0 =1.2, 1.6-1.7 respectively) (Zvuloni et al. 2009; Zvuloni et al. 2015). However, at the peak of this outbreak, R_{eff} reached 1.22. High transmission within 15 meters may help explain why the outbreak grew and crashed quickly as reflected by the temporal variation in FOI and R_{eff}. In acute outbreaks, R_{eff} decreases when the number of susceptible individuals is depleted below some threshold, forcing the outbreak to die out. In this study, the total number of susceptible individuals (where classification was determined by visual surveys only) never dropped below the number of diseased individuals (Figure 4.2). However, the local pool of susceptible individuals (within 15 m) was partially depleted by the peak of the outbreak (Figure 4.7), which may have contributed to the outbreak dying out globally. However, this parameter alone cannot completely explain why the outbreak declined so quickly. It is also valuable to place this outbreak in context of the reef's recent natural history.

Likely the outbreak ended due to multiple factors acting in concert, such as natural host immunity and environmental conditions. The assumption that $R_0>1$ is required for an

outbreak to persist assumes that all non-infected colonies are susceptible, however, if there is variation in natural resistance to disease, this assumption is violated. It was not possible to test this relationship directly because diagnostic tools for this emerging disease do not exist yet. Another possibility is that an acute environmental stress triggered the disease outbreak, either with the introduction of pathogenic bacteria or by inducing natural microbiota to become pathogenic, and as that stress abated disease transmission halted.

The presumed absence of oceanic barriers to disease transmission suggests that disease spread should be more rapid in marine systems compared to their terrestrial counterparts; yet, our study suggests disease spread can also be locally constrained within marine seascapes. While it is often argued that marine populations are 'open' systems, habitat patches, chemical gradients and hydrodynamics may create barriers restricting pathogen spread. Thus, even though there are some notable marine disease outbreaks that have caused widespread mass moralities (e.g., abalone Lafferty & Kuris 1993; seafans Kim and Harvell 2004; seastars Eisenlord et al. 2016) it is unclear whether these disease patterns are linked to population connectivity. For marine organisms in general, long-distance dispersal usually occurs during the planktonic larval stage, and there is currently no evidence that larvae serve as adequate hosts for marine pathogens. In contrast, dispersal in terrestrial ecosystems is more common in subadults and adults. For corals in particular, local and patchy disease transmission more likely arises because of limited local genetic diversity compared to other marine and terrestrial animals, thus increasing the potential for localized disease transmission. *Montipora*

capitata for example, has uniformly low estimates of dispersal in the Hawaiian Islands, with over 90 % self-recruitment within sites (Concepcion, Baums, and Toonen 2014). Our results suggest that in certain cases, such as a coral disease outbreak, marine disease transmission can occur on more localized scales than previously thought.

Investigating infectious disease dynamics in wildlife is of academic interest, but also important for conservation and management. A major topic of interest in infectious disease ecology is the influence of pathogens on community structure and function. In this study we demonstrate that host and seascape heterogeneity influence disease transmission. These results compliment a simulation study of white plague disease spreading through a heterogeneous reefscape and could lead to similar changes in coral cover (Brandt and McManus 2009). For instance, the tissue loss disease described in this study has the potential to alter *M. capitata* size-frequency distributions, which could have cascading effects throughout the local reef ecosystem by affecting habitat availability and coral-associated communities. Coral diseases in the Pacific Ocean are a major conservation concern (Sutherland et al. 2015), threatening an already vulnerable ecosystem (Carpenter et al. 2008); therefore the results of our study are important for coral-specific conservation initiatives. However, placing studies such as this one in a broader context is more widely valuable as infectious wildlife diseases pose a serious threat to global biodiversity (Daszak, Cunningham, and Hyatt 2000) and threaten many species with extinction, particularly for diseases that spread through close contact (Pedersen et al. 2007). Thus, managing wildlife populations is important for the conservation of nature and ecosystem services.

Table 4.1 Measurements of host and seascape heterogeneity. Disease pressure metrics are average values for the three nearest infected neighbors to each initially healthy focal colony. Initial measurements of disease pressure were collected four days prior to the monitoring period. Final measurements of disease pressure were collected one to three days after the monitoring period. For disease pressure metric 1, low corresponds to <25 % of the colony affected, moderate corresponds to between 25 % and 75 % of the colony affected and high corresponds to above 75 % of the colony affected by disease. Disease pressure metric 2 was calculated as the size of the colony multiplied by the percentage of actively affected tissue. Disease pressure metric 3 was calculated as the amount of actively affected tissue (i.e., metric 2) divided by $\exp^{-distance}$.

Scale	Metric description	Range
Host	Host size (maximum diameter)	12-135 cm
Host	Depth	0.5-7 m
Host	Position on reef	Flat, Crest, Slope
Host	Sediment cover	0-33 % of tissue covered
Seascape	Host cover	4-67 % cover of *M. capitata* colonies in 2 m^2
Seascape	Coral cover	11-100 % cover in 2 m^2
Seascape	Disease pressure metric 1: neighborhood severity	Initial: low-high
		Final: moderate-high
Seascape	Disease pressure metric 2: area of infectious tissue	Initial: 4-90 cm^2
		Final: 9-150 cm^2
Seascape	Disease pressure metric 3: area of infectious tissue scaled by distance	Initial: 0.05-2643
		Final: 0.21-256

Table 4.2 Comparison of top four models explaining infection likelihood.

Coefficients for each variable are listed with the standard error of the mean in parentheses. Colony size was measured as the longest horizontal axis. Position on reef refers to flat, crest or slope. Coefficients for reef crest (upper number) and slope (lower number) are provided in relation to reef flat (baseline). Baseline hazard is the baseline level of risk for any individual without accounting for host and seascape heterogeneity. Model fit was assessed using Akaike information criterion (AIC) with the best fit model described by the lowest AIC value.

Model	Colony size	Position on reef	Initial neighborhood severity	Infected individuals within 15 m	Baseline hazard	AIC	ΔAIC
1	2.46^{-4} (1.5^{-4})	0 (0.006)	0.109 (0.006)	3.87^{-3} (0.001)	6.39^{-6}	946.44	0
		0.002 (0.006)	0.519 (0.006)				
2	N/A	0 (0.004)	0.13 (0.005)	0.004 (0.001)	6.51^{-3}	955.4	8.96
		0.002 (0.006)	0.796 (0.005)				
3	2.52^{-4} (1.4^{-4})	N/A	0.118 (0.005)	3.8^{-3} (0.001)	4.64^{-6}	941.44	5
			0.593 (0.005)				
4	3.28^{-4} (1.5^{-4})	0 (0.006)	N/A	4.41^{-3} (0.002)	4.54^{-13}	953.79	7.35
		0.005 (0.005)					

Table 4.3 Comparison of different distance thresholds in infection likelihood. Coefficients for each variable are listed with the standard error of the mean in parentheses. Distance threshold is the radius of concentric circles tested in the spatio-temporal point process regression model, where zero indicates colonies were touching.

Model	Size	Initial average severity	Distance threshold (m)	Within distance threshold	AIC
1	4.42^{-4} (1.58^{-4})	0.157 (0.05) 0.879 (0.05)	0	0 (0.025)	958.15
2	4.38^{-4} (1.57^{-4})	0.152 (0.05) 0.8 (0.05)	1	0.0114 (0.015)	957.54
3	2.54^{-4} (1.54^{-4})	0.126 (0.06) 0.599 (0.06)	5	8.89^{-3} (3.54^{-3})	946.54
4	3.11^{-4} (1.52^{-4})	0.118 (0.05) 0.758 (0.06)	10	4.45^{-3} (1.54^{-3})	943.71
5	**2.58^{-4} (1.41^{-4})**	**0.112 (0.05)** **0.539 (0.05)**	**15**	**3.85^{-3} (1.11^{-3})**	**941.44**
6	2.70^{-4} (1.49^{-4})	0.0119 (0.06) 0.003 (0.002)	20	2.45^{-3} (8.25^{-4})	946.90
7	2.30^{-04} (1.48^{-04})	0.119 (0.05) 0.0423 (0.006)	50	8.9^{-04} (2.9^{-04})	948.34
8	2.52^{-04} (1.5^{-04})	0.126 (0.05) 0.497 (0.06)	100	6.87^{-04} (2.6^{-04})	949.21

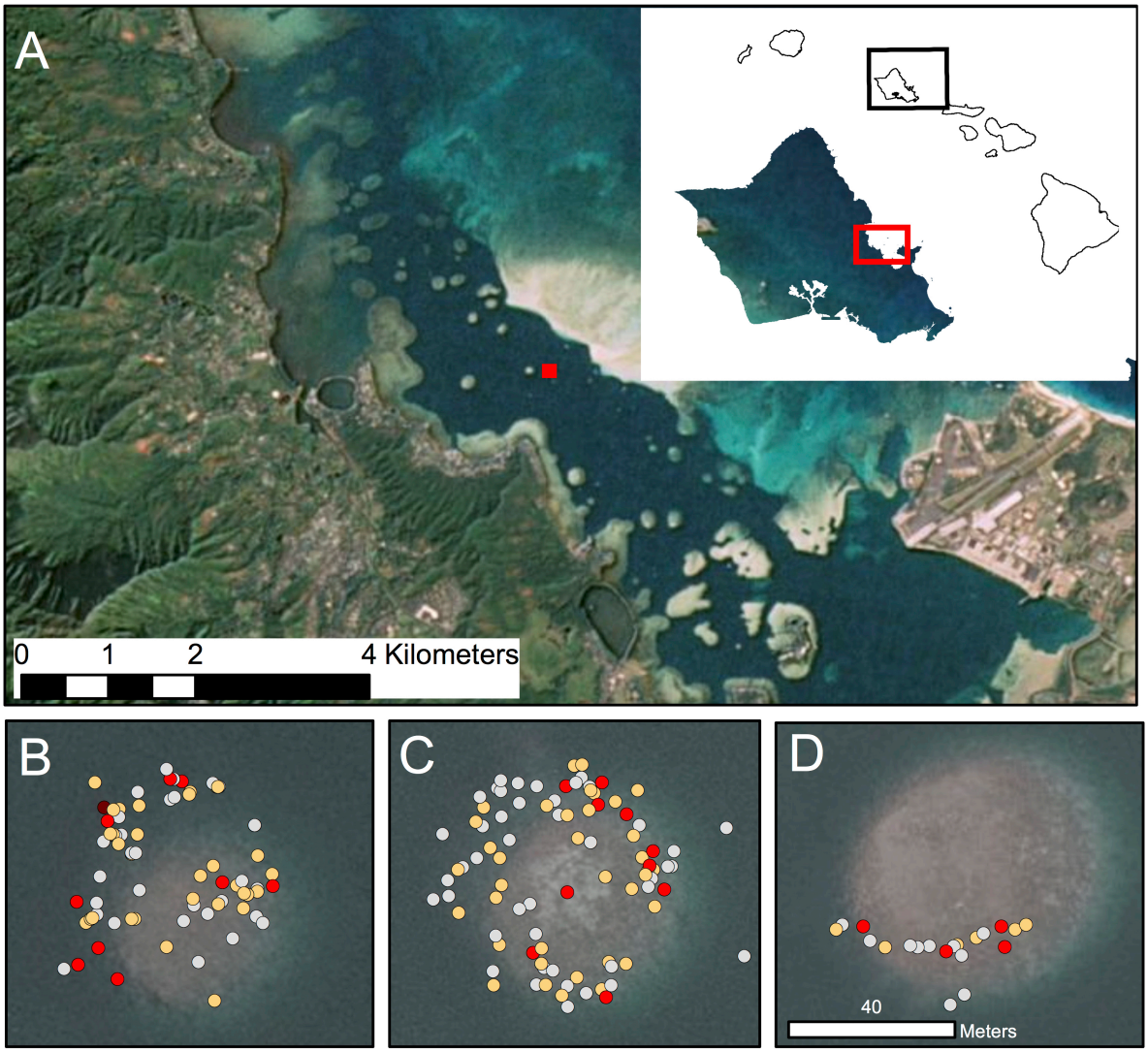

Figure 4.1 Survey sites. Map inset shows Main Hawaiian Islands with O‘ahu enlarged. A) Kāne‘ohe Bay, O‘ahu, Hawai‘i. Survey sites included B) Reef 21, C) Reef 22 and D) Reef 23. Dots represent the 200 focal colonies monitored over the course of the study. Grey dots indicate colonies that remained visually healthy through the study period; orange dots indicate colonies with a severity 1 infection (≤25 % of surface tissue actively affected); red dots indicate colonies with a severity 2 infection (between 25 % and 75 % tissue actively affected); maroon dot indicates the single colony with a severity 3 infection (≥75 % tissue actively affected).

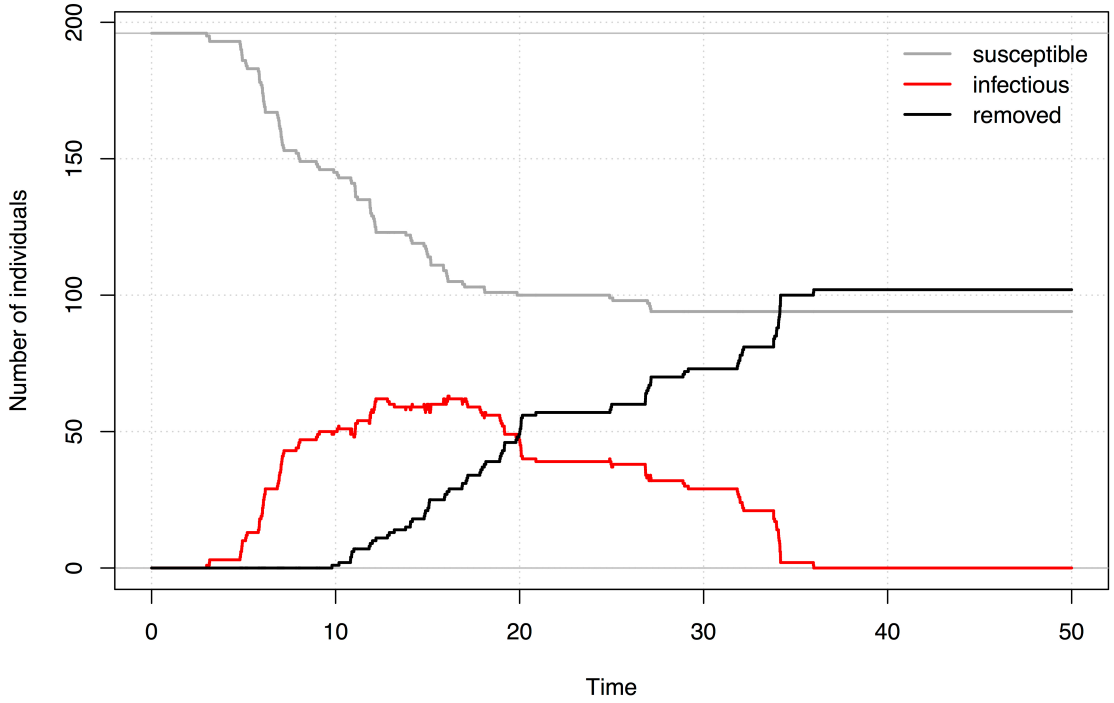

Figure 4.2 Susceptible infectious removed plot. Trajectories of the susceptible proportion of the population (grey line), infectious proportion of the population (red line) and removed proportion of the population (black line) over the course of the coral disease outbreak.

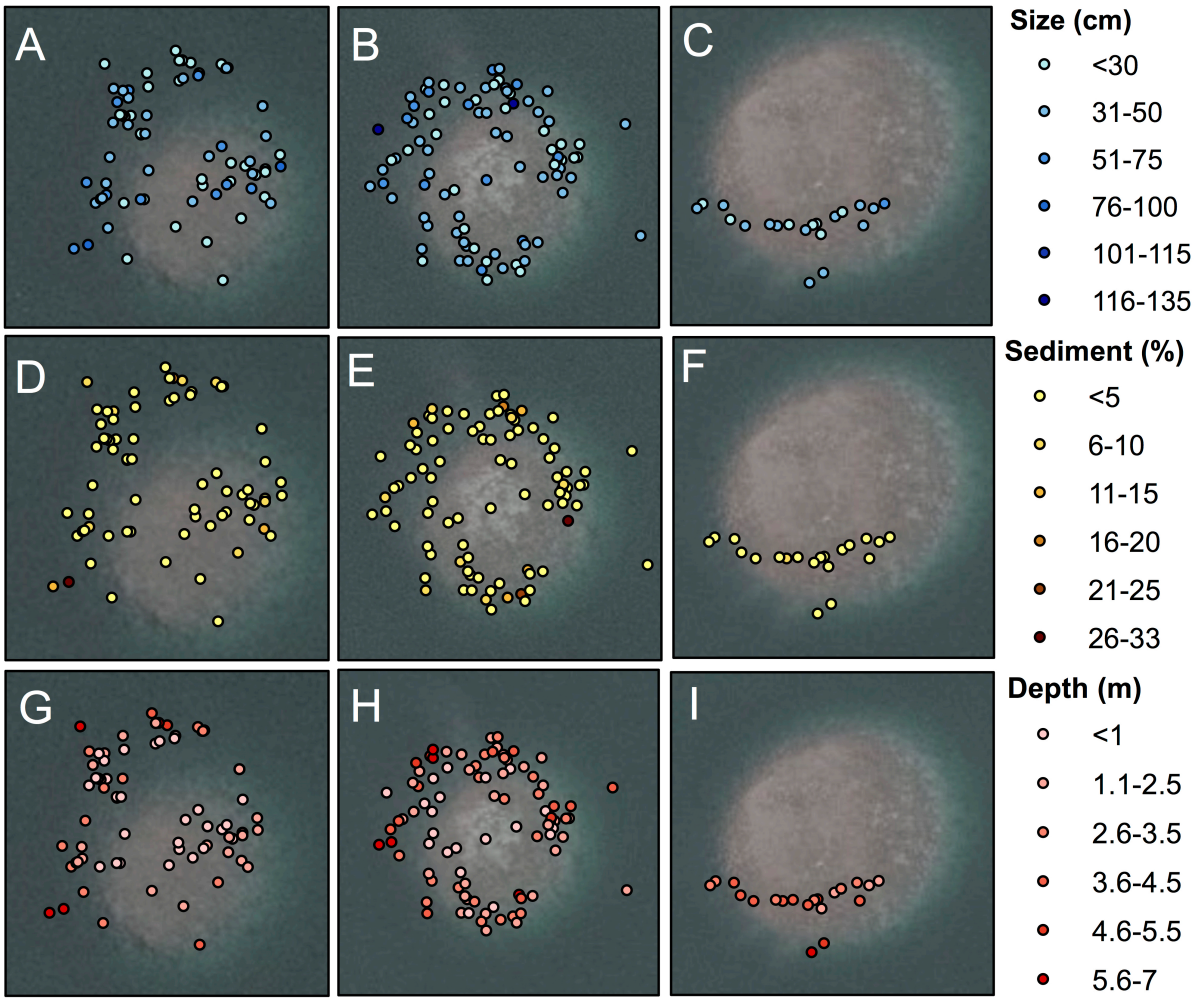

Figure 4.3 Spatial variation in host traits. Variation in (A) host size, (B) sediment cover and (C) depth for focal coral colonies.

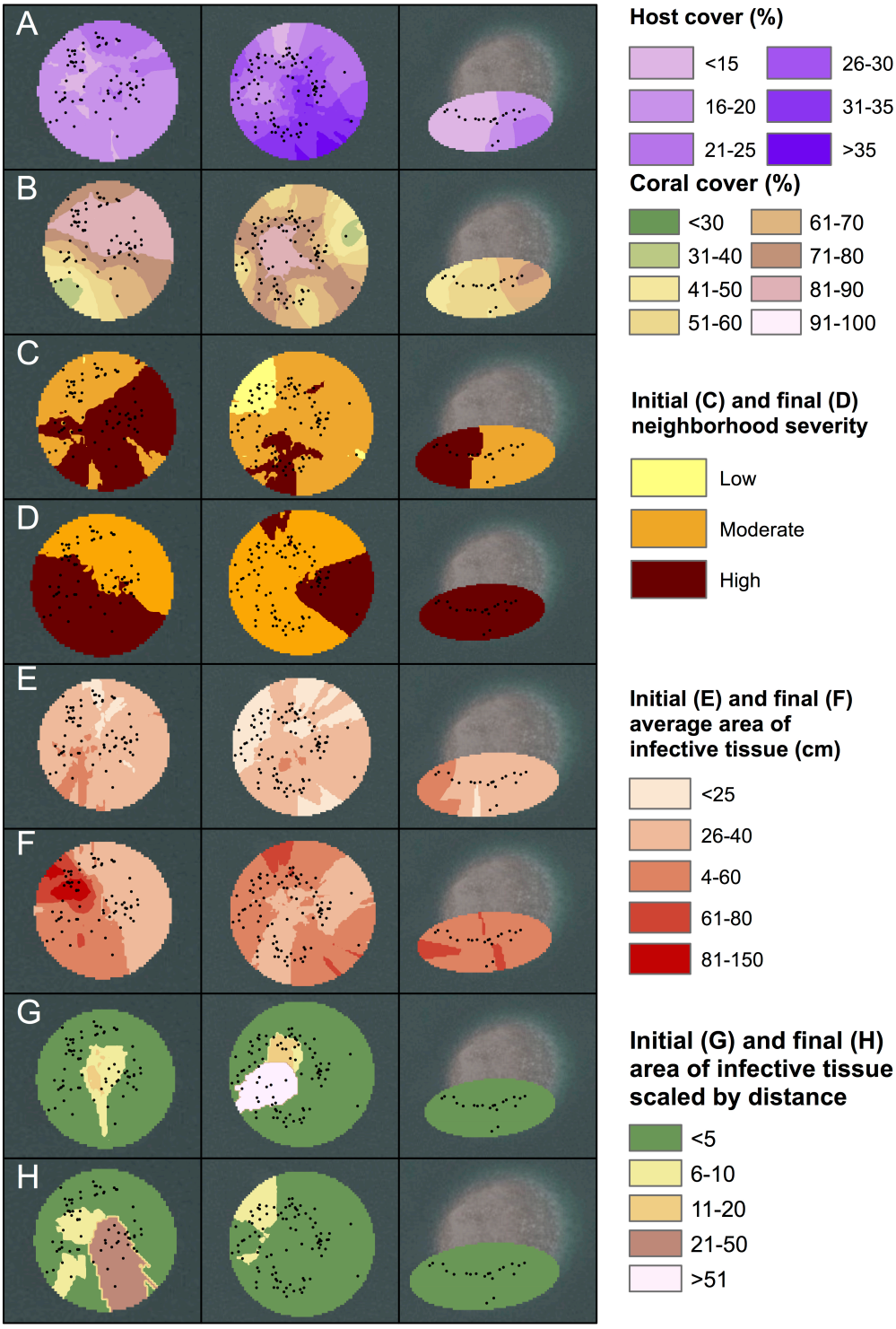
A
B
C
D
E
F
G
H
Host cover (%)
<15
16-20
21-25
26-30
31-35
>35
Coral cover (%)
<30
31-40
41-50
51-60
61-70
71-80
81-90
91-100
Initial (C) and final (D) neighborhood severity
Low
Moderate
High
Initial (E) and final (F) average area of infective tissue (cm)
<25
26-40
4-60
61-80
81-150
Initial (G) and final (H) area of infective tissue scaled by distance
<5
6-10
11-20
21-50
>51

Figure 4.4 Spatial variation in seascape characteristics. Variation in (A) host cover, (B) coral cover, (C) initial neighborhood severity, (D) final neighborhood severity, (E) initial area of affected tissue, (F) final area of affected tissue, (G) initial area of affected tissue scaled by distance and (H) final area of affected tissue scaled by distance. The left panel is a map of patch reef 21, the central panel is a map of patch reef 22 and the right panel is a map of patch reef 23. Dots overlaying interpolated data represent the locations of the 200 focal colonies monitored during this study. Maps were interpolated from data collected surrounding each focal colony using the kriging function in ArcMap 10.4.

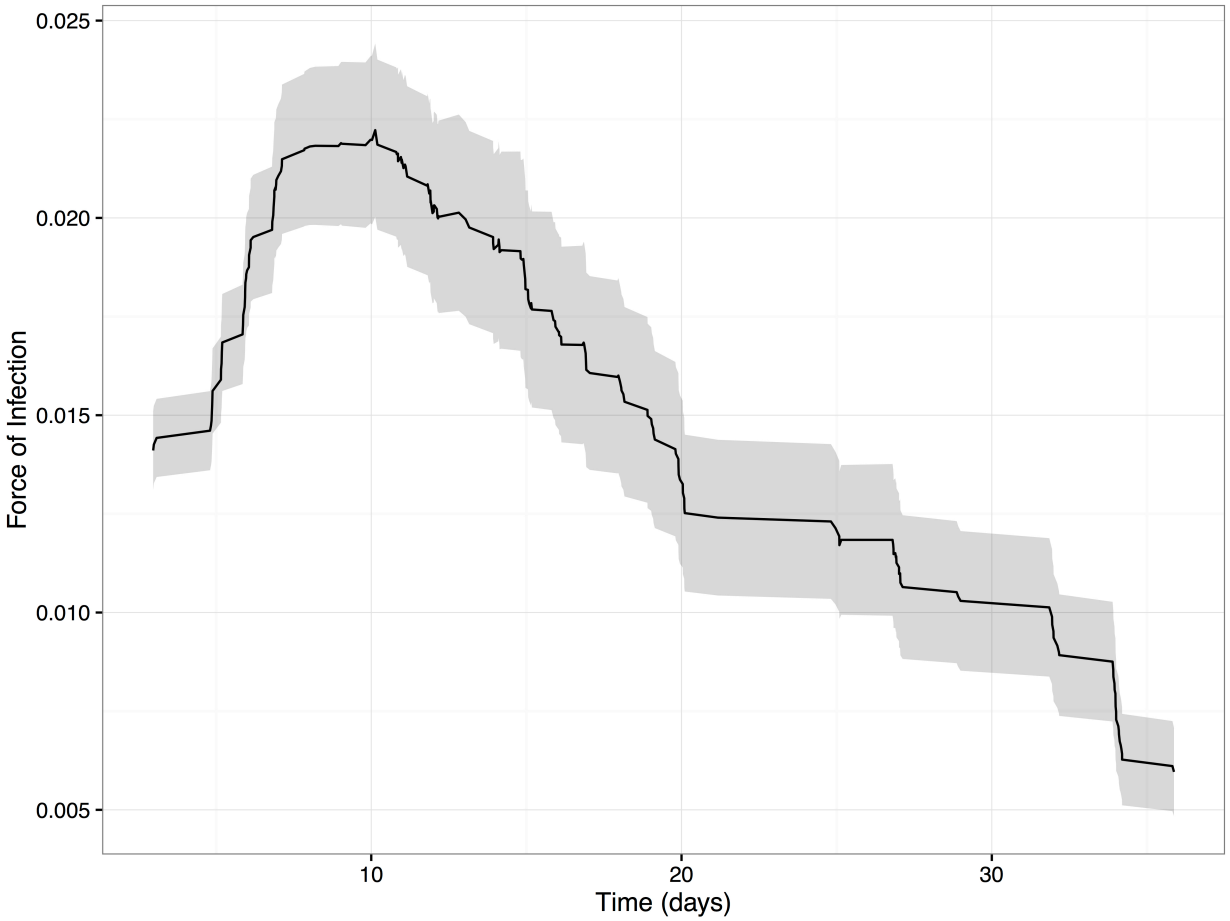

Figure 4.5 Force of infection through time. Average daily FOI over the course of the outbreak; shaded area represents ± standard error of the mean.

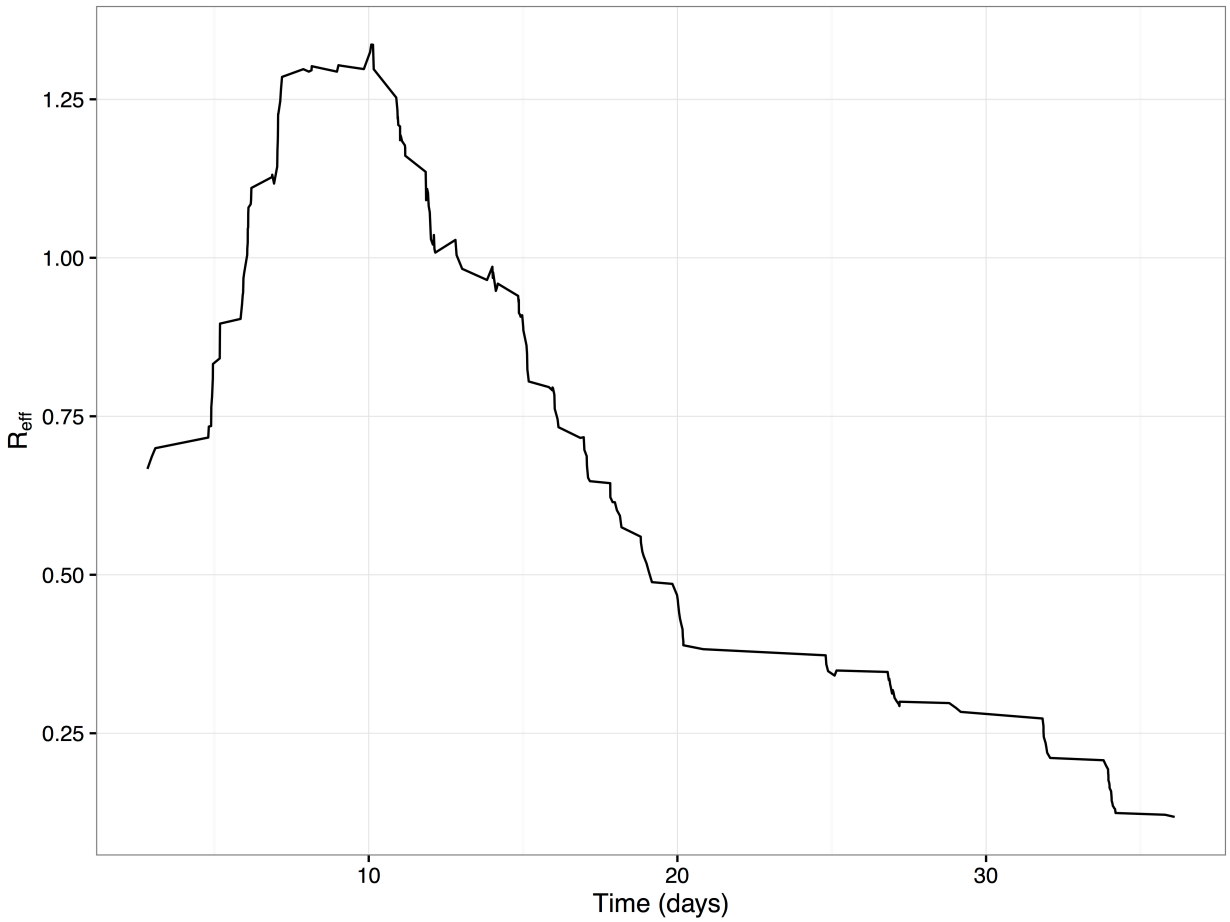

Figure 4.6 Effective reproductive ratio. Average daily R_{eff} over the course of the outbreak.

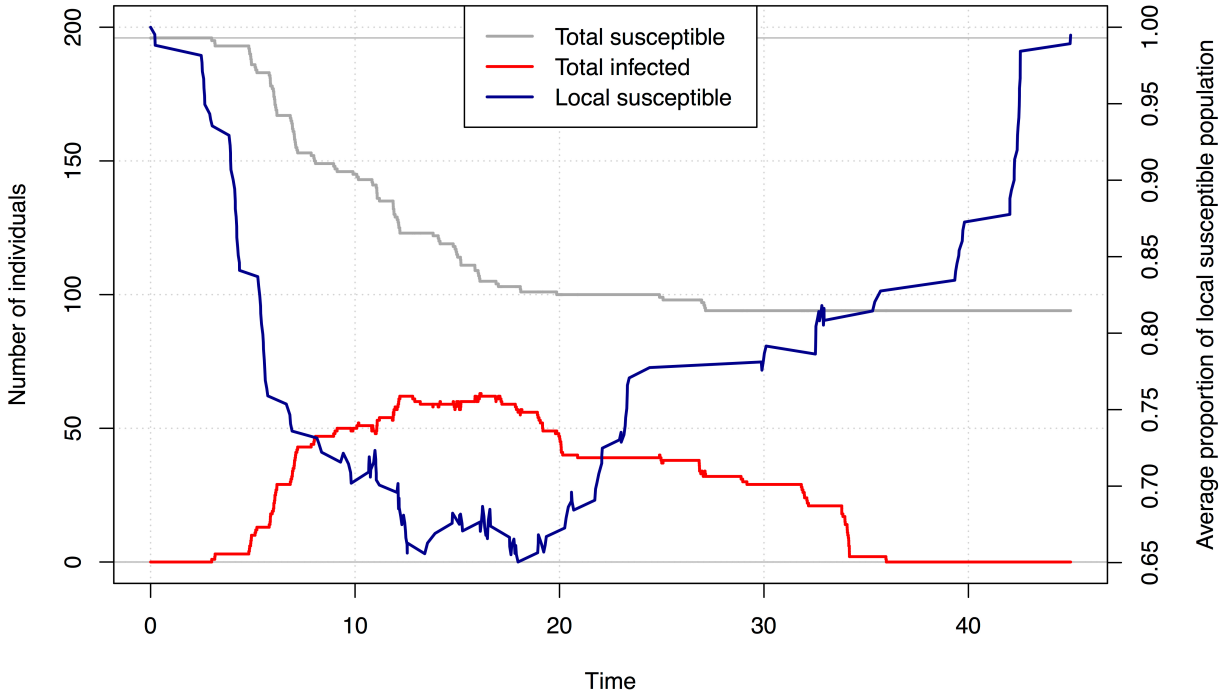

Figure 4.7 Susceptible infected plot. Trajectories of the globally susceptible proportion of the population (grey line), locally susceptible proportion of the population (blue line) and infectious proportion of the population (red line) over the course of the coral disease outbreak.

CHAPTER 5

INTRA-COLONY DISEASE PROGRESSION INDUCES FRAGMENTATION OF CORAL FLUORESCENT PIGMENTS

To be submitted as:

Caldwell J, Ushijima B, Couch C and Gates R. 2017. Intra-colony disease progression induces fragmentation of coral fluorescent pigments to Scientific Reports.

Abstract

We show that changes in the micro-scale spatial distribution of coral fluorescence reflects a distinct tissue loss disease response in the Hawaiian coral *Montipora capitata*, and these patterns can be used to assess sub-lethal disease responses in living coral colonies. We characterized the emission spectra and the spatial distribution of fluorescent pigments in *M. capitata* and determined that the fluorescent signature remains constant across a depth gradient but differs between healthy and diseased colonies. Both healthy and diseased colonies exhibited emission spectra resembling cyan fluorescent protein (450 nm - 495 nm) and chlorophyll-*a* fluorescence (650 nm - 680 nm) when simultaneously exposed to excitation spectra at 405 nm and 561 nm under a confocal microscope. On average, healthy coral fragments had greater overall coverage and more evenly distributed fluorescence compared to diseased coral fragments, whereas naturally diseased and laboratory infected coral systematically exhibited fragmented and disorganized distributions of fluorescent pigments adjacent to the disease front as indicated by several measures of fragmentation (e.g., number of patches, edge to area ratio). Our histology results further supported these findings. Fluorescent pigment fragmentation indicates a disruption in the coral tissue that likely impedes translation of energy within the colony. However, the area of fragmented fluorescent pigments in diseased coral extended 3.03 mm ± 1.8 mm directly adjacent to the disease front, indicating pathogenesis is highly localized rather than systemic. Our study shows that quantifying micro-scale spatial changes in coral fluorescence can be used as a non-invasive indicator of coral health state, and, such patterns can help refine our hypotheses about modes of pathogenesis.

Introduction

Natural fluorescence is ubiquitous in scleractinian corals, although their biological function remains unresolved. Coral pigmentation is produced by fluorescent proteins found in coral tissue (i.e., green fluorescent protein and its homologues) (Dove, Hoegh-Guldberg, and Ranganathan 2001; Johnson and Goulet 2007; Alieva et al. 2008) and photosynthetic pigments produced by symbiotic dinoflagellates, *Symbiodinium* spp. (i.e., chlorophyll-*a*, chlorophyll c_2, peridinin, diadinoxanthin, diatoxanthin, β,β-carotene, dinoxanthin) (Apprill, Bidigare, and Gates 2007). The functional role(s) of fluorescent proteins (FPs) in coral is currently unresolved; however there are several leading hypotheses. The most well supported hypothesis suggests that coral FPs are photoprotective, dissipating energy in excessive sunlight (Salih et al. 2000). Other studies suggest FPs may also play a role in immune function, including response to stressful temperatures (Roth, Fan, and Deheyn 2013), mechanical damage, infestation, infection, and tissue regeneration (Palmer, Mydlarz, and Willis 2008; Palmer, Modi, and Mydlarz 2009; Palmer, Bythell, and Willis 2010; D'Angelo et al. 2012; van de Water et al. 2015).

Despite a limited understanding of the function of fluorescence, natural fluorescence has been used as a non-invasive intrinsic marker of coral physiological condition and may be particularly suitable for investigating coral disease. In laboratory experiments, coral fluorescence has been used as a proxy for photochemical efficiency and growth in response to temperature stress, wounding, epibiont infestation, and recovery (Roth et al. 2010; D'Angelo et al. 2012; Roth, Goericke, and Deheyn 2012). There is evidence that

fluorescence may be involved in other facets of the innate immune system as well, such as inflammatory responses typical of coral diseases (Palmer, Mydlarz, and Willis 2008; Palmer, Roth, and Gates 2009; Palmer et al. 2011). Several studies discovered that higher concentrations of FPs were found in immunocompromised tissue compared to healthy colony tissue (Palmer, Mydlarz and Willis, 2008; Palmer, Roth and Gates, 2009; van de Water *et al.*, 2015). In the case of *Porites* trematodiasis, Palmer et al. (2009) showed that increased red FP production occurred within disease lesions. One hypothesis for the increased concentration of FPs in immunocompromised and diseased tissue is that FPs can efficiently scavenge hydrogen peroxide (Palmer, Modi, and Mydlarz 2009), a reactive oxygen species that is elevated in infected coral, causing oxidative stress to the coral host and its symbionts (Martindale and Holbrook 2002; Mydlarz and Harvell 2007). Another hypothesis is that tissue regeneration is associated with increased FP concentration (D'Angelo et al. 2012), which is important for recovery from infection.

Monitoring changes in the spatial distribution of endogenous fluorescence may allow for the identification of sub-lethal disease signs and improve our understanding of intra-colony disease progression. Several studies have used total fluorescence concentration or expression as a proxy for coral physiological condition (e.g., Palmer, Roth, et al. 2009; Roth et al. 2012; van de Water et al. 2016). New technology, such as live-imaging confocal microscopy, now allows for micro-scale investigation of the spatial distribution of fluorescent pigments over fine spatial scales, which may highlight variation in fluorescent pigments across the coral surface that cannot be captured by quantifying

total fluorescence concentration or expression alone. Fluorescent pigments are heterogeneously distributed across the coral tissue making physical features of the coral easily distinguishable in spectral images (Hill et al. 2004; Treibitz et al. 2015). Characterizing disease-induced changes in the spatial arrangement of coral fluorescence could support different hypotheses about modes of infection and disease progression. For instance, different patterns of fluorescence may arise from diseases that move across a colony surface versus move through the gastrovascular canal versus direct attack to *Symbiodinium*. These different patterns in fluorescence could emerge from two different mechanisms: i) the pathogen's assault, or ii) the coral's immune response. Investigation of these fluorescence changes through time may also reveal important information about intra-colony disease progression.

Here, we investigated the coral response to infection by quantifying disease-induced changes in coral fluorescence associated with tissue loss diseases in *Montipora capitata*, a common reef-building coral found throughout Hawai'i. *M. capitata* is affected by both a slow-moving tissue loss disease referred to as chronic *Montipora* white syndrome and a rapid tissue loss disease referred to as acute *Montipora* white syndrome (Aeby et al. 2010; Aeby et al. 2016). Both forms of this disease manifest as tissue degradation with a clear boundary between apparently healthy tissue and exposed skeleton. Different bacterial pathogens have been shown to cause chronic and acute white syndromes in *M. capitata* in Hawai'i (Ushijima et al. 2012; Ushijima et al. 2014). Currently, the coral pathogens that cause *Montipora* white syndrome have not been localized in histology samples, however, researchers have successfully used

histology to identify several secondary invaders such as ciliates, helminthes, and chimeric parasites (Work, Russell, and Aeby 2012). These secondary invadors cause different types of injury in the coral host and could support one of two contradictory modes of disease progression: localized or systemic. To determine if fluorescence is a viable physiological proxy for coral health and disease progression, we investigated spatially explicit patterns of natural fluorescence in healthy and diseased *M. capitata*. To distinguish natural variability in fluorescence from the distinct patterns associated with disease progression, we used live-imaging laser-scanning confocal microscopy to characterize the emission spectra and the spatial distribution of fluorescence (emission signature) in healthy coral fragments across different habitats, and compared this emission signature to the fluorescence patterns from naturally diseased and laboratory inoculated coral fragments. We complimented this analysis with histology to determine whether differences in fluorescence were attributed to patterns in the distribution of *Symbiodinium*.

Results

Natural variability in coral fluorescence across habitats

Spectral signatures were similar for visually healthy coral fragments from all three depths (1 m, 3 m and 5 m). Coral fragments emitted cyan fluorescence between 450 and 495 nm and red fluorescence between 650 and 680 nm in response to simultaneous excitation at 405 nm and 561 nm. These emission spectra resemble the emission spectra of cyan fluorescent protein (483 nm – 495 nm found in Salih et al. 2000; Alieva et al. 2008; D'Angelo et al. 2008; Roth, Fan, and Deheyn 2013) and

chlorophyll-*a* (peak ~685 nm found in Mazel, 1997). We found no significant difference between the ratio of cyan to red fluorescence at the polyp scale or at the branch scale based on results from one-way analysis of variance (ANOVAs) with depth as a factor. The spatial distribution of fluorescent pigments revealed distinctly different patterns between coenosarc (tissue overlying the coral skeleton) and polyps (Figure 5.1), and those patterns were consistent across all fragments within and between depths. We found no significant difference in the number of intact polyps across depths at the branch scale based on results of a one-way ANOVA. We also found no differences in the spatial distribution of fluorescent pigments across depths at the branch scale in any of the five metrics of landscape structure we evaluated using one-way ANOVAs: total area of fluorescence, area of edge, edge to area ratio, number of patches (contiguous breaks in fluorescence) and area of patches (Figure 5.1).

Differences in fluorescence between healthy and naturally diseased coral fragments

While there was no difference in the emission spectra of visually healthy and diseased coral fragments, the spatial pattern of fluorescence for visually healthy and diseased fragments differed by most landscape metrics based on t-tests and Wilcoxon rank-sum tests. In diseased fragments, the average area of affected fluorescence extended 3.03 mm ± 1.8 mm beyond the disease front (visual lesion edge) (Figure 5.2). The emission spectra (ratio of cyan to red fluorescence) of healthy and diseased fragments did not differ at either the polyp scale or the branch scale (Table 5.1). In contrast, the spatial distribution of fluorescent pigments at the branch scale indicated significant differences between healthy and diseased fragments (Table 5.1; Figure 5.1I,J). Mean area of

fluorescence was 1.7 times greater in healthy fragments compared to diseased fragments (t=-2.7, df=29, p=0.01; Table 5.1; Figure 5.3A) and there were 3.4 times as many intact polyps in healthy fragments compared to diseased fragments (t=-4.9, df=26, p=0.002; Figure 5.3B). On average, diseased fragments had 1.4 times greater area of edge (t=2.8, df=30, p=0.01; Table 5.1; Figure 5.3C), 1.8 times greater edge to area ratio (t=3.6, df=22, p=0.002; Table 5.1; Figure 5.3D) and 1.5 times as many patches relative to healthy fragments (t=2.5, df=32, p=0.02; Table 5.1; Figure 5.3E). There was no significant difference between patch area in healthy and diseased fragments.

Histological investigation of visually healthy and diseased coral

Mean *Symbiodinium* density in visually healthy fragments (22.71 ± 3.08) did not differ from diseased fragments (17.57 ± 3.26) (t=0.96, df=20, p=0.35). However, density was higher in the surface (27.71 ± 3.26) compared to the basal (14.04 ± 2.07) body wall (t=3.6, df=26, p=0.001). Symbiont abundance per contour length of surface body wall did not change with distance from the lesion margin in naturally diseased corals (R^2=-0.022, p=0.92).

Differences in fluorescence between healthy and laboratory infected coral fragments

Laboratory inoculated coral fragments showed similar patterns of fluorescence to those of naturally diseased coral fragments; however, there was high individual variability in the rate of disease progression, obscuring any distinct temporal changes in disease progression. We found no significant differences in emission spectra or the spatial distribution of fluorescent pigments between fragments sampled 8, 9, 10 and 11 hours

post-inoculation using repeated measures mixed effects models. Combining inoculated fragments from all time points, we compared spectral and landscape metrics between fresh seawater control, negative bacterial control, and pathogen treatments based on two-way ANOVAs with treatment and colony as random effects. The ratio of cyan to red fluorescence did not differ at the polyp scale or branch scale, and there were no differences across treatments in total area of fluorescence, number of patches or patch area. Mean area of edge ($F_{df=2,df=5}$=39.4, p=0.002) and edge to area ratio ($F_{df=2,df=5}$=109.7, p=0.0003) were higher and number of intact polyps ($F_{df=2,df=5}$=39.7, p=0.002) was lower in the inoculated treatment compared to the control groups (Figure 5.4A-C).

Discussion

Confocal microscopy images of *Montipora capitata* fluorescence reflected distinct structural components of the coral tissue, and these patterns were consistent for coral across a range of depths. These results suggest that *M. capitata* maintains the same type and arrangement of fluorescent pigments across shallow water habitats where light attenuation is most dynamic. Interestingly, a recent study showed that cyan fluorescent protein was dominant in *Leptastrea spp.* collected from shallow habitats while green fluorescent protein was dominant in *Leptastrea spp.* collected from deep habitats (Roth et al. 2015), suggesting the relationships between fluorescent pigments and light quality and light quantity may vary among different coral species.

The distribution of fluorescent pigments in healthy coral systematically differed from

naturally diseased and laboratory infected coral in this study, indicating sub-lethal changes in the coral tissue that cannot be seen with the human eye. Our results show that healthy coral fluorescence patterns were structured and predictable, whereas diseased coral fluorescence was disorganized and fragmented within a boundary directly adjacent to the visual disease lesion. In this disease front boundary, there was less total coverage of fluorescence and the fluorescent pigments were not distributed equally across the coral, suggesting a disruption in the coenosarc and gastrodermis, which may impede translocation of energy between polyps. Beyond the disease front boundary, polyps had distended or fractured tentacles, or were completely disintegrated (indicated by empty corallites), which inhibits heterotrophic feeding. The sub-lethal coral disease response extended directly from the disease front suggesting that pathogenesis is highly localized, potentially spreading across the tissue surface, which can be tested in future studies. This study builds on other research efforts that show fluorescence expression is altered in response to temperature stress, wounding and epibiont infestation, and recovery (Roth et al. 2010; D'Angelo et al. 2012; Roth, Goericke, and Deheyn 2012).

Histology showed intact, brown *Symbiodinium* in the endoderm supporting the hypothesis that the *Symbiodinium* maintain their physiological function while the coral is infected, which is similar to what has been found for *Acropora* white syndrome on the Great Barrier Reef (Roff et al. 2008). However, the Roff et al. (2008) study found that the abundance of *Symbiodinium* in *Acropora* white syndrome was maintained in the coral tissue directly adjacent to and eight centimeters away from the disease lesion. In

contrast, we found that the total area of red fluorescence decreased both directly adjacent to and several centimeters away from the disease front in chronic and acute *Montipora* white syndrome. Histological analyses revealed that *Symbiodinium* density per unit area of gastrodermis was not reduced, thus, the decrease in red fluorescence reflects less coverage of the gastrodermis overall rather than a loss of symbionts. We also found that symbiont density was significantly higher in the surface body wall compared to the basal body wall suggesting that *Symbiodinium* are not migrating deeper into the tissue.

Our study lays the foundation to address several other questions regarding disease progression using natural fluorescence as a proxy of health state for coral or for other naturally fluorescent organisms. In this particular study, we were interested in how coral responds to two widespread tissue loss diseases. Our results indicate that healthy and diseased coral have distinctive patterns of fluorescent pigment distributions. This approach could provide valuable complementary information about the spatial scale of a disease response for other coral where fluorescent protein concentrations are known to change in response to disease. While we were able to reproduce the fluorescence response in laboratory inoculations, we found large individual variation in the rate of disease progression (likely due to the low sample size and use of replicate coral fragments) making it difficult to investigate disease patterns through time. Future studies could explore temporal trends in infection, investigate mode of infection using fluorescently tagged pathogenic bacteria, and compare fluorescence responses across a variety of coral diseases and species, or even investigate disease responses in other

naturally fluorescent organisms. Investigating changes in the spatial arrangement of fluorescent pigments is a new approach to assess disease lesions and within-individual stress responses. Our results indicate that confocal microscopy is a powerful tool that can complement more commonly used disease methods such as histology. In particular, confocal microscopy provides the unique ability for researchers to study *living* organisms, and thus, it can be used to study physiological changes within individuals over time and between individuals across different treatments.

Methods

Collections of healthy coral fragments

We collected 21 4 cm^2 fragments of visually healthy *Montipora capitata* from red, branching colonies between 25 and 35 cm maximum length from Coconut Island in Kāneʻohe Bay, Oʻahu, Hawaiʻi. To capture the natural variability in coral fluorescence from colonies living in different habitats, we collected coral samples from five colonies at one, three and five meter depths, for a total of 15 colonies. All fragments were allowed to acclimate in a water table for at least 24 hours prior to microscopy.

Collections of naturally diseased coral fragments

To characterize fluorescence in naturally diseased colonies, we collected 4 cm^2 coral fragments with partially healthy and partially diseased tissue for 16 colonies exhibiting signs of chronic *Montipora* white syndrome (tissue loss disease with slow progression rate). Diseased fragments were collected from red, branching *M. capitata* colonies between 25 and 35 cm maximum length from ~2 m depth off Coconut Island (same size

and site of healthy fragment collections). All fragments were allowed to acclimate in aquaria for at least 24 hours prior to microscopy.

Collection of healthy and diseased coral for histology

We collected six pairs of coral fragments for histological investigation. We collected 4 cm^2 coral fragments from pairs of visually healthy and diseased red, branching *M. capitata* colonies (colony size ranged from 25-35 cm maximum length) located within 1 m of each other at ~2 m depth off Coconut Island. All colonies were scarified for histological investigation after confocal microscopy.

Histology

After we collected visually healthy and diseased *M. capitata* coral fragments from the field, they were placed in Whirl-paks®, imaged under the confocal microscope and then immediately fixed in 1:4 zinc-buffered formalin (Z-Fix Concentrate, Anatech, Ltd.) diluted with artificial seawater for histological analysis. All fixed samples were rinsed thoroughly in deionized water and then decalcified in 1% formic acid for 1 to 2 days followed by 2 % formic acid for another 1 to 2 d or until fully decalcified. Samples were trimmed to 3 cm^2, placed in cassettes, rinsed thoroughly and then placed in 70 % ethanol. Samples were embedded in paraffin wax, cross sectioned at 5 μm thickness and mounted on slides at Histo Techniques, LTD. De-paraffinized sections were stained with hematoxylin and eosin and cover-slipped prior to light microscopy. To determine whether *Symbiodinium* density varied between health states or location within the tissue, *Symbiodinium* were counted along the contour length of gastrodermis within the surface

and basal body walls for all coral fragments. For diseased tissue, *Symbiodinium* were quantified in the intact tissue directly adjacent to the lesion margin. We normalized counts of zooxanthellae by dividing numbers of each of *Symbiodinium* by contour length (i.e., number of *Symbiodinium* per unit length of tissue) for each health state and location within the tissue (surface or basal body wall).

Laboratory inoculations

To monitor changes in coral fluorescence over time during an infection, we collected 21 visually healthy fragments from three *M. capitata* colonies for laboratory inoculations. Experimental set up and bacterial inoculation was conducted as previously described (Ushijima *et al.*, 2016). Briefly, for each of the three replicate colonies (with seven replicate fragments per colony), four fragments were inoculated with a bacterial pathogen (OCN008), one fragment was inoculated with the non-pathogenic negative control bacterium *Alteromonas* sp. strain OCN004, one fragment was kept in an aquarium with only filtered seawater, and one fragment was left untreated after sampling and kept in a flow-through water table. OCN008 is a strain of *Vibrio coralliilyticus* known to cause acute *Montipora* white syndrome (Ushijima et al. 2014). To limit the handling time of any one coral fragment, we imaged a unique replicate fragment inoculated with the bacterial pathogen at 8, 9, 10 and 11 hours post-inoculation (in contrast to repeatedly imaging the same coral fragment at each sampling time point). All aquariums were maintained at 25 °C under ambient sunlight. The final inoculum concentration used, for both the pathogen and control bacterium, was calculated to be 10^8 CFU per ml of aquarium water.

All marine bacteria were grown in a modified version of glycerol artificial seawater (GASW) media (Ushijima et al. 2012), which was supplemented with 15 g/l of agar prior to autoclaving for solid media. Marine bacteria were kept in cryopreservation at -80 °C until needed, at which stocks were streaked out onto GASW plates and incubated overnight at 29 °C. Colonies from this plate were used to start liquid cultures for downstream uses (e.g. inoculation of coral fragments).

Confocal microscopy

We imaged natural fluorescence of living coral fragments using a Zeiss LSM 710 live-imaging laser-scanning confocal microscope (LSCM). We used excitation lasers at 405 nm and 561 nm and captured emission spectra at 32 wavelengths between 405 and 755 nm. To characterize overall diversity of natural fluorescence and to spatially localize the arrangement of fluorescent pigments, we imaged coral samples at two spatial scales corresponding to the coral branch (image coverage of ~50 mm^2 using a 2.5x objective) and the coral polyp (image coverage of ~1 mm^2 using a 10x objective).

Image analysis

We quantified confocal microscopy spectral images using Photometrica 7.0 (Westboro Photonics). We parsed each confocal image into separate layers corresponding to fluorescence produced in the red and cyan emission spectrum (Figure 5.1D,E,F). Across both fluorescence layers, we delineated and classified key physiological features such as polyps using Area of Interest (AOI) classifiers in Photometrica. Within specified

AOIs (i.e., polyp, branch), we calculated the ratio of total cyan to red fluorescence. At the branch scale (25x objective), we quantified the spatial distribution of fluorescent pigments for each image using five metrics of landscape structure: total area of fluorescence (number of contiguous pixels greater than 400 pixels with luminosity greater than 0.22 Watts), area of edge (perimeter of contiguous patches of fluorescence), edge to area ratio, number of patches (number of AOIs within image corresponding to black areas in Figure 5.1C,J) and area of patches. At the branch scale, we also quantified number of intact polyps based on tentacle and oral disk structure.

Statistical analyses

We analyzed the ratio of cyan to red fluorescence and metrics of landscape structure from the image analysis in R statistical software (version 3.3.1). We compared fluorescence across habitats using one-way analysis of variance tests (ANOVAs) and across inoculation treatments and colony using two-way ANOVAs. We pooled healthy samples from all depths and compared visually healthy and naturally diseased coral using two-sample t-tests for normally distributed and/or transformed variables with normal distributions and Wilcoxon rank sum tests for non-normally distributed variables (Table 5.1). To compare *Symbiodinium* density between visually healthy and naturally diseased corals and between the surface and basal body walls, we first log transformed *Symbiodinium* density and then conducted paired t-tests. To compare fluorescence over time for the inoculation experiment, we conducted repeated measures mixed effects models on replicate fragments from the same coral colony imaged over time.

Table 5.1 Analysis of spatial distribution of fluorescent pigments and ratio of fluorescence emission spectra.

Variable	Healthy group mean	Diseased group mean	Degrees of freedom	P-value
Total area fluorescence (mm)	44	37	29	0.01
Number of intact polyps	5.4	1.6	6	0.002
Area of edge (mm)	5.8	8	30	0.01
Number of patches	3.17	4.82	32	0.02
Area of patches* (mm)	0.02	0.05	-	0.30
Edge:area ratio	0.14	0.25	22	0.002
Cyan:red fluorescence ratio*	0.0001	0.05	-	0.20
Cyan:red fluorescence ratio*†	44	3.9	-	0.13

*Non-parametric Wilcoxon rank sum test

† Measurement taken using 10x objective (polyp scale)

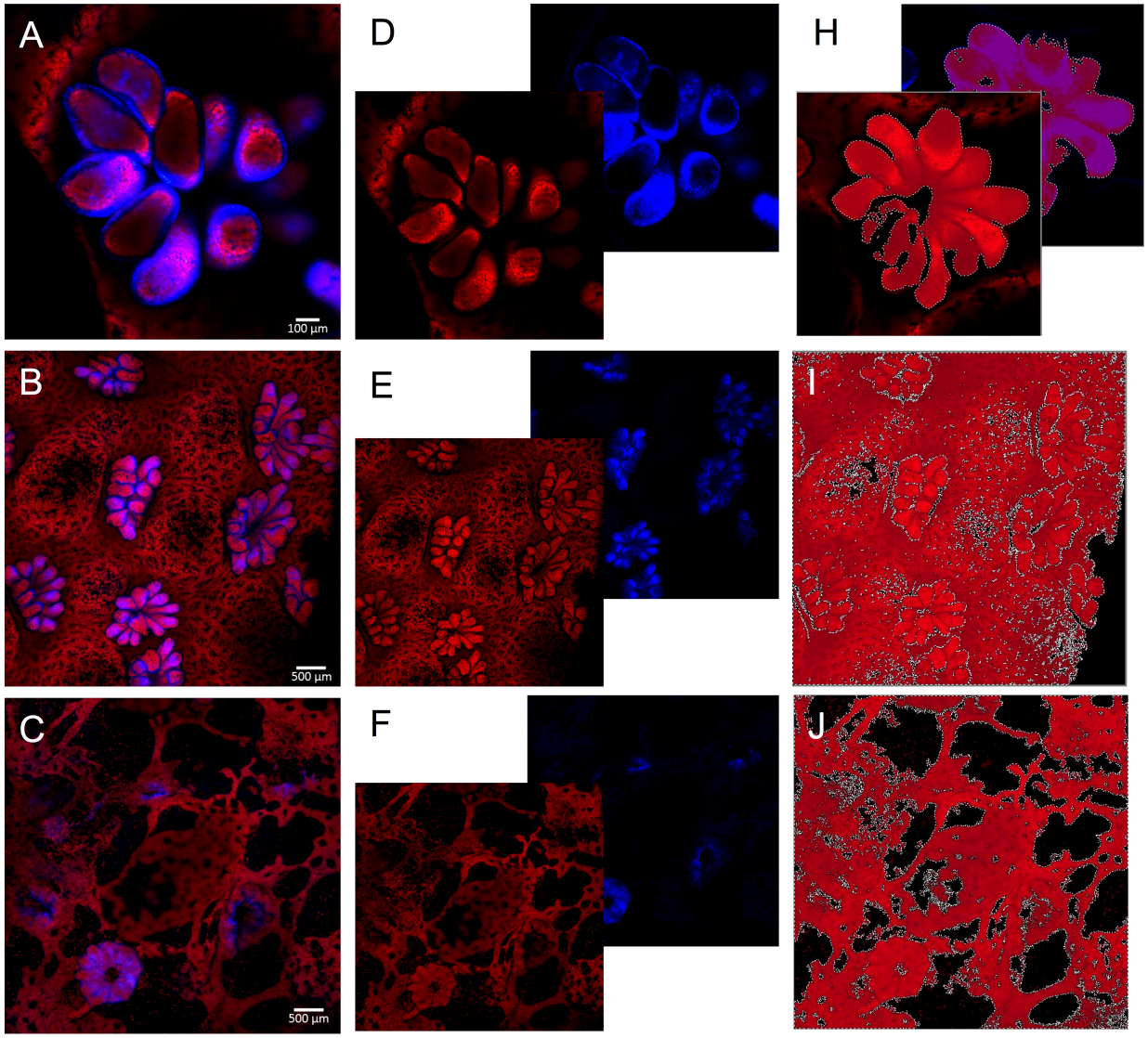

Figure 5.1 Confocal microscopy imagery and analysis. Confocal images of live *M. capitata* specimens at the A) polyp scale (10x objective) and B-C) branch scale (25x objective). Imagery was exported in layers corresponding to dominant emission spectra (D-F). Photometrica 7.0 was used to identify areas of interest to compare ratio of cyan to red fluorescence (H) and to compare measures of landscape structure (I-J). In images I-J, the area highlighted in red reflects total area of fluorescence; black regions indicate patches and white lines indicate edges.

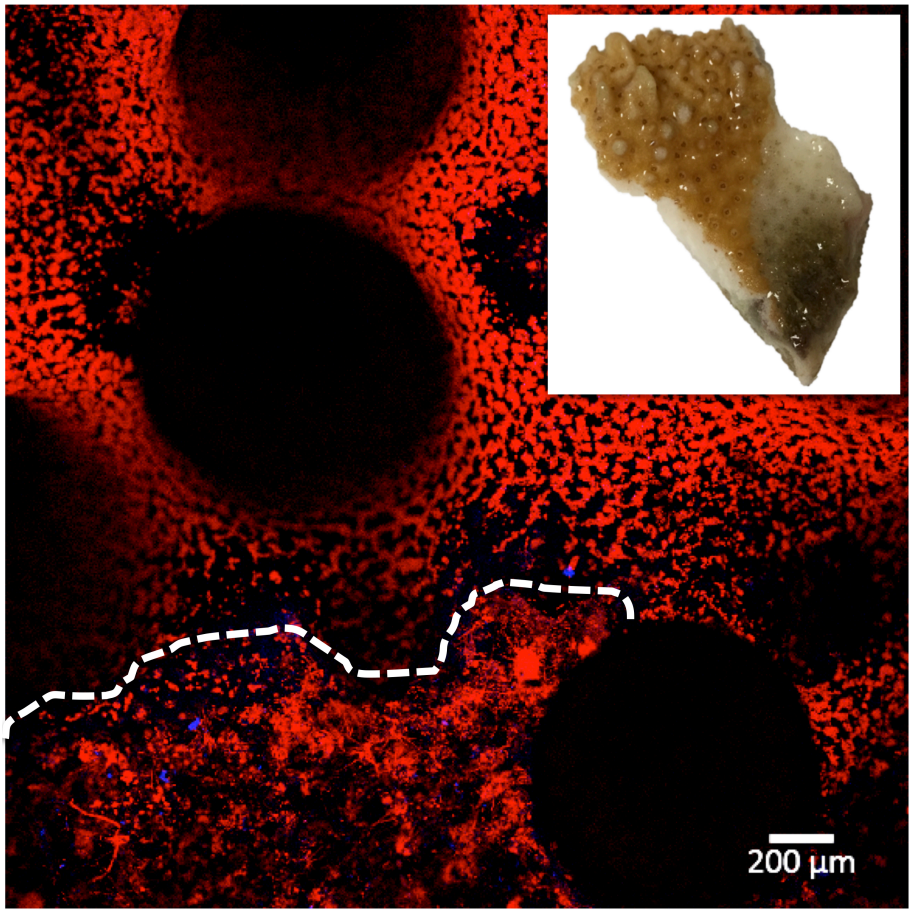

Figure 5.2 Linear extension of disease front. White dotted line indicates the extent of fluorescence area affected in a diseased fragment directly adjacent to the disease front (microscopy image). Inset image shows the diseased coral fragment corresponding to the microscopy image.

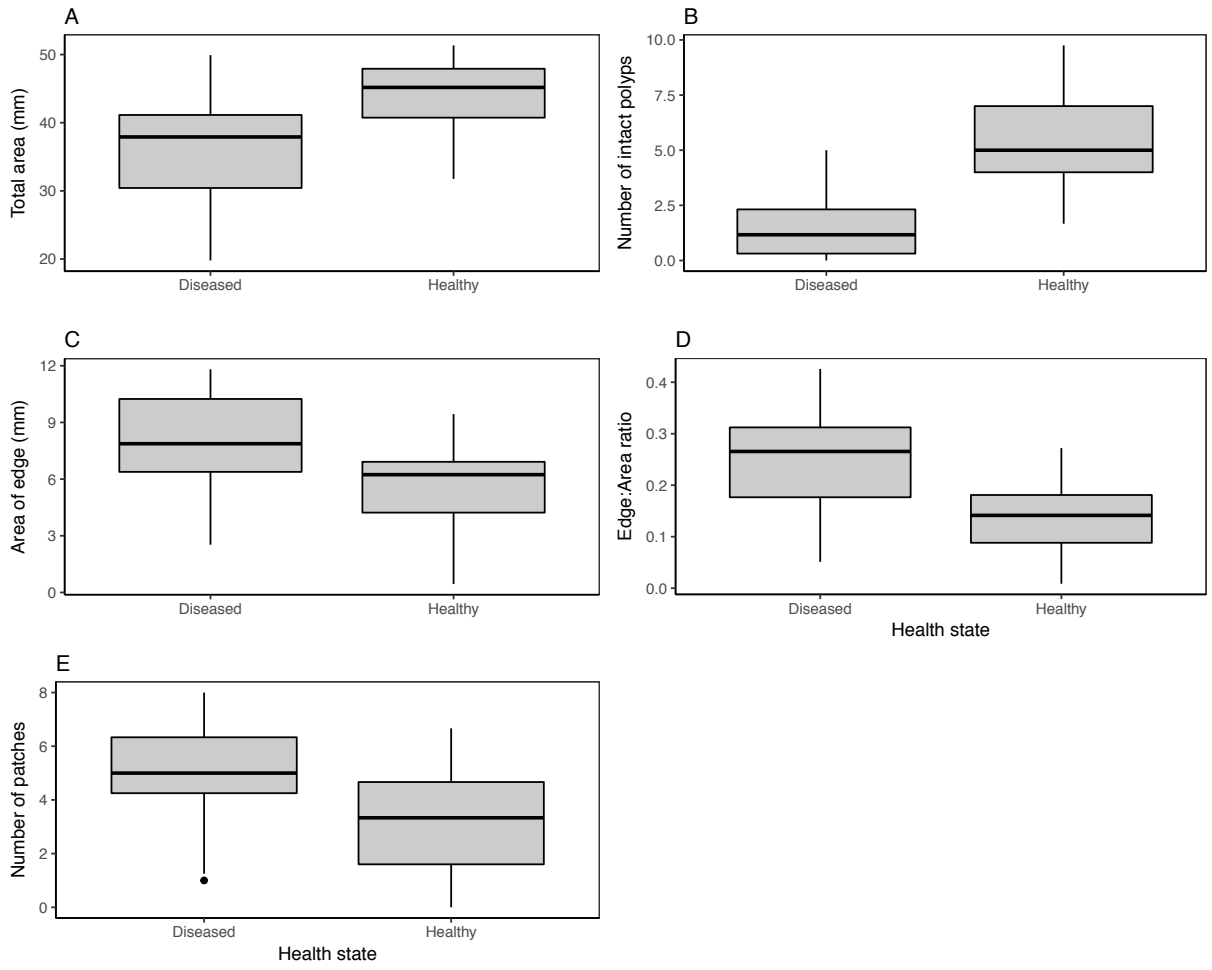

Figure 5.3 Differences in landscape structure between healthy and naturally diseased coral. Boxplots showing significant differences between healthy and diseased coral colonies in A) total area of fluorescence, B) number of intact polyps, C) mean area of edge, D) mean edge to area ratio, and E) mean number of patches within image frame (~55 mm^2). Boxplot whiskers indicate 95% confidence intervals. The black point indicates an outlier, which was kept in the dataset for analysis.

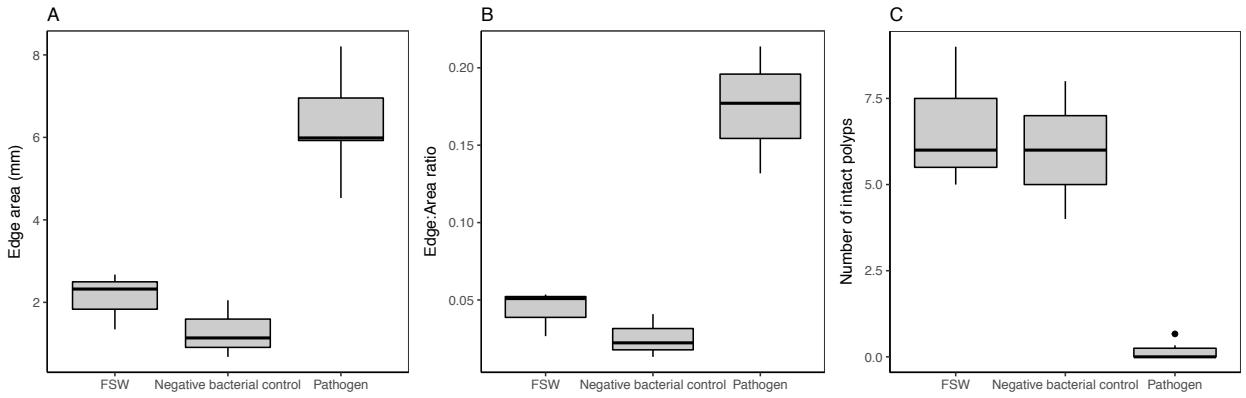

Figure 5.4 Differences in landscape structure between healthy and laboratory inoculated corals. Boxplots showing significant differences across treatments in A) mean area of edge and B) mean edge to area ratio, and C) number of intact polyps within image frame (~55 mm^2). Boxplot whiskers indicate 95% confidence intervals. The black point indicates an outlier, which was kept in the dataset for analysis.

CHAPTER 6

DISCUSSION

Diseases appear to be increasing in many marine invertebrates and vertebrates around the world (Ward and Lafferty 2004), yet our fundamental understanding of how diseases spread in the ocean remains limited. Most marine disease research is based on terrestrial epidemiology, but research advancements over the last few decades suggests that disease processes may substantially differ between terrestrial and marine systems because of differences in taxonomic diversity, life history traits and modes of transmission (McCallum et al. 2004). To address this knowledge gap, my dissertation research examined host-pathogen-environment interactions for several coral diseases to improve our understanding of disease risk and transmission in the marine environment at various spatial scales.

At broad spatial scales, variation in coral disease prevalence in the Hawaiian archipelago was associated with habitat structure and environment. Spatial patterns in disease prevalence based on 12 years of observational data indicated that disease prevalence varied across sites within the same region of coastline. This variation was partially explained by habitat structure (e.g., host density, water motion and fish abundance) and environmental variation (e.g., temperature and rainfall anomalies). Together, these results suggest that local biotic and abiotic habitat features can mitigate or amplify stress from anomalous environmental conditions and influence disease risk. These results are valuable for untangling natural variation in disease prevalence, with increased disease risk due to human activities.

At the scale of an individual patch reef, host traits and coral reef configuration influenced coral disease risk and transmission rates. Coral colony size, severity of diseased neighbors and number of diseased neighbors were associated with disease risk during an emerging tissue loss disease outbreak. Transmission rates were highest within a very localized area (~15 m) indicating disease spread can be highly constrained within the ocean, despite the potential for pathogens to disperse broadly via waterborne transmission. Disease transmission rates also changed dramatically over the course of a relatively short time period (days to weeks). Therefore, it is important consider that epidemiology parameters that describe the speed and strength of a disease outbreak (e.g., effective reproductive ratio, force of infection) could be constantly changing for coral diseases, and without accounting for that temporal variation, outbreak impact could be substantially underestimated.

Within individual coral colonies, spatial patterns in natural coral fluorescence revealed distinctive disease lesions adjacent to the disease front. Compared to healthy coral, colonies exhibiting signs of chronic and acute *Montipora* white syndrome had spatially fragmented fluorescence and that disruption in pigment structure was highly localized near the disease front, potentially indicating that the pathogen moves directly away from the disease front rather than spreading systemically throughout the coral colony. The histology results further indicate that the pathogen targeted coral tissue rather than *Symbiodinium.* These spatially explicit intra-colony patterns indicated that, in diseased colonies, there is substantial variation in health state between polyps across a single colony.

Overall, my dissertation demonstrates that marine disease spread is limited by multiple interacting factors on different spatial scales, which should be considered when assessing disease prevalence within the context of climate change. Although there are some notable widespread marine disease outbreaks (e.g., seastar wasting disease, Eisenlord et al. 2016; eelgrass wasting disease, Short et al. 1987), this research suggests coral disease may be constrained within local areas. It is likely that there may be unique physical barriers to disease transmission in the marine environment that do not apply to terrestrial systems, such as eddies, persistent fronts and internal tides. In general, epidemics are projected to become more frequent and intense in the future due to ongoing climate change (Harvell et al. 2002). However, this research indicates that habitat structure, coral configuration, host traits and even intra-colony immune responses can slow or prevent disease spread despite increasing climatic stress.

These results also provide a pathway to discuss concrete solutions for managing coral health over short- and long-term time scales. Corals are currently facing an unprecedented amount of environmental stress. In my dissertation, I have highlighted several conditions that increase coral susceptibility to disease and described short- and long-term management strategies. In the short-term, we can use early warning systems that remotely monitor anomalous environmental conditions to provide rough estimates of disease risk up to six months prior to an expected outbreak event. To complement early warning systems, management strategies should aim to reduce and/or remove chronic stressors from the environment, such as nitrogen, phosphorus and other toxins found in fertilizer runoff from agriculture and golf courses. In addition, management

strategies should consider how physical features of the environment, such as wave exposure, and habitat composition, such as host density, affects coral health. An important next step for future research should take a mechanistic approach to better understand how these stressors (and others) relate to disease onset for a variety of coral diseases.

At the present time, a major knowledge gap within the field of marine disease ecology, and in particular for coral diseases, is disease control strategies. Many effective wildlife disease control strategies in terrestrial systems, such as vaccination and culling, are not feasible in the marine environment. A number of interventions have been proposed to prevent marine disease outbreaks or reduce their impact, such as activities that boost host immunity (using healthy cell micro-biota as probiotics, Ritchie 2006), reduce pathogen abundance (phage therapy to attack pathogenic bacteria, Cohen et al. 2012), and reduce rates of pathogen transmission (disrupting pathogenic cell-cell communications, Teplitski and Ritchie 2009). While these experimental strategies are promising, they could not easily be implemented at the appropriate spatial scales. Biological control strategies may be one method to reduce pathogenic organisms in the ocean. For example, filter feeding organisms such as oysters could be placed in coastal areas with high runoff to improve water quality. Controling marine diseaeses will likley require multiple strategies such as biocontrol methods, early warning systems and adaptive management practices. Interdisciplinary and adaptive management strategies are needed to improve coral reef health and can be used to support marine conservation initiatives more broadly, which, in the face of climate change and ocean

acidification is more important than ever before.

References

Acevedo-Whitehouse K, Gulland F, Greig D, and Amos W. 2003. Inbreeding: Disease Susceptibility in California Sea Lions. *Nature* 422 (6927): 35.

Aeby GS. 2005. Outbreak of Coral Disease in the Northwestern Hawaiian Islands. *Coral Reefs* 24 (3): 481.

Aeby GS, Kenyon JC, Maragos JE, and Potts DC. 2003. First Record of Mass Coral Bleaching in the Northwestern Hawaiian Islands. *Coral Reefs* 22 (3): 256.

Aeby GS. 2009. Baseline Levels of Coral Disease in the Northwestern Hawaiian Islands. Coral Health and Disease in the Pacific: Vision for Action. NOAA Technical Memorandum NOS NCCOS 97: 168.

Aeby GS, Ross M, Williams GJ, Lewis TD, and Work TM. 2010. Disease Dynamics of *Montipora* White Syndrome within Kāneʻohe Bay, Oʻahu, Hawaiʻi: Distribution, Seasonality, Virulence, and Transmissibility. *Diseases Of Aquatic Organisms* 91 (1): 1.

Aeby GS, Callahan S, Cox EF, Runyon C, Smith A, Stanton FG, Ushijima B, and Work TM. 2016. Emerging Coral Diseases in Kāneʻohe Bay, Oʻahu, Hawaiʻi (USA): Two Major Disease Outbreaks of Acute *Montipora* White Syndreom. *Diseases Of Aquatic Organisms* 119: 189.

Aeby G, Williams GJ, Franklin EC, Haapkyla J, Harvell CD, Neale S, Page C, Raymundo L, vargas-Angel B, Willis BL, Work TM, and Davy SK. 2011. Growth Anomalies on the Coral Genera *Acropora* and *Porites* Are Strongly Associated with Host Density and Human Population Size across the Indo-Pacific. *PloS One* 6 (2): e16887.

Aeby G, Williams GJ, Franklin EC, Kenyon J, Cox EF, Coles S, and Work TM. 2011. Patterns of Coral Disease across the Hawaiian Archipelago: Relating Disease to Environment. *PLoS One* 6 (5): e20370.

Aeby GS, Work TM, Runyon CM, Shore-Maggio A, Ushijima B, and Videau P. 2015. First Record of Black Band Disease in the Hawaiian Archipelago: Response, Outbreak Status, Virulence, and a Method of Treatment. *PloS One* 10 (3): e0120853.

Alieva NO, Konzen KA, Field SF, Meleshkevitch EA, Hunt ME, Beltran-Ramirez V, Miller DJ, Wiedenmann J, Salih A, and Matz MV. 2008. Diversity and Evolution of Coral Fluorescent Proteins. *PloS One* 3 (7): e2680.

Altizer S, Dobson A, Hosseini P, Hudson P, Pascual M, and Rohani P. 2006. Seasonality and the Dynamics of Infectious Diseases. *Ecology Letters* 9 (4): 467.

Altizer S, Harvell D, and Friedle E. 2003. Rapid Evolutionary Dynamics and Disease Threats to Biodiversity. *Trends in Ecology and Evolution* 18 (11): 589.

Altizer S, Ostfeld RS, Johnson PTJ, Kutz S, and Harvell CD. 2013. Climate Change and Infectious Diseases: From Evidence to a Predictive Framework. *Science* 341 (6145): 514.

Alvarez-Filip L, Dulvy NK, Gill JA, Côté IM, and Watkinson AR. 2009. Flattening of Caribbean Coral Reefs: Region-Wide Declines in Architectural Complexity. *Proceedings. Biological Sciences / The Royal Society* 276 (1669): 3019.

Anderson RM. 1978. The Regulation of Host Population Growth by Parasitic Species. *Parasitology* 76 (2): 119.

Apprill AM, Bidigare RR, and Gates RD. 2007. Visibly Healthy Corals Exhibit Variable

Pigment Concentrations and Symbiont Phenotypes. *Coral Reefs* 26: 387.

Aronson RB and Precht WF. 2001. White-Band Disease and the Changing Face of Caribbean Coral Reefs. *Hydrobiologia* 460: 25.

Augustin R and Bosch T. 2010. Cnidarian Immunity: A Tale of Two Barriers. Invertebrate Immunity in Advances in Experimental Medicine and Biology 708: 1.

Ban SS, Graham NAJ, and Connolly SR. 2014. Evidence for Multiple Stressor Interactions and Effects on Coral Reefs. *Global Change Biology* 20 (3): 681.

Beeden R, Maynard JA, Marshall PA, Heron SF, and Willis BL. 2012. A Framework for Responding to Coral Disease Outbreaks That Facilitates Adaptive Management. *Environmental Management* 49 (1): 1.

Ben-Haim Y and Rosenberg E. 2002. A Novel *Vibrio* sp. Pathogen of the Coral *Pocillopora damicornis*. *Marine Biology* 141 (1): 47.

Bertuzzo E, Casagrandi R, Gatto M, Rodriguez-Iturbe I, and Rinaldo A. 2010. On Spatially Explicit Models of Cholera Epidemics. *Journal of the Royal Society, Interface* 7 (43): 321.

Brandt ME and McManus JW. 2009. Dynamics and Impact of the Coral Disease White Plague: Insights from a Simulation Model. *Diseases Of Aquatic Organisms* 87: 117.

Bruckner AW and Hill RL. 2009. Ten Years of Change to Coral Comunities off Mona and Desecheo Islands, Puerto Rico, from Disease and Bleaching. *Diseases of Aquatic Organisms* 87: 19.

Bruno JB, Ellner SP, Vu I, Kim K, and Harvell CD. 2011. Impacts of Aspergillosis on Sea Fan Coral Demography: Modeling a Moving Target. *Ecological Monographs* 81 (1): 123.

Bruno JF, Selig ER, Casey KS, Page CA, Willis BL, Harvell CD, Sweatman H, and Melendy AM. 2007. Thermal Stress and Coral Cover as Drivers of Coral Disease Outbreaks. *PLoS Biology* 5 (6): e124.

Burge CA, Eakin CM, Friedman CS, Froelich B, Hershberger PK, Hofmann EE, Petes LE,Prager KC, Weil E, Willis BL, Ford SE, and Harvell CD. 2014. Climate Change Influences on Marine Infectious Diseases: Implications for Management and Society. *Annual Review of Marine Science* 6: 249.

Burge CA, Kim K, Lyles JM, and Harvell CD. 2013. Special Issue Oceans and Humans Health: The Ecology of Marine Opportunists. *Microbial Ecology* 65 (4): 869.

Burns J and Takabayashi M. 2011. Histopathology of growth anomaly affecting the coral, *Montipora capitata*: implications on biological functions and population viability. PLoS One 6 (11): e28854.

Caldwell JM, Heron SF, Eakin CM, and Donahue MJ. 2016. Satellite SST-Based Coral Disease Outbreak Predictions for the Hawaiian Archipelago. *Remote Sensing* 8 (2): 93.

Caldwell JM, Burns JHR, Couch C, Ross M, Runyon C, Takabayashi M, Vargas-Ángel B, Walsh W, Walton M, White D, Williams G, and Heron SF. 2016. Hawai‘i Coral Disease Database (HICORDIS): Species-Specific Coral Health Data from across the Hawaiian Archipelago. *Data in Brief*.

Cappelle J, Girard O, Fofana B, Gaidet N, and Gilbert M. 2010. Ecological Modeling of the Spatial Distribution of Wild Waterbirds to Identify the Main Areas Where Avian Influenza Viruses Are Circulating in the Inner Niger Delta, Mali. *EcoHealth* 7: 283.

Carpenter KE, Abrar M, Aeby G, Aronson RB, Banks S, Bruckner A, Chiriboga A, et al.

2008. One-Third of Reef-Building Corals Face Elevated Extinction Risk from Climate Change and Local Impacts. *Science* 321 (5888): 560.

Casey KS, Brandon TB, Comillon P, and Evans R. 2010. The Path, Present, and Future of the AVHRR Pathfinder SST Program in *Oceanography from Space* 273.

Cervino JM, Hayes RL, Polson SW, Polson SC, Goreau TJ, Martinez RJ, and Smith GW. 2004. Relationship of *Vibrio* Species Infection and Elevated Temperatures to Yellow Blotch/Band Disease in Caribbean Corals. *Applied and Environmental Microbiology* 70 (11): 6855.

Chapin III FS, Walker BH, Hobbs RJ, Hooper DU, Lawton JH, Osvaldo ES, and Tilman D. 1997. Biotic Control over the Functioning of Ecosystems. *Science* 277 (5325): 500.

Cohen Y, Pollock JF, Rosenberg E, and Bourne DG. 2012. Phage Therapy Treatment of the Coral Pathogen *Vibrio coralliilyticus*. *Microbiology Open* 2 (1): 64.

Combosch DJ and Vollmer SV. 2011. Population Genetics of an Ecosystem-Defining Reef Coral *Pocillopora damicornis* in the Tropical Eastern Pacific. *PLoS ONE* 6 (8): e21200.

Concepcion GT, Baums IB, and Toonen RJ. 2014. Regional Population Structure of *Montipora Capitata* across the Hawaiian Archipelago. *Bulletin of Marine Science* 90 (1): 257.

Couch CS, Garriques JD, Barnett C, Preskitt L, Cotton S, Giddens J, and Walsh W. 2014. Spatial and Temporal Patterns of Coral Health and Disease along Leeward Hawai‘i Island. *Coral Reefs* 33 (3): 693.

D’Angelo C, Smith EG, Oswald F, Burt J, Tchernov D, and Wiedenmann J. 2012.

Locally Accelerated Growth Is Part of the Innate Immune Response and Repair Mechanisms in Reef-Building Corals as Detected by Green Fluorescent Protein (GFP)-like Pigments. *Coral Reefs* 31 (4): 1045.

Darling E, Lorenzo A, Oliver T, McClanahan T, Cote I and Bellwood D. 2012. Evaluating life-history strategies of reef corals from species traits. *Ecology letters* 15 (12): 1378-1386.

Daszak P, Cunningham AA, and Hyatt AD. 2000. Emerging Infectious Diseases of Wildlife—Threats to Biodiversity and Human Health. *Science* 287: 443.

Department of Land and Natural Resources, Division of Aquatic Resources. 2015. Record Ocean Temperatures Causing Coral Bleaching Across Hawai‘i. Honolulu. http://dlnr.hawaii.gov/blog/2015/09/11/nr15-135/.

Dove SG, Hoegh-Guldberg O, and Ranganathan S. 2001. Major Colour Patterns of Reef-Building Corals Are due to a Family of GFP-like Proteins. *Coral Reefs* 19 (3): 197.

Dube D, Kim K, Alker AP, and Harvell CD. 2002. Size Structure and Geographic Variation in Chemical Resistance of Sea Fan Corals *Gorgonia ventalina* to a Fungal Pathogen. *Marine Ecology Progress Series* 231: 139.

Dunn SR. 2010. Immunorecognition and Immunoreceptors in the Cnidaria. *Invertebrate Survival Journals* 6 (1): 7.

Eakin CM, Morgan JA, Heron SF, Smith TB, Liu G, Alvarez-Filip L, Baca B, et al. 2010. Caribbean Corals in Crisis: Record Thermal Stress, Bleaching, and Mortality in 2005. *PloS One* 5 (11): e13969.

Eisenlord ME, Groner ML, Yoshioka RM, Elliott J, Maynard J, Fradkin S, Turner M,

Pyne K, Rivlin N, van Hooidonk R, and Harvell CD. 2016. Ochre Star Mortality during the 2014 Wasting Disease Epizootic: Role of Population Size Structure and Temperature. *Philosophical Transactions of the Royal Society B, Biological Sciences* 371 (1689): 20150212.

Elith J, Leathwick JR, and Hastie T. 2008. A Working Guide to Boosted Regression Trees. *Journal of Animal Ecology* 77: 802.

Ellis RP, Parry H, Spicer JI, Hutchinson TH, Pipe RK, and Widdicombe S. 2011. Immunological Function in Marine Invertebrates: Responses to Environmental Perturbation. *Fish & Shellfish Immunology* 30 (6): 1209.

Finlay BB and McFadden G. 2006. Anti-Immunology: Evasion of the Host Immune System by Bacterial and Viral Pathogens. *Cell* 124 (4): 767.

Fisher MC, Henk DA, Briggs CJ, Brownstein JS, Madoff LC, McCraw SL, and Gurr SJ. 2012. Emerging Fungal Threats to Animal, Plant and Ecosystem Health. *Nature* 484 (7393): 186.

Franklin EC, Jokiel PL, and Donahue MJ. 2013. Predictive Modeling of Coral Distribution and Abundance in the Hawaiian Islands. *Marine Ecology Progress Series* 481: 121.

Frazier AG, Giambelluca TW, Diaz HF, and Needham HL. 2016. Comparison of Geostatistical Approaches to Spatially Interpolate Month-Year Rainfall for the Hawaiian Islands. *International Journal of Climatology* 36 (3): 1459.

French MD, Churcher TS, Webster JP, Fleming FM, Fenwick A, Kabatereine NB, Sacko M, Garba A, Toure S, Nyandindi U, Mwansa J, Blaire L, Bosque-Oliva E, and Basanez BG. 2015. Estimation of changes in the force of infection for intestinal and

urogenital schistosomiasis in countries with schistosomiasis control initiative-assisted programmes. *Parasites & Vectors* 8: 558.

Frydenborg BR, Krediet CJ, Teplitski M, and Ritchie KB. 2013. Temperature-Dependent Inhibition of Opportunistic *Vibrio* Pathogens by Native Coral Commensal Bacteria. *Microbial Ecology* 67 (2): 392.

Gachon CMM, Strittmatter M, Müller DG, Kleinteich J, and Küpper FC. 2009. Detection of Differential Host Susceptibility to the Marine Oomycete Pathogen *Eurychasma Dicksonii* by Real-Time PCR: Not All Algae Are Equal. *Applied and Environmental Microbiology* 75 (2): 322.

Gove Jamison M, Williams GJ, McManus MA, Heron SF, Sandin SA, Vetter OJ, and Foley DG. 2013. Quantifying Climatological Ranges and Anomalies for Pacific Coral Reef Ecosystems. *PloS One* 8 (4): e61974.

Groner ML, Burge CA, Couch CS, Kim CJS, Siegmund GF, Singhal S, Smoot SC, Jarrell A, Gaydos JK, Harvell CD, and Wyllie-Echeverria S. 2014. Host Demography Influences the Prevalence and Severity of Eelgrass Wasting Disease. *Diseases of Aquatic Organisms* 108 (2): 165.

Guzner B, Novplansky A, Shalit O, and Chadwick NE. 2010. Indirect Impacts of Recreational Scuba Diving: Patterns of Growth and Predation in Branching Stony Corals. *Bulletin of Marine Science* 86 (3): 727.

Haapkylä J, Melbourne-Thomas J, Flavell M, and Willis BL. 2013. Disease Outbreaks, Bleaching and a Cyclone Drive Changes in Coral Assemblages on an Inshore Reef of the Great Barrier Reef. *Coral Reefs* 32 (3): 815.

Haapkylä J, Seymour AS, Trebilco J, and Smith D. 2007. Coral Disease Prevalence and

Coral Health in the Wakatobi Marine Park, South-East Sulawesi, Indonesia. *Journal of the Marine Biological Association of the UK* 87 (2): 403.

Haapkylä J, Unsworth RKF, Flavell M, Bourne DG, Schaffelke B, and Willis BL. 2011. Seasonal Rainfall and Runoff Promote Coral Disease on an Inshore Reef. *PloS One* 6 (2): e16893.

Harvell, CD, Mitchell CE, Ward JR, Altizer S, Dobson AP, Ostfeld RS, and Samuel MD. 2002. Climate Warming and Disease Risks for Terrestrial and Marine Biota. *Science* 296 (5576): 2158.

Harvell CD, Aronson R, Baron N, Connell J, Dobson A, Ellner S, Gerber L, Kim K, Kuris A, McCallum H, Lafferty K, McKay B, Porter J, Pascual M, Smith G, Sutherland K, and Ward J. 2004. The Rising Tide of Ocean Diseases: Unsolved Problems and Research Priorities. *Ecology* 2 (7): 375.

Hatcher MJ, Dick JTA, and Dunn AM. 2006. How Parasites Affect Interactions Between Competitors and Predators. *Ecology Letters* 9 (11): 1253.

Hatcher MJ, Dick JTA, and Dunn AM. 2014. Parasites That Change Predator or Prey Behaviour Can Have Keystone Effects on Community Composition. *Biology Letters* 10 (1): 20130879.

Hawley DM and Altizer SM. 2011. Disease Ecology Meets Ecological Immunology: Understanding the Links between Organismal Immunity and Infection Dynamics in Natural Populations. *Functional Ecology* 25 (1): 48.

Heenan A, Ayotte P, Gray A, Lino K, McCoy K, Zamzow J, and Williams I. 2014. Ecological Monitoring 2012-2013 - Reef Fishes and Benthic Habitats of the Main Hawaiian Islands, American Samoa, and Pacific Remote Island Areas. National

Oceanic and Atmospheric Administration Report.

Hens N, Aerts M, Faes C, Shkedy Z, Lejeune O, Van Damme P, and Beutels P. 2010. Seventy-Five Years of Estimating the Force of Infection from Current Status Data. *Epidemiology and Infection* 138 (6): 802.

Heron SF, Willis BL, Skirving WJ, Eakin CM, Page CA, and Miller IR. 2010. Summer Hot Snaps and Winter Conditions: Modelling White Syndrome Outbreaks on Great Barrier Reef Corals. *PloS One* 5 (8): e12210.

Hill R, Schreiber U, Gademann R, Larkum AWD, Kohl M, and Ralph PJ. 2004. Spatial Heterogeneity of Photosynthesis and the Effect of Temperature-Induced Bleaching Conditions in Three Species of Corals. *Marine Biology* 144 (4): 633.

Hobbs JPA, Frisch AJ, Newman SJ, and Wakefield CB. 2015. Selective Impact of Disease on Coral Communities: Outbreak of White Syndrome Causes Significant Total Mortality of *Acropora* Plate Corals. *PloS One* 10 (7): e0132528.

Howard SC and Donnelly CA. 2000. Estimation of a Time-Varying Force of Infection and Basic Reproduction Number with Application to an Outbreak of Classical Swine Fever. *Journal of Epidemiology and Biostatistics* 5 (3): 161.

Hughes TP and Jackson JB. 1980. Do Corals Lie about Their Age? Some Demographic Consequences of Partial Mortality, Fission, and Fusion. *Science* 209 (4457): 713.

Hughes TP, Rodrigues MJ, Bellwood DR, Ceccarelli D, Hoegh-Guldberg O, McCook L, Moltschaniwskyj N, Pratchett MS, Steneck RS, and Willis B. 2007. Phase Shifts, Herbivory, and the Resilience of Coral Reefs to Climate Change. *Current Biology* 17 (4): 360.

Islam S and Tanaka M. 2004. Impacts of Pollution on Coastal and Marine Ecosystems

Including Coastal and Marine Fisheries and Approach for Management: A Review and Synthesis. *Marine Pollution Bulletin* 48 (7): 624.

Johnson CE and Goulet TL. 2007. A Comparison of Photographic Analyses Used to Quantify Zooxanthella Density and Pigment Concentrations in Cnidarians. *Journal of Experimental Marine Biology and Ecology* 353: 287.

Johnson PTJ and Thieltges DW. 2010. Diversity, Decoys and the Dilution Effect: How Ecological Communities Affect Disease Risk. *The Journal of Experimental Biology* 213 (6): 961.

Jolles AE, Sullivan P, Alker AP, and Harvell CD. 2002. Disease Transmission of Aspergillosis in Sea Fans: Inferring Process from Spatial Pattern. *Ecology* 83 (9): 2373.

Kaczmarsky L. 2012. Coral Disease Dynamics in the Central Philippines. *Diseases of Aquatic organisms* 69 (1): 9.

Kauffman MJ and Jules ES. 2006. Heterogeneity Shapes Invasion: Host Size And Environment Influence Susceptibility To A Nonnative Pathogen. *Ecological Applications* 16 (1): 166.

Keesing F, Holt RD, and Ostfeld RS. 2006. Effects of Species Diversity on Disease Risk. *Ecology Letters* 9 (4): 485.

Kennedy S, Kuiken T, Jepson PD, Deaville R, Forsyth M, Barrett T, van de Bildt MWG, Osterhaus AD, Eybatov T, Duck C, Kydymanov A, Mitrofanov I, and Wilson S. 2000. Mass Die-Off of Caspian Seals Caused by Canine Distemper Virus. *Emerging Infectious Diseases* 6 (6): 637.

Kermack WO and McKendrick AG. 1927. A Contribution to the Mathematical Theory of

Epidemics. *Proceedings of the Royal Society A: Mathematical, Physical and Engineering Sciences* 115 (772): 700.

Kim K and Harvell CD. 2004. The Rise and Fall of a Six-Year Coral-Fungal Epizootic. *The American Naturalist* 164: 52.

Kimes NE, Grim CJ, Johnson WR, Hasan NA, Tall BD, Kothary MH, Kiss H, Munk AC, Tapia R, Green L, Detter C, Bruce DC, Brettin TS, Colwell RR, and Morris PJ. 2012. Temperature Regulation of Virulence Factors in the Pathogen *Vibrio coralliilyticus*. *ISME Journal* 6 (4): 835.

Kramer AM, Pulliam JT, Alexander LW, Park AW, Rohani P, and Drake JM. 2016. Spatial Spread of the West Africa Ebola Epidemic. *Royal Society Open Science* 3: 160294.

Lafferty KD. 2009. The Ecology of Climate Change and Infectious Diseases. *Ecology* 90 (4): 888.

Lafferty KD and Kuris AM. 1993. Mass Mortality of Abalone *Haliotis cracherodii* on the California Channel Islands: Tests of Epidemiological Hypotheses. *Marine Ecology Progress Series* 96: 239.

Lafferty KD, Allesina S, Arim M, Briggs CJ, De Leo G, Dobson AP, Dunne JA, Johnson PTJ, Kuris AM, Marcogliese DJ, Martinez ND, Memmott J, Marquet PA, McLaughlin JP, Mordecai EA, Pascual M, Poulin R, and Thieltges DW. 2008. Parasites in Food Webs: The Ultimate Missing Links. *Ecology Letters* 11 (6): 533.

Lafferty KD and Mordecai EA. 2016. The Rise and Fall of Infectious Disease in a Warmer World. *F1000 Research* 5.

Lasker HR and Coffroth MA. 1999. Responses of Clonal Reef Taxa to Environmental

Change. *American Zoology* 39: 92.

Lecky J. 2016. Ecosystem Vulnerability and Mapping Cumulative Impacts on Hawaiian Reefs. Master's thesis, University of Hawai'i at Manoa.

Lentz JA, Blackburn JK, and Curtis AJ. 2011. Evaluating Patterns of a White-Band Disease (WBD) Outbreak in *Acropora palmata* Using Spatial Analysis: A Comparison of Transect and Colony Clustering. *PloS One* 6 (7): e21830.

Lirman D. 2000. Fragmentation in the Branching Coral *Acropora palmata* (Lamarck): Growth, Survivorship, and Reproduction of Colonies and Fragments. *Journal of Experimental Marine Biology and Ecology* 251 (1): 41.

Liu G, Heron SF, Eakin CM, Muller-Karger F, Vega-Rodriguez M, Guild L, De La Cour J, Geiger EF, Skirving WJ, Burgess TFR, Strong AE, Harris A, Maturi E, Ignatov A, Sapper J, Li J, and Lynds S. 2014. Reef-Scale Thermal Stress Monitoring of Coral Ecosystems: New 5-Km Global Products from NOAA Coral Reef Watch. *Remote Sensing* 6 (11): 11579.

Lloyd-Smith JO, Cross PC, Briggs CJ, Daugherty M, Getz WM, Latto J, Sanchez MS, Smith AB, and Swei A. 2005. Should We Expect Population Thresholds for Wildlife Disease? *Trends in Ecology & Evolution* 20 (9): 511.

Martindale JL and Holbrook NJ. 2002. Cellular Response to Oxidative Stress: Signaling for Suicide and Survival. *J Cell Physiol* 192 (1): 1.

Maynard JA, Anthony KRN, Harvell CD, Burgman MA, Beeden R, Sweatman H, Heron SF, Lamb JB, and Willis BL. 2011. Predicting Outbreaks of a Climate-Driven Coral Disease in the Great Barrier Reef. *Coral Reefs* 30: 485.

Mazel C. 1997. Coral Fluorescence Characteristics: Excitation-Emission Spectra,

Fluorescence Efficiences, and Contribution to Apparent Reflectance. *SPIE* 2963: 240.

McCallum H, Barlow N, and Hone J. 2001. How Should Pathogen Transmission Be Modelled? *Trends in Ecology & Evolution* 16 (6): 295.

Mccallum HI, Kuris A, Harvell CD, Lafferty KD, Smith GW, and Porter J. 2004. Does Terrestrial Epidemiology Apply to Marine Systems? *Trends in Ecology and Evolution Evolution* 19 (11): 585.

McNew GL. 1960. The Nature, Origin, and Evolution of Parasitism in Plant Pathology: An Advanced Treatise. New York, Academic Press.

Miller AW and Richardson LL. 2014. Emerging Coral Diseases: A Temperature-Driven Process? *Marine Ecology*, 36 (3): 278.

Miller J, Muller E, Rogers C, Waara R, Atkinson A, Whelan KRT, Patterson M, and Witcher B. 2009. Coral Disease Following Massive Bleaching in 2005 Causes 60% Decline in Coral Cover on Reefs in the US Virgin Islands. *Coral Reefs* 28 (4): 925.

Muench H. 1934. Derivation of Rates from Summation Data by the Catalytic Curve. *Journal of the American Statistical Association* 29 (185): 25.

Mullen KM, Peters EC, and Harvell CD. 2004. Coral Resistance to Disease in Coral Health and Disease 337.

Mydlarz LD and Harvell CD. 2007. Peroxidase Activity and Inducibility in the Sea Fan Coral Exposed to a Fungal Pathogen. *Comparative Biochemistry and Physiology - A Molecular and Integrative Physiology* 146 (1): 54.

NOAA Coral Reef Watch -- 2014 Annual Summaries of Thermal Conditions Related to Coral Bleaching for U.S. National Coral Reef Monitoring Program (NCRMP)

Jurisdictions. 2014. http://coralreefwatch.noaa.gov/satellite/analyses_guidance/2014_annual_summaries_thermal_stress_conditions_NCRMP.pdf?

Palmer CV and Traylor-Knowles N. 2012. Towards an Integrated Network of Coral Immune Mechanisms. *Proceedings of the Royal Society B: Biological Sciences* 279 (1745): 4106.

Palmer CV, Bythell JC, and Willis BL. 2010. Levels of Immunity Parameters Underpin Bleaching and Disease Susceptibility of Reef Corals. *FASEB Journal* 24 (6): 1935.

Palmer CV, Modi CK, and Mydlarz LD. 2009. Coral Fluorescent Proteins as Antioxidants. *PloS One* 4 (10): e7298.

Palmer CV, Mydlarz LD, and Willis BL. 2008. Evidence of an Inflammatory-like Response in Non-Normally Pigmented Tissues of Two Scleractinian Corals. *Proceedings of the Royal Society B: Biological Sciences Biological Sciences* 275 (1652): 2687.

Palmer CV, Roth MS, and Gates RD. 2009. Red Fluorescent Protein Responsible for Pigmentation in Trematode-Infected *Porites Compressa* Tissues. *The Biological Bulletin* 216: 68.

Palmer CV, Traylor-Knowles NG, Willis BL, and Bythell JC. 2011. Corals Use Similar Immune Cells and Wound-Healing Processes as Those of Higher Organisms. *PloS One* 6 (8): e23992.

Pedersen AB, Jones KE, Nunn CL, and Altizer S. 2007. Infectious Diseases and Extinction Risk in Wild Mammals. *Conservation Biology* 21 (5): 1269.

Pollock FJ, Lamb JB, Field SN, Heron SF, Schaffelke B, Shedrawi G, Bourne DG, and

Willis BL. 2014. Sediment and Turbidity Associated with Offshore Dredging Increase Coral Disease Prevalence on Nearby Reefs. *PLoS ONE* 9 (7): e102498.

Preston DL, Mischler JA, Townsend AR, and Johnson PTJ. 2016. Disease Ecology Meets Ecosystem Science. *Ecosystems* 19 (4): 737.

R Core Team: A Language and Environment for Statistical Computing. 2014. http://www.r-project.org.

Randall CJ and van Woesik R. 2015. Contemporary White-Band Disease in Caribbean Corals Driven by Climate Change. *Nature Climate Change* 5 (4): 375.

Reiner RC, Stoddard ST, Forshey BM, King AA, Ellis AM, Lloyd AL, Long KC, Rocha C, Vilcarromero S, Astete H, Bazan I, Lenhard A, Vazquez-Prokopec GM, Paz-Soldan VA, McCall PJ, Kitron U, Elder JP, Halsey ES, Morrison AC, Kochel TJ, and Scott TW. 2014. Time-Varying, Serotype-Specific Force of Infection of Dengue Virus. *Proceedings of the National Academy of Sciences* 111 (26): E2694.

Reshef L, Koren O, Loya Y, Zilber-Rosenberg I, and Rosenberg E. 2006. The Coral Probiotic Hypothesis. *Environmental Microbiology* 8 (12): 2068.

Reytar K, Spalding M, and Perry A. 2011. *Reefs at Risk Revisited*. Washington, D.C.

Ritchie KB. 2006. Regulation of Microbial Populations by Coral Surface Mucus and Mucus-Associated Bacteria. *Marine Ecology Progress Series* 322: 1.

Rizzo DM and Garbelotto M. 2003. Sudden Oak Death : Endangering California and Oregon Forest Ecosystems. *Frontiers in Ecology and the Environment* 1 (4): 197.

Roff G, Kvennefors ECE, Ulstrup KE, Fine M, and Hoegh-Guldberg O. 2008. Coral Disease Physiology: The Impact of Acroporid White Syndrome on *Symbiodinium*. *Coral Reefs* 27 (2): 373.

Roff G, Kvennefors ECE, Fine M, Ortiz J, Davy JE, and Hoegh-Guldberg O. 2011. The Ecology of 'Acroporid White Syndrome', a Coral Disease from the Southern Great Barrier Reef. *PloS One* 6 (12): e26829.

Ross M, Stender Y, White D, and Aeby G. 2012. Outbreak of the coral disease, *Montipora* White Syndrome in Maui, Hawai'i. Proceedings of the 12th International Coral Reef Symposium, Cairns, Australia July 9-13.

Roth MS, Fan TY, and Deheyn DD. 2013. Life History Changes in Coral Fluorescence and the Effects of Light Intensity on Larval Physiology and Settlement in *Seriatopora hystrix*. *PLoS ONE* 8 (3): e59476.

Roth MS, Goericke R, and Deheyn DD. 2012. Cold Induces Acute Stress but Heat is Ultimately More Deleterious for the Reef-Building Coral A*cropora yongei*. *Scientific Reports* 2 (240): 1.

Roth MS, Latz MI, Goericke R, and Deheyn DD. 2010. Green Fluorescent Protein Regulation in the Coral *Acropora yongei* during Photoacclimation. *The Journal of Experimental Biology* 213: 3644.

Roth MS, Padilla-Gamiño JL, Pochon X, Bidigare RR, Gates RD, Smith CM, and Spalding HL. 2015. Fluorescent Proteins in Dominant Mesophotic Reef-Building Corals. *Marine Ecology Progress Series* 521: 63.

Ruiz-Moreno D, Willis BL, Page AC, Weil E, Cróquer A, Vargas-Angel B, Jordan-Garza AG, Jordán-Dahlgren E, Raymundo L, and Harvell CD. 2012. Global Coral Disease Prevalence Associated with Sea Temperature Anomalies and Local Factors. *Diseases Of Aquatic Organisms* 100 (3): 249.

Salih A, Larkum A, Cox G, Kühl M, and Hoegh-Guldberg O. 2000. Fluorescent

Pigments in Corals Are Photoprotective. *Nature* 408 (6814): 850.

Scott ME and Dobson A. 1989. The Role of Parasites in Regulating Host Abundance. *Parasitology Today* 5 (6): 176.

Selig ER, Casey KS, and Bruno JF. 2010. New Insights into Global Patterns of Ocean Temperature Anomalies: Implications for Coral Reef Health and Management. *Global Ecology and Biogeography* 19: 397.

Sheridan C, Baele JM, Kushmaro A, Frejaville Y, and Eeckhaut I. 2014. Terrestrial Runoff Influences White Syndrome Prevalence in SW Madagascar. *Marine Environmental Research* 101: 44.

Shnit-Orland M and Kushmaro A. 2009. Coral Mucus-Associated Bacteria: A Possible First Line of Defense. *FEMS Microbiology Ecology* 67 (3): 371.

Short FT, Muehlstein LK, and Porter D. 1987. Eelgrass Wasting Disease: Cause and Recurrence of a Marine Epidemic. *Biological Bulletin*, 173: 557.

Skerratt LF, Berger L, Speare R, Cashins S, McDonald KR, Phillott AD, Hines HB, and Kenyon N. 2007. Spread of Chytridiomycosis Has Caused the Rapid Global Decline and Extinction of Frogs. *EcoHealth* 4 (2): 125.

Smart CD and Fry WE. 2002. Invasions by the Late Blight Pathogen: Renewed Sex and Enhanced Fitness. *Biological Invasions* 3: 235.

Smith DL, Lucey B, Waller LA, Childs JE, and Real LA. 2002. Predicting the Spatial Dynamics of Rabies Epidemics on Heterogeneous Landscapes. *Proceedings of the National Academy of Sciences of the United States of America* 99 (6): 3668.

Sokolow S. 2009. Effects of a Changing Climate on the Dynamics of Coral Infectious Disease: A Review of the Evidence. *Diseases of Aquatic Organisms* 87: 5.

Stimson J. 2010. Ecological Characterization of Coral Growth Anomalies on *Porites compressa* in Hawai'i. *Coral Reefs* 30 (1): 133.

Storlazzi C, McManus M, Logan J, and McLaughlin B. 2006. Cross-shore velocity shear, eddies and heterogeneity in water column properties over fringing coral reefs: West Maui, Hawai'i. *Continental Shelf Research* 26 (3): 401.

Sutherland KP, Porter JW, and Torres C. 2004. Disease and Immunity in Caribbean and Indo-Pacific Zooxanthellate Corals. *Marine Ecology Progress Series* 266: 273.

Sutherland WJ, Clout M, Depledge M, Dicks LV, Dinsdale J, Entwistle AC, Fleishman E, Gibbons DW, Beim B, Lickorish FA, Monk KA, Ockendon N, Peck LS, Pretty J, Rockstrom J, Spalding MD, Tonneijck FH, and Wintle BC. 2015. A Horizon Scan of Global Conservation Issues for 2015. *Trends in Ecology & Evolution* 30 (1): 17.

Teplitski M and Ritchie K. 2009. How Feasible Is the Biological Control of Coral Diseases? *Trends in Ecology and Evolution Evolution* 24 (7): 378.

Travers MA, Basuyaux O, Le Goic N, Huchette S, Nicolas JL, Koken M, Paillard C. 2009. Influence of Temperature and Spawning Effort on *Haliotis tuberculata* Mortalities Caused by *Vibrio harveyi*: An Example of Emerging Vibriosis Linked to Global Warming. *Global Change Biology* 15 (6): 1365.

Treibitz T, Neal BP, Kline DI, Beijbom O, Roberts PLD, Mitchell BG, and Kriegman D. 2015. Wide Field-of-View Fluorescence Imaging of Coral Reefs. *Scientific Reports* 5: 7694.

Ushijima B, Smith A, Aeby GS, and Callahan SM. 2012. *Vibrio owensii* Induces the Tissue Loss Disease *Montipora* White Syndrome in the Hawaiian Reef Coral *Montipora capitata*. *PloS One* 7 (10): e46717.

Ushijima B, Videau P, Burger AH, Shore-Maggio A, Runyon CM, Sudek M, Aeby GS, and Callahan SM. 2014. *Vibrio coralliilyticus* Strain OCN008 Is an Etiological Agent of Acute *Montipora* White Syndrome. *Applied and Environmental Microbiology* 80 (7): 2102.

Ushijima B, Videau P, Poscablo D, Stengel JW, Beurmann S, Burger AH, Aeby GS, and Callahan SM. 2016. Mutation of the toxR or mshA Genes from *Vibrio coralliilyticus* Strain OCN014 Reduces Infection of the Coral *Acropora cytherea*. *Environmental Microbiology* 18 (11): 4055.

van de Water JAJM, Lamb JB, Heron SF, van Oppen MJH, and Willis BL. 2016. Temporal Patterns in Innate Immunity Parameters in Reef‐building Corals and Linkages with Local Climatic Conditions. *Ecosphere* 7 (11): e01505.

van de Water JAJM, Ainsworth T, Leggat W, Bourne DG, Willis BL, and van Oppen MJH. 2015. The Coral Immune Response Facilitates Protection against Microbes during Tissue Regeneration. *Molecular Ecology*, 24 (13): 3390.

Vanoy RW, Tamplin ML, and Schwarz JR. 1992. Ecology of *Vibrio vulnificus* in Galveston Bay Oysters, Suspended Particulate Matter, Sediment and Seawater: Detection by Monoclonal Antibody — Immunoassay — Most Probable Number Procedures. *Journal of Industrial Microbiology* 9 (3): 219.

Vega Thurber RL, Burkepile DE, Fuchs C, Shantz AA, McMinds R, and Zaneveld JR. 2013. Chronic Nutrient Enrichment Increases Prevalence and Severity of Coral Disease and Bleaching. *Global Change Biology* 20 (2): 544.

Vollmer SV and Palumbi SR. 2006. Restricted Gene Flow in the Caribbean Staghorn Coral *Acropora cervicornis*: Implications for the Recovery of Endangered Reefs.

The Journal of Heredity 98 (1): 40.

Vredenburg VT, Knapp RA, Tunstall TS, and Briggs CJ. 2010. Dynamics of an Emerging Disease Drive Large-Scale Amphibian Population Extinctions. *Proceedings of the National Academy of Sciences of the United States of America* 107 (21): 9689.

Ward JR, Kim K, and Harvell CD. 2007. Temperature Affects Coral Disease Resistance and Pathogen Growth. *Marine Ecology Progress Series* 329: 115.

Ward JR and Lafferty KD. 2004. The Elusive Baseline of Marine Disease: Are Diseases in Ocean Ecosystems Increasing? *PLoS Biology* 2 (4): 542.

Williams GJ, Knapp IS, Work TM, and Conklin EJ. 2011. Outbreak of *Acropora* White Syndrome Following a Mild Bleaching Event at Palmyra Atoll, Northern Line Islands, Central Pacific. *Coral Reefs* 30 (3): 621.

Williams GJ, Aeby GS, Cowie ROM, and Davy SK. 2010. Predictive Modeling of Coral Disease Distribution within a Reef System. *PloS One* 5 (2): e9264.

Work T. 2015. Diagnostic Case Report. Honolulu.

Work TM, Russell R, and Aeby GS. 2012. Tissue Loss (White Syndrome) in the Coral *Montipora capitata* Is a Dynamic Disease with Multiple Host Responses and Potential Causes. *Proceedings of the Royal Society B Biological Sciences* 279 (1746): 4334.

Zvuloni A, Artzy-Randrup Y, Katriel G, Loya Y, and Stone L. 2015. Modeling the Impact of White-Plague Coral Disease in Climate Change Scenarios. *PLoS Computational Biology* 11 (6): e1004151.

Zvuloni A, Artzy-Randrup Y, Stone L, Kramarsky-Winter E, Barkan R, and Loya Y. 2009.

Spatio-Temporal Transmission Patterns of Black-Band Disease in a Coral Community. *PloS One* 4 (4): e4993.